DEVELOPMENT OF AN *EX VIVO* ASSAY TO EXAMINE TRANSCRIPTION FACTORS REQUIRED FOR ENDOTHELIAL TO HEMATOPOIETIC TRANSITION

by

AMANDA LORRAINE FENTIMAN

B. Sc., University of Victoria, 2011

A THESIS SUBMITTED IN PARTIAL FULFILLMENT OF THE REQUIREMENTS FOR THE DEGREE OF

MASTER OF SCIENCE

in

The Faculty of Graduate and Postdoctoral Studies

(Interdisciplinary Oncology)

THE UNIVERSITY OF BRITISH COLUMBIA

(Vancouver)

July 2014

Abstract

Hematopoietic stem cells (HSCs) arise from a specialized population of endothelial cells, termed hemogenic endothelium (HE). HE was first identified in the murine dorsal aorta (DA) at embryonic day (E) 10.5. This process is known as endothelial to hematopoietic transition (EHT). Our aim was to identify genes crucial for the development of embryonic HSCs from the endothelium through the process of EHT. We accomplished this through the use of a transgenic mouse model which expresses GFP under the control of an intronic enhancer of the HE gene *Runx1*. The expression of this enhancer was combined with endothelial and hematopoietic markers to sort specialized endothelial cell populations from the DA of E10.5 embryos. RNA-seq data was generated from these sorted cell populations and 9 possible upstream transcription factors were identified. These candidate transcription factors include both known and novel regulators of EHT, including a novel regulator *Meis1*.

Additionally, endothelial cell populations isolated from E9.5 embryos were sorted and cultured to develop an *ex vivo* co-culture assay that supports differentiation of pre-HE cells to HSCs. The effect of oxygen tension on endothelial and hematopoietic cell growth was investigated as a means to better support endothelial and hematopoietic cells. Oxygen transition during culture was found to significantly increase the proportion of wells which produced hematopoietic cells, and may aid in HE cell maintenance in culture. To examine the possibility of using this model to study regulators of EHT, the effect of blocking Notch signalling with a γ-secretase inhibitor added to our *ex vivo* culture was examined. Inhibition of Notch signalling did not significantly affect the generation of hematopoietic cells in our assay. Additionally, we evaluated the hematopoietic activity of tissue isolated from E9.5 $Meis1^{fl/fl\ VeCre}$ null embryos in this assay. No differences in hematopoietic cell generation were observed between wild-type and $Meis1^{fl/fl\ VeCre}$ null tissues in culture. Characterization of these embryos at E14.5 suggests that there exists a potential defect in $Meis1^{fl/fl\ VeCre}$ null embryos in later stages of embryonic hematopoiesis. This project contributes to the further understanding of genes important in EHT, while potentially defining transcriptional networks involved in HSC development.

Preface

The hypothesis, aims of this study and experimental design were developed by Amanda Fentiman with guidance from Dr. Aly Karsan. Cell collection strategy for RNA-seq library construction was designed with Dr. Jeremy Parker. RNA-seq library construction took place at Canada's Michael Smith Genome Sciences Centre. Libraries were sequenced as part of the SOF4 Chimeric Transcript Project led by Dr. Inanc Birol in collaboration with Amanda Fentiman and Dr. Aly Karsan. All *ex vivo* assays and *in vitro* experiments were performed by Amanda Fentiman. Mouse colony maintenance, genotyping and timed matings were performed by Amanda Fentiman, Megan Fuller and Patricia Umlandt. Embryo dissections were completed by Amanda Fentiman with help from Justin Smrz, and Rachelle Huot. All cell sorting took place within the Terry Fox Laboratory Flow Core by David Ko, Wenbo Xu, and Gayle Thornbury. All other flow cytometry was completed by Amanda Fentiman, with the exception of the ESLAM experiment which included help from Dr. Joanna Wegrzyn. Expertise and protocols in relation to the *Meis1*$^{fl/fl}$ mouse model was provided by Patty Rosten, Courteney Lai, and Justin Smrz.

All mouse work and methods were approved by the University of British Columbia's Committee on Animal Care; project title: Endothelial to Hematopoietic Transdifferentiation. Certificate #s A10-0331 and A12-0164.

Table of Contents

Abstract ii
Preface iii
Table of Contents iv
List of Tables vi
List of Figures vii
List of Abbreviations and Symbols viii
Acknowledgements x
1. Introduction 1
1.1 The Composition, Origin and Maintenance of Blood During Development 1
1.1.1 Development of the Hematopoietic Hierarchy 1
1.1.2 Temporospatial Hematopoietic Development in the Mouse Embryo 3
1.1.3 Relationship Between Fetal and Adult HSCs 6
1.2 Detecting and Quantifying Mouse HE and HSCs 7
1.2.1 Cell Surface Markers and Flow Cytometry 7
1.2.2 Whole Organ *Ex vivo* Culture 12
1.2.3 *Ex vivo* Cellular Co-culture 13
1.2.5 Colony-forming Cell Assays 15
1.2.6 Embryo Derived HSC Transplantation 15
1. 3 Genes Involved in Embryonic Hematopoiesis 16
1.3.1 Runt-related Transcription Factor 1 – *Runx1* 16
1.3.2 *Notch1* 20
1.3.3 Growth Factor Independent 1/1b - *Gfi1* and *Gfi1b* 23
1.3.4 Sry Related High Mobility Group Box Protein 17 – *Sox17* 23
1.3.5 Homeobox A3 - *Hoxa3* 24
1.3.6 Myeloid Ecotropic Viral Integration Site 1 - *Meis1* 25
1.4 Scope, Hypothesis and Aims of Present Study 26
2. Methods 29
2.1 Transgenic Mice 29
2.1.1 Runx1+24mCNE-GFP Transgenic Mouse 29
2.1.2 Meis1$^{fl/fl\ VeCre}$ Transgenic Mouse 29
2.2 Timed Matings and Embryo Generation 33
2.3 Embryo Dissection 34
2.4 FACS 36
2.5 Library Construction 39
2.6 Hierarchy Validation 41
2.7 *Ex vivo* Assay 42

2.7.1 OP9 Co-culture 42
2.7.2 Notch Inhibition 44
2.8 Meis1$^{fl/fl\ VeCre}$ Embryo Characterization 44
2.8.1 Phenotype Analysis 44
2.8.2 Percentage of Cells containing Excised *Meis1*$^{fl/fl}$ Exon 8 44
2.8.3 ESLAM Analysis of E14.5 FLs 45
2.8.4 Immunofluorescence Staining 46
2.9 Statistical Analysis 47
3. Results 48
3.1 RNA-seq Library Construction 48
3.2 Analysis of Whole Transcriptome Data 48
3.3 Hierarchy Validation 49
3.4 *Ex vivo* Assay 52
3.4.1 Oxygen Tension in E9.5 *Ex vivo* Co-culture 52
3.4.2 Effect of Oxygen Tension Change During Culture 57
3.4.3 Notch Inhibitor Manipulation 59
3.5 Meis1$^{fl/fl\ VeCre}$ Embryos 61
3.5.1 Percent Excision of *Meis1*$^{fl/fl}$ Exon 8 in VEC^{pos} Cells 61
3.5.2 Quantification of ESLAM^{pos} Cells in E14.5 FL 63
3.5.3 Hemorrhagic Phenotype in *Meis1*$^{fl/fl\ VeCre}$ Null Embryos 63
3.5.4 Whole DA Culture of Meis1$^{fl/fl\ VeCre}$ Embryos 66
3.5.5 Immunofluorescent Staining of Meis1$^{fl/fl\ VeCre}$ Embryos 66
4. Discussion 70
4.1 Analysis of RNA-seq Libraries 70
4.2 Validation of RNA-seq Results 73
4.3 *Ex vivo* Co-culture Assay 73
4.4 Effect of Oxygen Tension During *Ex vivo C*ulture 78
4.5 Shear Stress and Nitric Oxide in *Ex vivo* Culture 80
4.6 Effect of Notch Blockage in *Ex vivo* Culture 81
4.7 Analysis of Single Meis1$^{fl/fl\ VeCre}$ Embryos 82
4.8 Hemorrhagic Phenotype in Meis1$^{fl/fl\ VeCre}$ Embryos 83
4.9 *Ex vivo* Culture of E9.5 Meis1$^{fl/fl\ VeCre}$ Embryos 83
4.10 Quantification of ESLAM Cells in E14.5 Meis1$^{fl/fl\ VeCre}$ FL 84
4.11 The Role of Meis1 in the Endothelium and HSC 85
4.12 Summary and Future Directions 86
References 88
Appendix A: Additional information regarding RNA-seq Library Construction 95

List of Tables

Table 2.1 Genotyping primers for Meis1$^{fl/fl\ VeCre}$ embryos 33

Table 2.2 Interpretation of Meis1$^{fl/fl\ VeCre}$ genotyping results based on 4 primer sets..... 33

Table 2.3 Antibodies, antigens, and concentration for FACS experiments..... 37

Table 2.4 List of qRT-PCR primers..... 41

Table 2.5 List of qRT-PCR primers for percent excision..... 45

Table 3.1 Comparison of the expression of top hierarchy genes in E10.5 HE 52

List of Figures

Figure 1.1 Classical model of hematopoietic differentiation 2

Figure 1.2 Progression of primitive and definitive hematopoiesis in the mouse embryo..... 4

Figure 1.3 Comparison of mouse *Runx1* and Human *RUNX1* isoforms and +24mCNE transgenic mouse model..... 19

Figure 1.4 Notch signalling between endothelial cells 22

Figure 1.5 Known regulators in hematopoietic cluster formation and EHT..... 27

Figure 2.1 Mating scheme to generate *Meis1*$^{fl/fl\ VeCre}$ null embryos 30

Figure 2.2 Schematic of *Meis1* floxed exon 8 in uncollapsed and collapsed state..... 32

Figure 2.3 Dissection of E10.5 DA..... 35

Figure 2.4 Sorting scheme for library construction 38

Figure 3.1 Hierarchy of regulators involved in EHT at E10.5..... 50

Figure 3.2 qRT-PCR fold change for top hierarchy genes 51

Figure 3.3 Effect of O_2 tension on generation of CD45 and GFP in sorted cells..... 54

Figure 3.4 5% O_2 culture of CD45^{neg}GFP^{pos} and CD45^{neg}GFP^{neg} cell populations..... 55

Figure 3.5 Effect of O_2 tension transition during culture 58

Figure 3.6 The effect of 0.1 μM DFPAA addition to *ex vivo* culture 60

Figure 3.7 Flow analysis of single DAs from E10.5 and E11.5 embryos..... 62

Figure 3.8 Number of ESLAM cells in E14.5 FL of Meis1$^{fl/fl\ VeCre}$ embryos..... 64

Figure 3.9 Phenotypic examination of E14.5 Meis1$^{fl/fl\ VeCre}$ embryos 65

Figure 3.10 Analysis of Meis1$^{fl/fl\ VeCre}$ E9.5 DAs in *ex vivo* culture..... 67

Figure 3.11 Enumeration of CD41^{pos} cells in E10.5 DA sections 68

Figure 3.12 Immunofluorescence imaging of E10.5 Meis1$^{fl/fl\ VeCre}$ DAs..... 69

List of Abbreviations and Symbols

β-gal	β-galactosidase
AGM	Aorta-gonad-mesonephros
AML	Acute myeloid leukemia
AML1	Acute myeloid leukemia 1 protein
APC	Allophycocyanin
bFGF	Basic fibroblast growth factor
bp	Base pair
CBFα2	Core binding factor alpha 2
CBFβ	Core binding factor beta
cDNA	complimentary DNA
CFC	Colony forming cell
CLP	Common lymphoid progenitor
CMP	Common myeloid progenitor
CNE	Conserved non-coding enhancer
Cre	Cre recombinase
DA	Dorsal aorta
DAPI	4',6-diamidino-2-phenylindole
DAPT	(N-[N-(3,5-Difluorophenacetyl)-L-alanyl]-S-phenylglycine t-butyl ester)
DFPAA	((2S)-2-([(3,5-Difluorophenyl)acetyl]amino)-*N*-[(3S)-1-methyl-2-oxo-5-phenyl-2,3-dihydro-1*H*-1,4-benzodiazepin-3-yl]propanamide)
Dll1	Delta-like-ligand 1
DMSO	Dimethyl sulfoxide
DNase	Deoxyribonuclease
E	Embryonic day
ECR	Evolutionarily conserved region
ee	Embryo equivalents
EHT	Endothelial to hematopoietic transition
EMP	Erythroid/Myeloid progenitor
EPO	Erythropoietin
ES	Embryonic stem
ESLAM	Primitive hematopoietic stem cell
FACS	Fluorescence-activated cell sorting
FITC	Fluorescein isothiocyanate
FL	Fetal liver
fl	floxed
g	Gauge
Gy	Gray
G-CSF	Granulocyte-colony stimulating factor
GFP	Green fluorescent protein
GM-CSF	Granulocyte macrophage-colony stimulating factor
GMP	Granulocyte-macrophage progenitor
GSC	Canada's Michael Smith Genome Sciences Centre
GSI	γ-secretase inhibitor
Gy	Gray

HE	Hemogenic endothelium
HI-FBS	Heat inactivated-fetal bovine serum
Hox	Homeobox
Hoxa3	Homeobox family member A3
HSC	Hematopoietic stem cell
IL-3	Interleukin 3
LSK	Primitive hematopoietic stem cell
LT-HSC	Long-term hematopoietic stem cell
M-CSF	Macrophage-colony stimulating factor
Meis1	Myeloid ecotropic viral integration site 1
MHC	Major histocompatibility complex
MPP	Multipotent progenitor
mRNA	Messenger RNA
NICD	Notch intracellular domain
NK	Natural killer
NO	Nitric oxide
OCT	Optimal cutting temperature
OP9	Fibroblast cell line isolated from *Op/Op* mouse model
O_2	Oxygen
OSM	Oncostatin M
PBS	Phosphate buffered saline
PE	Phycoerythrin
PFA	Paraformaldehyde
PGC	Primitive germ cell
PSG	Penicillin-streptomycin-glutamine
qRT-PCR	Quantitative real time-polymerase chain reaction
RCF	Relative centrifugal force
RNA-seq	RNA sequencing
ROS	Reactive oxygen species
RPKM	Reads per kilobase per million mapped reads
RT	Room temperature
SCF	Stem cell factor
SEM	Standard error of the mean
SNS	Sympathetic nervous system
Sox17	Sry related high mobility group box protein 17
SSEA-1	Stage specific embryonic antigen 1
ST-HSC	Short-term hematopoietic stem cell
TF	Transcription factor
TFBS	Transcription factor binding site
UA	Umbilical artery
VA	Vitelline artery
VEC	Vascular endothelial cadherin
VEGF	Vascular endothelial growth factor
YS	Yolk sac

Acknowledgements

I would like to acknowledge all of the members of the Karsan Lab who assisted me with experiments contained in this thesis, including early morning dissections, and late night discussions. I am grateful to Dr. Aly Karsan for seeing my potential as a researcher and thankful for his encouraging discussions when “science doesn’t work”. I would like to thank Dr. Jeremy Parker who took a chance on a co-op student who used to study sea creatures, and got me excited about hemogenic endothelium. I am grateful for my committee members Dr. Connie Eaves, and Dr. Andrew Weng for their insightful perspective on my project. I would like to thank Dr. Linda Chang for sharing with me her extensive knowledge of development and endothelial cell biology. I would certainly have been late for my sort time if not for the work of numerous co-op, students who helped me dissect embryos early in the morning. I would also like to thank the funding I received from the Stem Cell Network to attend workshops and conferences to interact with scientists from around the country, as well as the Heart and Stroke Foundation, and CIHR.

Lastly, I wouldn’t have been able to do this without the support from family, and friends. I am forever indebted to my Mom and Dad, who have always been extremely supportive of my education, and the multiple moves between land masses I took to accomplish it. I am thankful for my friends who understood when I needed to go into work on the weekends, even if they could never figure out why a mouse’s pregnancy was so important to me.

1. Introduction

1.1 The Composition, Origin and Maintenance of Blood During Development

1.1.1 Development of the Hematopoietic Hierarchy

All blood cells in adult mammals are produced from specialized multipotential stem cells located within the bone marrow, known as hematopoietic stem cells (HSCs) [1]. HSCs were first hypothesized to exist as early as 1909 by Russian scientist Alexander Maximow [2]. Adult HSCs have historically been defined by two major characteristics, the ability to self-renew for the lifetime of an organism, and to divide and differentiate into all mature blood cells. Theoretically, HSCs may divide symmetrically, to expand the population of HSCs or generate two more differentiated progeny, and asymmetrically, into one HSC and a single differentiated progenitor [1, 3-5]. As HSCs are not morphologically nor always phenotypically distinct from many progenitors, the most reliable test of an HSC is through the use of a functional assay, such as transplantation of cells into irradiated adult recipients at limiting dilution [3, 4]. HSCs must be capable of maintaining the population of mature blood cells during homeostasis, and in the stress of immune system challenge. The balance between HSC self-renewal and blood production is crucial for survival.

HSCs situated at the apex of the hematopoietic hierarchy, are termed long-term or LT-HSCs. Most LT-HSCs are able to engraft into the bone marrow of an irradiated adult recipient and produce both myeloid and lymphoid blood cells for the lifetime of the animal (Figure 1.1) [6, 7]. LT-HSCs have been shown to be comprised of multiple sub-populations referred to as

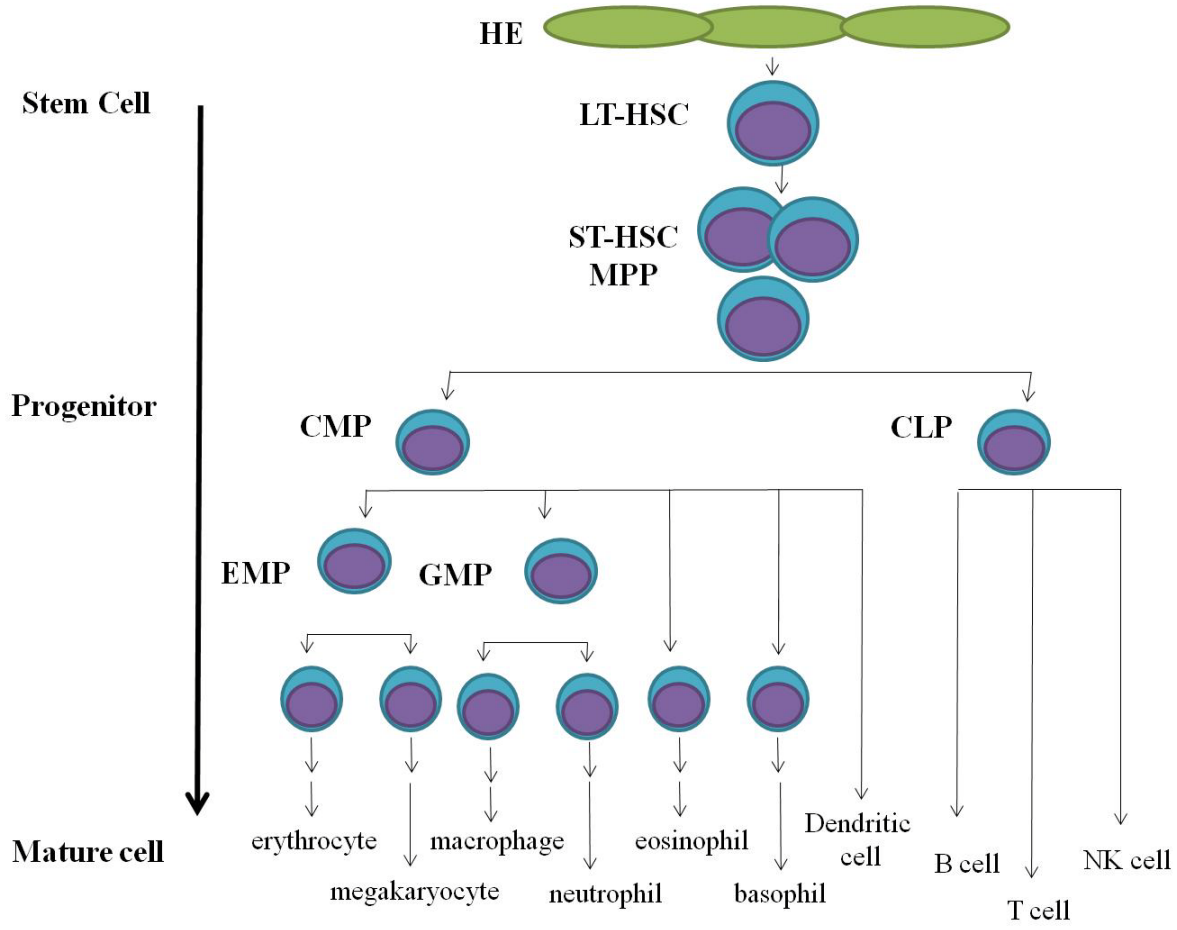

Figure 1.1 Classical model of hematopoietic differentiation

Hierarchy displaying generalized development of hematopoietic cells from hemogenic endothelium (HE). All mature blood cells descend from long-term hematopoietic stem cell (LT-HSC) and short-term hematopoietic stem cell (ST-HSC) or multipotent progenitor (MPP) cells, followed by more committed common myeloid progenitors (CMP), and common lymphoid progenitors (CLP). CMPs are further divided into erythroid-myeloid progenitors (EMPs) and granulocyte-macrophage progenitors (GMPs). Adaptation of the classical model from Reya *et al.* [8]. It is important to note that alternative models exist, often including more flexibility in lymphoid progenitors' ability to contribute to the myeloid lineage, or dispute on the origin of HSCs [9-11].

α-HSCs, which are lymphoid-deficient, and β-HSCs which are able to efficiently generate both lymphoid and myeloid cells [4]. Subdividing HSCs further in relation to their longevity has allowed the identification of short-term, ST-HSCs, and multipotential progenitors (MPPs) [6, 7]. ST-HSCs and MPPs share multiple surface markers, persist for a reduced time in comparison to LT-HSCs, and are thought to take on the major burden of expansion of blood cell progenitors within the body [6]. Both allow the generation of myeloid and lymphoid progenitors, but possess a restriction on self-renewal, exhausting before the end of an organism's life [6, 7]. Following these multipotent stem cells, the hierarchy is broken into more lineage-restricted progenitors known as common myeloid progenitors (CMP), and common lymphoid progenitors (CLP) [12, 13]. CMPs produce all myeloid cells though erythroid-myeloid progenitors (EMP) which produce erythrocytes, and megakaryocytes and granulocyte-macrophage progenitors (GMP) which produce macrophages and neutrophils, as well as eosinophils, basophils, and dendritic cells [12]. CLPs produce all lymphoid progeny including B, T, and Natural killer (NK) cells [12, 13]. During development the first LT-HSCs, capable of long-term adult repopulating activity and the production of blood throughout an organism's lifetime, arise within the embryo [14].

1.1.2 Temporospatial Hematopoietic Development in the Mouse Embryo

In the mouse, embryonic hematopoiesis can be classified roughly as occurring in two waves, which are able to fulfill the needs of the embryo at different stages of development (Figure 1.2). In the mouse, before the embryo has reached embryonic day E7.0, the structure is simple enough that diffusion will supply the growing embryo with oxygen (O_2). Once the embryo becomes more complex, the first wave of primitive hematopoiesis begins at E7.0-E7.5 in blood islands of the yolk sac (YS), producing nucleated erythrocytes [15, 16]. These primitive blood cells are thought to arise from a bi-potential mesodermal precursor, capable of generating

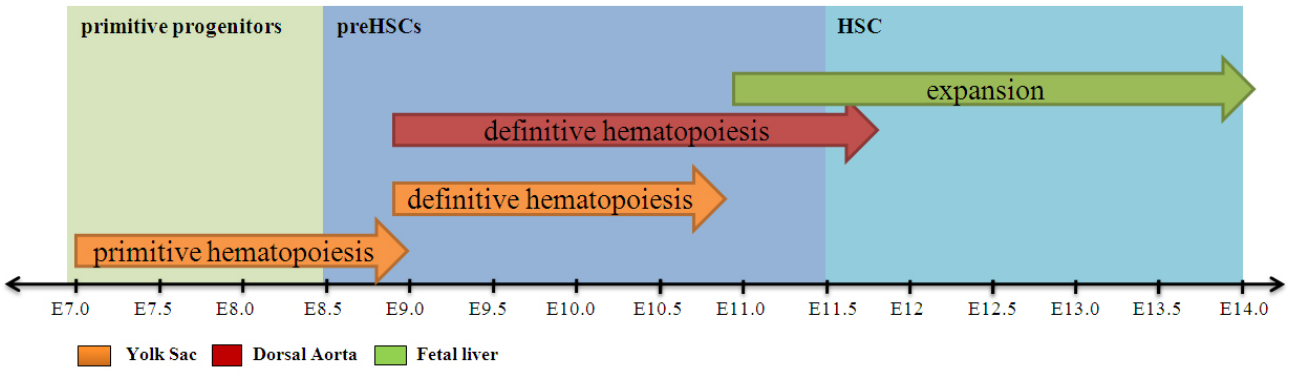

Figure 1.2 Progression of primitive and definitive hematopoiesis in the mouse embryo

Embryonic hematopoiesis shifts through multiple sites through embryonic development. The horizontal axis shows embryonic time-point in embryonic days (E) from E7.0 to E14.0, after which hematopoiesis shifts to the developing bone marrow. The coloured blocks represent when hematopoietic stem cells or precursors are produced within the organs shown. The yolk sac (YS), dorsal aorta (DA) and fetal liver (FL) are represented here by coloured arrows. Contribution from organs such as the umbilical artery (UA), vitelline artery (VA), placenta, head, and endocardium are not shown. Adapted from Mikkola and Orkin [17].

both endothelial and hematopoietic cells. This cell is termed the hemangioblast, and HSCs have not yet been identified at this early time-point [18]. Around E9.5 the second wave of hematopoiesis begins within the aorta-gonad-mesonephros (AGM) region of the embryo. This second wave generates MPPs and HSCs from specialized endothelial cells termed hemogenic endothelium (HE) [19].

The intra-embryonic origin of HSCs was proposed in 1916, when clusters of cells were observed within the vasculature of developing chicken embryos [20]. Since then the endothelial origin of HSCs has been debated alongside the hypothesis that all blood cells arose from a bipotential hemangioblast [18]. In 2010, Boisset *et al.* showed cells expressing endothelial markers rounding up and budding off of the wall of the dorsal aorta (DA) and into the lumen [21]. Although some scientists still support the existence of the definitive hemangioblast, it is now thought to only be present during the first wave of hematopoiesis in the YS, originating from the primitive streak [10, 17]. Regions of the embryo containing HE include the umbilical artery (UA), vitelline artery (VA), endocardium, head, and placenta [22-25]. The term for the development of HSCs from HE is endothelial to hematopoietic transition (EHT) [26].

The first HSC capable of reconstituting the hematopoietic system of an irradiated adult recipient is found in the DA at E10.5 [17, 27-29]. This first HSC is estimated to be present at a frequency of 1 per embryo in this organ at this time [17, 27-29]. Immature HSCs present from E9.5-E10.5, are referred to as pre-HSCs due to their need for maturation before they can successfully engraft in an adult recipient. This maturation can be achieved by culturing the whole organ *ex vivo*, or through transplantation into a more permissive niche [28, 30, 31]. By E11.5 some pre-HSCs are mature enough to allow long term adult engraftment as HSCs following direct transplantation [29]. From E12.5-E14.5 hematopoiesis shifts from the DA to the fetal liver

(FL), although no HSCs arise *de novo* in this organ [22-25, 31, 32]. Instead pre-HSCs from the DA, YS, UA, VA, head and placenta migrate to the FL [22-25, 31, 32]. This allows HSCs to expand, before they colonize the spleen and bone marrow of the embryo at E16.5 [17]. The bone marrow retains this population of HSCs and is the primary site of hematopoiesis in the adult.

1.1.3 Relationship Between Fetal and Adult HSCs

As the mouse embryo develops and nears birth, blood production declines within the FL, and HSCs generated within the embryo go on to seed the developing bone marrow, providing the HSC pool needed for the lifetime of the organism [17, 29]. Tracing experiments using labelled embryonic HSCs have helped determine the source and proportion of fetal HSCs present in the adult bone marrow. Chen *et al.* used a mouse model containing endothelial cells permanently marked throughout development, to determine their contribution to adult bone marrow [26]. Upon examination of an adult mouse containing this endothelial marker, they determined that 96% of hematopoietic cells within the bone marrow developed from endothelial cells [26]. Zovein *et al.* employed a similar model to determine the contribution of endothelial cells specifically within the AGM at mid-gestation to adult bone marrow [33]. Their mouse model expressed an inducible marker, which upon injection of Tamoxifen at E9.5, permanently labelled endothelial cells of the DA [33]. This enabled them to identify the progeny of E9.5 HE cells at later time-points in the embryo and adult mouse, determining the contribution of E9.5 HE to hematopoiesis [33]. When these embryos were allowed to progress to adulthood, 2-24% of total adult bone marrow cells were positive for the marker induced at E9.5, and therefore arose from endothelial cells in the AGM at mid-gestation [33].

Although adult HSCs arise from the FL HSCs which first colonize the bone marrow, HSCs isolated from fetal or adult tissues differ in noticeable ways. One difference includes both

the rate and degree to which fetal and adult HSCs engraft in an irradiated adult recipient [34]. Fetal HSCs maintain an increased rate of cell cycling, until about 3 weeks after birth [35-37]. The increased rate of cycling in fetal HSCs as compared to adult HSCs is associated with a higher degree of engraftment when similar cell numbers are transplanted into the same type of irradiated adult recipient [35, 37]. This is in contrast to adult HSCs which are largely quiescent, and display a lower rate of self-renewal divisions as compared to fetal HSCs [38].

In addition to some cell-intrinsic differences in fetal and adult HSC properties, the cell-extrinsic effects of fetal and adult niches can affect engraftment. E9.5-E10.5 pre-HSCs isolated from the DA have been shown to engraft in myeloablated neonates, but only rarely engraft in adult recipients [28-31, 39]. There may be differences in the homing capacity of pre-HSCs, as transplantation directly into the long bones of irradiated adult recipients has been reported to allow pre-HSC engraftment [17]. Although engraftment of HSCs isolated from E11.5 embryos is possible, the major expansion observed in the FL, combined with the fact that *de novo* generation of HSCs does not occur, suggests priming of HSCs may occur in this organ. This would explain the low engraftment observed in the direct transplant of E10.5 HSCs [29]. Due to the functional differences between fetal and adult HSCs, it is important to choose an appropriate assay for HSC quantitation, as adult transplantation is not always appropriate for embryo-derived cells.

1.2 Detecting and Quantifying Mouse HE and HSCs

1.2.1 Cell Surface Markers and Flow Cytometry

One of the key difficulties in examining the development of HSCs from endothelial precursors in the mouse embryo is the transitional nature of these cell populations. As cells are rapidly progressing through EHT, they express both endothelial and hematopoietic markers.

Flow cytometry and fluorescence-activated cell sorting (FACS) are important tools in interrogating these transitional cell populations based on specific subsets of markers that they express [40].

Despite the numerous endothelial and hematopoietic cell surface markers known, no accepted consensus exists for the identification of mouse HE. Combinations of both hematopoietic and endothelial markers are often used to identify these cells. A linear acquisition of endothelial to hematopoietic markers is often assumed when classifying cells undergoing EHT. At E10.5 in the mouse embryo, endothelial markers vascular endothelial cadherin (VEC, CD144) or platelet endothelial cell adhesion molecule (Pecam-1, CD31) are commonly used [21, 33, 39, 41, 42]. Basal HE, which lacks early hematopoietic markers stem cell growth factor receptor (CD117, c-Kit) and integrin alpha chain 2b (CD41), expresses both VEC and CD31 [21, 33, 39, 41, 42]. As cells mature and emerge from the endothelium, they gain c-Kit and CD41 surface expression, followed by the expression of the pan-hematopoietic marker, leukocyte common antigen CD45 [39, 41]. CD45 is used within the mouse embryo to label differentiated hematopoietic cells [39, 41].

The labelling of endothelial cells expressing VEC has been an important tool for fate tracing experiments which determined the embryonic origin of adult HSCs mentioned in 1.1.3 [26, 33]. Mice engineered to express Cre recombinase driven by the VEC promoter, *Cdh5*, are crossed with Rosa26R-lacZ reporter mice [43, 44]. Rosa26R-lacZ reporters contain the gene for β-galactosidase (β-gal) production, *lacZ*, inactivated with a floxed stop codon [43, 44]. Cre expression excises the stop codon, allowing *lacZ* expression, and the production of β-gal which cleaves the colourless substrate X-gal, into a blue compound [43, 44]. Both cells presently expressing VEC and their progeny, which have expressed VEC previously during development,

can be identified in situ by β-gal staining with this mouse model [26]. When Chen *et al.* observed embryos generated by crossing these transgenic mice, the sites of VEC expression were congruent with areas of embryonic hematopoiesis [26, 43, 44]. The first sites of VEC expression are the YS and embryonic mesoderm, followed by the placenta and UA at E9.5 [26]. At E10.5 Chen *et al.* observed clusters in the DA, UA, and VA that were marked with β-gal expression [26]. In addition 85% of hematopoietic cells within the FL at E15. 5 arise from VEC^{pos} cells [26]. Zovein *et al.* used an inducible model of Cre expression, driven by Tamoxifen injection into pregnant mice, to determine the contribution of VEC^{pos} cells from embryos at mid-gestation [33]. VEC^{pos} cells present within the embryo at E9.5-E11.5 were labelled upon Tamoxifen injection at E9.5. β-gal positive cells in the E11.5 AGM were found to provide LT-HSC engraftment in adult recipients [33]. *VEC* is important for definitive hematopoietic development. Mice lacking expression of *VEC* die at E9.5, although they contain some primitive hematopoietic cells in the YS before death [45].

Another marker of endothelium, CD31, is expressed on endothelial cells of the DA [39]. Although they are somewhat redundant in their marking of endothelial cells, VEC and CD31 are often used interchangeably as markers of HE in the AGM [45, 46]. When CD31 is combined with the early hematopoietic marker c-Kit, $CD31^{pos}$c-Kit^{pos} cells isolated from E9.5 and E10.5 embryos are able to repopulate busulfan-conditioned neonates [39].

c-Kit, CD117, is a ligand for Stem Cell Factor (SCF) [47]. c-Kit is first expressed on a small population of cells within the DA at E9.5, increasing in number at E10.5 [42]. Embryos lacking exon 4 of the gene *Runx1*, which is required for embryonic hematopoiesis, do not produce hematopoietic clusters or c-Kit^{pos} cells in the AGM [42]. c-Kit^{pos} cells are also found in populations of non-hematopoietic primitive germ cells (PGCs) which mark as c-$Kit^{pos}CD31^{pos}$

SSEA-1^{pos} [42]. It is important to include sex specific embryonic antigen-1 (SSEA-1) as a marker when using CD31 and c-Kit to identify intra-aortal clusters as these developing germ cells are closely associated with HE, but do not contribute to hematopoiesis directly [42]. c-Kit^{pos} cell populations had previously been found to contain LT-HSCs. When cells sorted from E11.5 AGM marked as c-Kit^{pos}, c-Kit^{lo} and c-Kit^{neg} were transplanted into irradiated adult recipients, only c-Kit^{pos} cells repopulated recipients [48].

CD41 is a marker for the earliest hematopoietic cells in the mouse embryo, observed first in E8.0-E8.5 YS vasculature, and E10.5 AGM [17, 21, 30, 49, 50]. Whole embryo imaging experiments allowed the visualization of CD41^{pos} cells emerging from the walls of the DA [21]. Transplants of cell populations expressing different levels of CD41 showed that only CD41^{mid} cells sorted from E11.5 AGM showed engraftment in irradiated adult recipients [51]. No engraftment was achieved with CD41^{neg} or CD41^{hi} cells [51]. This was also true in colony forming cell (CFC) assays which revealed higher progenitor capacity in CD41^{pos} cells isolated from E9.5 YS and E10.5 AGM compared to CD41^{neg} cells [50]. At E12.5 in the placenta, and E14.5 in the FL, this effect was lost, as only CD41^{neg} cells repopulated recipients [51]. Again, at E13.5 higher progenitor activity was observed in CFC assays of CD41^{neg} cells isolated from FLs than CD41^{pos} cells [50]. These findings suggest that CD41 expression is down-regulated by HSCs upon their move to the FL [17, 50]. Later as a fraction of these cells mature into platelets and megakaryocytes in the adult, CD41 expression is regained [17, 50].

Combinations of these endothelial and hematopoietic markers are used in flow cytometry analysis of isolated tissues from E7.5-E14.5 mouse embryos. Alternatively, whole mounted embryos or tissue sections may be stained *in situ* to determine the relative location of these cells within an embryo. Later in development at E12.5-E14.5, LSK (Lin^{neg}Sca1^{pos}c-Kit^{pos}) and

ESLAM ($CD45^{pos}EPCR^{pos}CD48^{neg}CD150^{pos}$) marker combinations commonly used for adult HSCs, can be used in the embryo once pre-HSCs have matured and display a transplantable HSC phenotype [4, 26, 52, 53]. LSK staining marks a relatively HSC-enriched cell population, identified in part by a lack of expression of lineage markers (Lin^{neg}), Mac1 (CD11b), Gr1, CD45R, B220, Ter119, CD4, CD8, in combination with positive Sca1 and c-Kit expression [52, 53]. ESLAM cells are an even more HSC-enriched population, with about 50% of cells exhibiting this immunophenotype representing LT-HSCs as determined by functional assays [4]. Lineage staining must be used with caution on embryonic HSCs as they have been observed to express Mac1 [17].

In addition to cell surface markers, the use of green fluorescent protein (GFP) driven by a relevant promoter or enhancer is a key tool in identifying HE cells undergoing EHT. Both *Runx1* and the surface marker Sca1 have been shown to be important for the process of EHT through the use of GFP to label proteins [25, 46, 54]. Mice are generated which express transgenes that contain coding sequence for GFP under the control of promoters or other regulatory sequences of the gene of interest. Ng *et al.* created a transgenic mouse containing a fusion gene linking a minimal heat-shock promoter, which was activated by the binding of transcription factors (TFs) to the sequence unique to an intronic enhancer of *Runx1*, resulting in the transcription of GFP fused to this enhancer sequence [46]. This enhancer's activity, through the expression of GFP, was found to be present in endothelial cells of the DA undergoing EHT [46]. However this enhancer was not active in all endogenous *Runx1* expressing cells, such as non-hematopoietic neuronal tissue, and mesoderm [46]. Sca1 marks the surface of HE cells within the DA at E10.5-E11.5 [25]. Using a transgene containing GFP driven by regulatory elements of *Ly6a*, the gene coding for Sca1 surface expression, the population of cells expressing this gene doubled. This

population of *Ly6a*-expressing cells was found to contain LT-HSCs, identifying a larger pool from which HSCs develop than by Sca1 surface expression alone [25, 54].

For the purposes of this thesis, I will refer to cells expressing CD31 or VEC on their surface as endothelial cells. The specific population of *Runx1*-expressing endothelial cells in E9.5 embryos will be referred to as pre-HE, and mature HE at E10.5 as HE. HE cells at E10.5 which have acquired surface expression of c-Kit will be referred to as cluster cells, as these cells are often present within intra-aortal clusters of the DA. Any cells within the embryo marked by CD45 expression will be referred to as hematopoietic cells.

1.2.2 Whole Organ *Ex vivo* Culture

HE cells undergoing EHT are located within a heterogeneous environment, exposed to signals from surrounding non-endothelial cells. All the necessary conditions for EHT to occur exist within the embryo itself. Many groups use whole organ culture, allowing the isolation of a specific organ such as the DA, to interrogate genes or inhibitors of hematopoietic development. This process does not include sorting or isolation of a particular cell population of interest, only isolating an organ of interest which contains multiple heterogeneous cell types. Medvinsky and Dzierzak were the first to use this technique when identifying HSC production in the AGM, culturing whole E10.5 DAs on a stainless steel filter mounted at the air-liquid interface [28, 55]. Cells were cultured in myeloid long-term media, without the addition of cytokines. After a short culture period, DAs were dissociated and transplanted into irradiated adult recipients [28, 29]. 24 of 27 recipients engrafted successfully with fetal HSCs when they received these E10.5 DAs which had been cultured prior to transplantation [28, 29]. This is a much higher proportion of positively engrafted recipients than when E10.5 DAs were transplanted directly without culture, which resulted in the successful engraftment of only 3 of 96 recipients [28, 29].

In addition to signals received by cells from neighbouring tissues, exogenously added cytokines show an effect on the transplant outcomes of cells cultured under such conditions. E11.5 DAs which were cultured in the presence of Interleukin 3 (IL-3) were found to engraft at a higher level, supplying more HSCs to recipient mice [55]. Embryos containing only one functional allele of *Runx1* display a reduction in HSC number due to this haploinsufficiency [55]. The addition of IL-3 to the culture media of E11.5 *Runx1*$^{+/-}$ DAs was found to rescue the negative effect of *Runx1* haploinsufficiency on HSC numbers [55]. These effects were not observed in whole DAs cultured with the addition of other cytokines tested, granulocyte macrophage-colony stimulating factor (GM-CSF), SCF, Oncostatin M (OSM), or basic Fibroblast Growth Factor (bFGF) [55].

1.2.3 *Ex vivo* Cellular Co-culture

When attempting to culture small HE cell populations capable of generating HSCs, it is important to provide supportive cells to approximate the *in vivo* niche. During development, HE cells are supported by stromal cells, including vascular endothelial cells lining the DA, and mesenchymal cells surrounding it [17]. OP9 cells are a feeder cell line which support hematopoietic cell growth *ex vivo*. This cell line was originally isolated from the *Op/Op* mouse strain which does not produce functional macrophage-colony stimulating factor (M-CSF) cytokines [56]. As the lack of M-CSF avoids promotion of macrophage development in culture, OP9 cells have been used for embryonic stem (ES) cell differentiation and embryo-derived hematopoietic organ culture [56, 57]. Besides the supportive niche created by feeder cells, the addition of cytokines in the cell culture media can be critical for providing signals to specific cell populations.

As was recognized with the use of OP9 cells lacking the production of M-CSF, cytokines are of critical importance in determining the outcome of a culture assay. IL-3 has been identified as a downstream target of Runx1 [55]. In addition to IL-3, SCF, Erythropoietin (EPO), and granulocyte-colony stimulating factor (G-CSF) are all commonly used to culture populations of cells isolated from early time-point DAs (E9.5-E11.5) [42, 58, 59]. The c-Kit receptor, which is expressed on early hematopoietic cluster cells, is activated by its ligand mSCF, allowing important interactions between hematopoietic cells and their niche [42, 47, 60]. EPO is required by erythroid progenitors, specifically definitive erythrocyte progenitors in the FL [61]. mG-CSF, was purified from mouse lungs, separately from GM-CSF in 1983, and stimulates the growth of granulocytes *ex vivo* [62]. bFGF is another mammalian growth factor which has been used in the *ex vivo* culture of E7.5 embryos [63, 64]. bFGF is thought to be important specifically for stimulating endothelial cells, and for sustaining human ES cells in culture [63, 64].

The cross reactivity potential of some cytokines allows the use of human-derived factors, in the *ex vivo* culture of mouse tissues and cell populations. IL-3 ligand does not cross react between species when binding to its receptor IL-3Rα, so mouse IL-3 must be used in the culture of mouse cells [35]. This is somewhat the case for SCF as hSCF is a relatively weaker stimulant of the mouse kit receptor [42, 47, 60]. hEPO, hG-CSF, and hbFGF are all active on the cognate mouse receptor, so they may be used in the culture of mouse tissues [61, 62, 64].

Changes in culture conditions can also affect the development of cells *ex vivo*. Mouse embryos develop in the genital tract at an O_2 tension of 2. 5-5% and mouse blastocysts have been observed to develop optimally at 5% O_2 [65]. Furthermore, the production of hypoxia-induced cytokines such as vascular endothelial growth factor (VEGF), EPO and bFGF by endothelial cells and fibroblasts is stimulated by exposure to low O_2 tensions [66-69]. The

culture of embryonic hematopoietic cells often takes place in atmospheric conditions, at 20% O_2. A recent study by Borges *et al.* used a technique whereby they cultured mesodermal precursors from E7.5 embryos at 5% O_2 to assay endothelial cell development, and 20% O_2 to assay hematopoietic development [63]. The culture of cells at 5% O_2 was said to be crucial for endothelial cell growth and development from cells of this earlier developmental stage [70].

1.2.5 Colony-forming Cell Assays

Colony-forming cell (CFC) assays are commonly used to determine the number and type of hematopoietic progenitors contained in a test cell population [71, 72]. Single cells are plated in semi-solid media containing hematopoietic cytokines, to constrain their progeny spatially into separate colonies, allowing the identification and quantification of the input CFCs. In the context of embryonic hematopoiesis, CFC assays are commonly used to determine differences in the number of hematopoietic progenitors produced by gene-targeted embryos, or phenotypically isolated cell populations of the DA at E11.5 or FL at E14.5 [17, 25]. CFC assays are not as meaningful when studying early time-points of EHT, as endothelial cells do not differentiate into hematopoietic colonies in this assay.

1.2.6 Embryo Derived HSC Transplantation

Due to differences in the properties of HSCs found at different embryonic time-points, cells isolated from embryos during development differ in their capacity to fulfill the functional requirement of HSCs. The first HSC capable of long term adult engraftment is found in the DA at E10.5 at a frequency of about 1 HSC per embryo [29]. Medvinsky *et al.* found that a whole organ culture period of 2-3 days greatly increased the number of HSCs present at E10.5, measured by engraftment in adult recipients [28]. Even cells isolated from embryos as young as E8.5 were capable of engraftment in irradiated adult recipients after culture [15]. It is thought

that culture allows the acquisition of additional properties needed for pre-HSCs to engraft in an adult recipient. The transplantation of cells into myeloablated neonates which have been conditioned with sub-lethal exposure to busulfan *in utero*, allows a more efficient detection of HSC potential in fetal cell populations [15, 31, 39]. These conditioned neonates allow the long-term engraftment of E9.5 and E10.5 pre-HSCs [15, 31, 39]. HSCs within the DA rely on blood circulation to migrate downstream to the FL. This passive migration is in contrast to homing mechanisms used by adult HSCs to locate the bone marrow niche, which fetal HSCs may not possess at this time [30]. To overcome this possible homing defect, it has been shown that direct transplantation of E10.5 pre-HSCs to the bone marrow can increase their engraftment in adult recipients [30]. Finally, immunocompromised recipients may be used to avoid the rejection of donor cells by the host immune system [15, 73]. Fetal cells may be targeted by NK cells due to the lack of major histocompatibility complex (MHC) I markers on E9.5-E10.5 fetal pre-HSCs [15, 73]. $Rag2^{-/-}\gamma C^{-/-}$ mice which have deficiencies in B, T and NK cells, allow the engraftment of these pre-HSCs despite their lack of MHC I "self" signals [15]. All of these assays provide powerful tools for interrogating the many genes involved in embryonic hematopoiesis.

1. 3 Genes Involved in Embryonic Hematopoiesis

1.3.1 Runt-related Transcription Factor 1 – *Runx1*

Runx1, also known as acute myeloid leukemia 1 (*AML1*), or core-binding factor alpha 2 (*CBFα2*), and its binding partner core-binding factor beta (*CBFβ*) are two of the most commonly rearranged genes in human leukemia [74]. Okuda *et al.* generated embryos homozygous for *Runx1* exon 5 deletion, $Runx1^{-/-}$, to interrogate normal gene function of *Runx1*, and found that the embryos died from E11.5- E12.5 [75]. These mice exhibited defects in definitive

hematopoiesis, but maintained the ability to produce primitive blood cells in the YS [75]. Other groups looked specifically at the expression of *Runx1* in mid-gestation embryos, and examined the effect of *Runx1* loss on intra-embryonic hematopoiesis. *Runx1* was observed to be expressed in all the major sites of hematopoiesis in the embryo through development [19]. *Runx1* expression was present at E7.5 in the neural plate, endoderm and mesoderm, followed by the YS at E8.0-E8.5, E10.5 in the AGM, VA, UA, and E11.5-E14.5 in hematopoietic cells of the FL [19]. Runx1$^{-/-}$ embryos displayed a lack of intra-aortal clusters in the E11.5 AGM, showed no circulating Runx1^{pos} cells, and their FL lacked Runx1^{pos} cells [19].

The temporal role of *Runx1* in hematopoiesis has been interrogated using Cre/Lox technology, allowing for Cre-mediated excision of loxP flanked *Runx1* in either VEC^{pos} endothelial cells, or Vav1^{pos} pan-hematopoietic cells [26]. 65% of embryos lacking both copies of *Runx1* in VEC^{pos} endothelium died by E11.5-E12.5, and showed a significant decrease in the number of c-Kit^{pos} clusters in the AGM at E10.5 [26]. At E12.5 10% of embryos showed hemorrhaging of the nervous system coupled with pale FLs, a phenotype congruent with full Runx1$^{-/-}$ null mice [19, 26]. In contrast, embryos containing *Vav-Cre* did not exhibit a significant difference in fetal viability as compared to controls [26]. *Vav-Cre* was found to be expressed in CD45^{pos}VEC^{neg} hematopoietic cells and not CD45^{neg}VEC^{pos} endothelial cells at E11.5 [26]. Embryos lacking both copies of *Runx1* in Vav1^{pos} cells instead showed an increase in the number of CFCs in the E15.5 FL [26]. This suggests that the lack of Runx1 expression in Vav1^{pos} cells causes a change in the maintenance but not generation of hematopoietic progenitors [26]. Adults homozygous for the deletion of *Runx1* in Vav1^{pos} cells showed no difference in survival or LT-HSC function when compared to wild-type controls in marrow transplant experiments, confirming the importance of *Runx1* in HE [26].

As Runx1 is expressed in other non-hematopoietic cells such as neurons and mesoderm, looking closer at its regulation has given us clues about its specific role in embryonic hematopoiesis. *Runx1* is controlled by both distal, and proximal promoters in mice and humans (Figure 1.3A) [37, 76]. Isoforms of human *RUNX1* and mouse *Runx1* that are driven by these promoters vary due to differences in alternative splicing of exon 7 and 6 respectively (Figure 1.3A and B) [77]. There are 5 isoforms of *Runx1* that have been identified in mice (Figure 1.3A) [77]. The distal promoter produces two isoforms termed *Runx1cEx6+* and *Runx1cEx6-* [77]. *Runx1cEx6+* contains all 8 exons of *Runx1* and is an orthologue of human *RUNX1c*. *Runx1cEx6-* possesses 7 exons, omitting exon 6 [77]. The proximal promoter generates 3 isoforms, *Runx1bEx6+*, *Runx1bEx6-* and *Runx1bEx6e* [77]. *Runx1bEx6+* lacks exons 1 and 2, is an orthologue of human *RUNX1b*, and *Runx1bEx6-* lacks these first two exons in addition to exon 6 [77]. The shortest transcript *Runx1bEx6e* is 4 exons long, lacking the first and last two exons, although it contains an extended exon 6 [77].

Both the distal and proximal promoters have been shown to be active in the mid-gestation embryo of mouse and human, however identification of an enhancer located between the distal and proximal promoters has allowed us closer examination of the role of *Runx1* in HE [37, 46, 76, 78]. This single enhancer, termed the +23 or +24 conserved non-coding enhancer (CNE), was identified by two separate groups [46, 78]. Using retroviral integration site mapping to identify this conserved enhancer of *Runx1*, Dr. Motomi Osato's lab, created a fusion protein consisting of minimal heat shock promoter 68 (hsp68) followed by the +24mCNE sequence, and finally the sequence for GFP (Figure 1.3C) [46]. Expression of this enhancer in the embryo recapitulated the timing and sites of HE cell development [46]. +24mCNE was first expressed in the YS at E8.0-E8.5, and then later in E10.5 UA, VA, YS, and DA [46]. The expression of

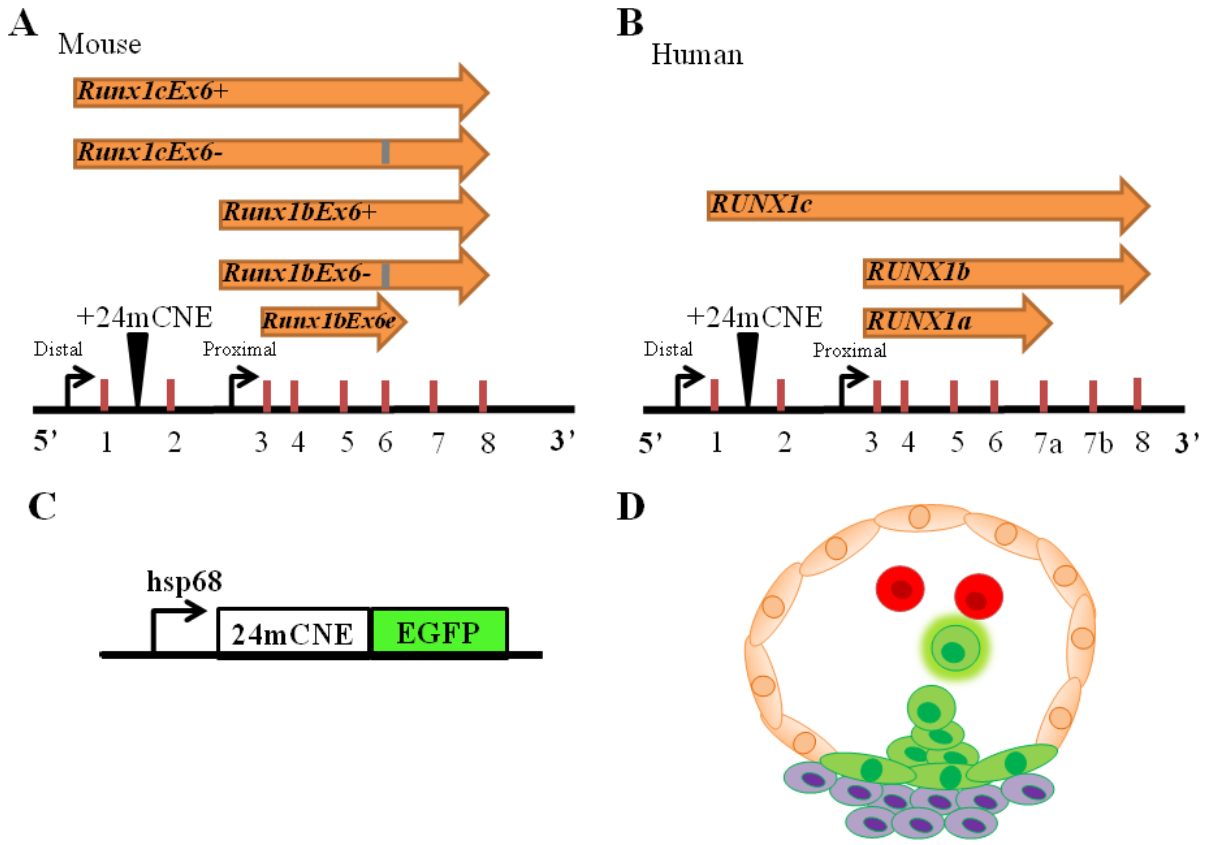

Figure 1.3 Comparison of mouse *Runx1* and Human *RUNX1* isoforms and +24mCNE transgenic mouse model

Diagram of mouse *Runx1* and human *RUNX1* with endogenous promoters shown as black arrows and exons shown as red bars. +24 conserved non-coding enhancer represented by black wedge [78]. Isoforms displayed as orange arrows spanning exons included in each transcript. Adapted from Komeno *et al.* [77]. A) Mouse *Runx1*, lack of exon 6 in alternatively spliced isoforms shown by grey bar. B) Diagram of human *Runx1*with 3 major isoforms shown. C) Diagram of the +24mCNE-GFP transgene containing minimal heat-shock promoter 68 (hsp68) followed by +24mCNE sequence and EGFP fusion. D) Cross section of E10.5 DA displaying non-HE cells in peach, Runx1+24mCNE-GFP expressing endothelial cells in green, hematopoietic stem cell in green glow, and red cells as differentiated blood cells no longer expressing Runx1+24mCNE-GFP. Mesenchymal cells surrounding DA in purple. Adapted from Ng *et al.* [46].

+24mCNE was also observed in LSKs isolated from adult bone marrow, and this population exhibited higher engraftment in transplant experiments [46]. Most importantly, the enhancer was not active in differentiated hematopoietic cells, only marking HE and primitive stem cells (Figure 1.3D) [46].

The role of *Runx1* in HE was critical in the development of tools to study EHT. The generation of transgenic mice allowing the identification of cells expressing the +24mCNE-GFP enhancer, allows the prospective identification of a more refined population of HE cells. The lack of clear definitive HE surface markers had previously prevented researchers from looking closer at the subpopulation of endothelial cells undergoing EHT. *Runx1* has also been shown to interact with another important signalling pathway in development, Notch [79-81]. *Runx1* has been observed to be down-regulated in the absence of Notch signalling, and its enforced expression rescues hemogenic function in E9.5 Notch1$^{-/-}$ DAs [79-81].

1.3.2 *Notch1*

The Notch signalling pathway is well known for its role in development, allowing organ specification in developing cells [82, 83]. *Notch1* expression has been identified in LSKs, and has been suggested to be important in EHT [80, 84]. Notch1$^{-/-}$ embryos appear to be stunted at E9.5 and none survive beyond E10.5 [85]. When examining hematopoietic development in Notch1$^{-/-}$ embryos, cultured E9.5 DAs showed a decrease in hematopoietic cell growth, and a decrease in CFC numbers when cultured cells were transferred to semisolid media [80]. However, primitive YS progenitors from Notch1$^{-/-}$ embryos still generated CFCs [80]. mRNA analysis showed that *Runx1* along with many other hematopoietic genes were down-regulated in Notch1$^{-/-}$ embryos, but no difference was observed in angiogenesis associated genes [80]. This

suggests that the role of *Notch1* in the endothelium is critical for hematopoietic development in the embryo at this time.

In contrast to its role in definitive hematopoiesis, Notch signalling is not necessary for primitive blood cell production [86]. Hadland *et al.* studied the relative contribution of both wild-type ES cells expressing *Notch1*, as well as ES cells with targeted deletion of Notch1$^{-/-}$ to a chimeric embryo during development [86]. Notch1$^{-/-}$ cells were observed contributing to early progenitors in the YS, and were present later in the E13.5-14.5 FL [86]. No LT-HSCs which arose from Notch1$^{-/-}$ cells were present in the bone marrow of adult mice, although they were present in other non-hematopoietic organs [86]. Based on the lack of Notch1$^{-/-}$ cells in definitive hematopoietic tissue of the embryo, Notch signalling is thought to differentiate between the primitive and definitive waves of hematopoiesis in the mouse embryo [86]. This distinction has also been observed in zebrafish models [87].

Another method to investigate the role of Notch signalling in hematopoiesis involves the culture of cells with γ-secretase inhibitors (GSI), such as DAPT (N-[N-(3,5-Difluorophenacetyl)-L-alanyl]-S-phenylglycine t-butyl ester) and DFPAA ((2S)-2-([(3,5-Difluorophenyl)acetyl] amino)-*N*-[(3S)-1-methyl-2-oxo-5-phenyl-2,3-dihydro-1*H*-1,4-benzodiazepin-3-yl]propanamide) [83]. These compounds prevent Notch cleavage, which normally allows the release of its intracellular domain, and downstream signalling by the molecule (Figure 1.4) [83]. Richard *et al.* measured the effect of DAPT in E9.5 DA culture [88]. With the addition of DAPT, CD45^{pos} cells produced by the organ *ex vivo* briefly increased, and then underwent apoptosis [88]. This lead to a trend of decreased CD45^{pos} cell counts in wells treated with DAPT, though this effect was not significant [88]. Additionally, DAPT treated wells produced fewer progenitors when cultured in CFC assays following *ex vivo* whole organ culture [88].

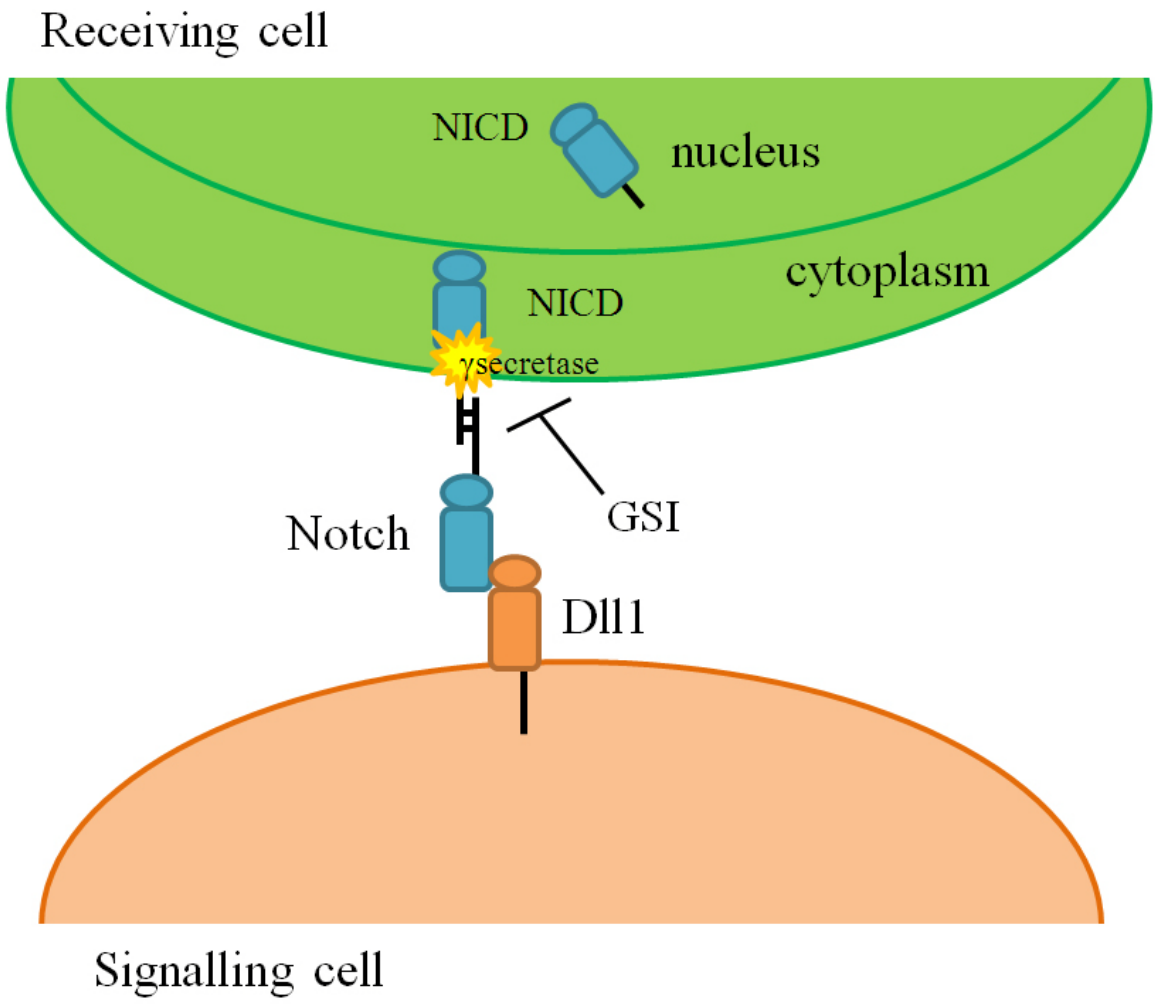

Figure 1.4 Notch signalling between endothelial cells

Diagram shows Notch receptor receiving signal from delta-like-ligand 1 (Dll1) causing cleavage of Notch intracellular domain (NICD) by γ-secretase, resulting in translocation to nucleus for further downstream signalling. γ-secretase inhibitors (GSI) such as DAPT inhibit activity of γ-secretase, preventing cleavage of the NICD and blocking notch signalling. Inhibition of Notch by GSI represented by T.

1.3.3 Growth Factor Independent 1/1b - *Gfi1* and *Gfi1b*

Adding to the network of genes involved in EHT, just as Notch$^{-/-}$ embryos show a decrease in *Runx1* expression, embryos lacking *Runx1* show a decrease in *Gfi1* and *Gfi1b* expression [89]. As is the case for mouse models lacking genes important for definitive hematopoiesis, embryos deficient in *Gfi1* and *Gfi1b* expression die during mid-gestation from E11.5- E12.5 [89]. These embryos show a decrease in erythrocyte counts as early as E8.5 in the YS, though colonies are formed in CFC assays at this time [89]. However at E10.5 no colonies are produced in CFC assays using cells isolated from the embryo proper [89]. CD41^{pos} cluster cells in the DA at E9.5 maintain early hematopoietic and endothelial gene expression at higher levels than wild-type cells which down-regulate these HE-associated genes at this time [89]. Therefore, it is hypothesized that *Gfi1* and *Gfi1b* suppress endothelial gene expression, and allow hematopoietic cluster development [89]. This capacity for encouraging cluster development was tested in Runx1$^{-/-}$ embryos which do not produce clusters [19]. Enforced expression of *Gfi1* and *Gfi1b* did not rescue cluster formation in Runx1$^{-/-}$ embryos [89]. *Gfi1* and *Gfi1b* are important for primitive erythrocyte development, as well as in EHT in the down-regulation of endothelial gene expression.

1.3.4 Sry Related High Mobility Group Box Protein 17 – *Sox17*

Sox17 is expressed in the endoderm and embryonic vasculature [90]. *Sox17* has been used to identify a population of ES cells which produced definitive progenitors in differentiation culture [91]. Clarke *et al.* recently identified *Sox17* as a candidate regulator of EHT [90]. Using mice which contain one allele of *Sox17* replaced with the coding sequence for GFP, both E10.5 endothelial cells and intra-aortal clusters were found to express *Sox17* [90, 92]. When cells were sorted from E11.5 embryos on the basis of *Sox17* expression, only double-positive

VEC^{pos}Sox17-GFP^{pos} cells showed engraftment in irradiated adult recipients [90]. Overexpression of *Sox17* in CD45^{lo}c-Kit^{hi} cells isolated from E10.5 embryos showed increased *Runx1* and *CD31* mRNA expression compared to controls [93]. In co-culture with OP9 cells *Sox17*-overexpressing cells generated fewer CD45^{pos} cells compared to un-transduced controls [93]. *Sox17* is thought to play a role in impairing hematopoietic differentiation, and supporting HE, and hematopoietic cluster maintenance [93]. When determining the relationship between *Sox17* and other known regulators of EHT, mouse ES cells lacking *Sox17* showed a decrease in *Notch1* expression [90]. No change was detected in *Runx1* or *Hoxa3* expression in these *Sox17* null ES cells [90].

1.3.5 Homeobox A3 - *Hoxa3*

Hoxa3 was found to play a suppressive role in EHT, encouraging cells to maintain an endothelial state [94]. The opposing activities of *Runx1* and *Hoxa3* are mirrored in their mutually exclusive expression beginning at E8.5, where *Runx1* is expressed in the YS and *Hoxa3* is expressed in the embryo [94]. Later at E10.5 *Hoxa3* is lost in the aortic endothelium and *Runx1* expression increases [94]. When *Hoxa3* expressing cells isolated from E10.5 AGM were cultured in OP9 cell co-culture, these cells produced fewer CD41^{pos} and CD45^{pos} cells and expressed *Hoxa3* in adherent cells [94]. Previous experiments by Iacovino *et al*. have shown that *Hoxa3* functions upstream of *Sox17*, leading to its upregulation upon *Hoxa3* overexpression in ES cells [94]. The repressive role of *Hoxa3* was found to be overcome by overexpression of *Runx1*, leading to *Sox17* repression [94]. This situates *Hoxa3* as maintaining endothelial identity in arterial endothelial cells, up until a certain level whereby it switches on *Sox17* expression, to allow cluster development [94]. The expression of *Runx1* is then able to override this process and allow hematopoietic development by down regulating *Sox17* in cluster cells [94]. This work, in

combination with our knowledge of the roles of *Runx1* and *Sox17* in EHT, identifies *Hoxa3* as both critical for HE development, while acting as a repressor of EHT in the embryo.

1.3.6 Myeloid Ecotropic Viral Integration Site 1 - *Meis1*

Although originally identified in a murine model of leukemic transformation, *Meis1*, like *Runx1*, is also expressed in acute myeloid leukemia (AML) patient samples [95, 96]. *Meis1* contains a homeobox binding domain, allowing it to bind DNA and interact with members of the Hox and Pbx families as a cofactor in Hox DNA binding [95-99]. As there are 39 Hox family members, but only 3 Meis proteins, loss of function studies examining the role of Hox proteins in hematopoiesis can be clouded due to their redundancy [100]. Instead the investigation of Meis1 in hematopoiesis may draw similar conclusions as to the role of Hox proteins in this process [100]. In normal mouse hematopoietic tissue, *Meis1* was found to be most highly expressed in primitive $Lin^{neg}Sca1^{pos}$ HSC-containing cell populations, isolated from E14.5 FL and adult bone marrow [98]. In contrast *Meis1* is nearly absent upon differentiation into progenitor populations expressing lineage markers [98].

Given its role in normal and leukemic hematopoiesis, *Meis1* has also been interrogated for its role in embryonic hematopoiesis, through the examination of embryos deficient for the gene [98, 100]. *Meis1* is expressed in the HSC compartment of the FL, in the mesenchyme, endothelium, and clusters of the AGM [100]. Embryos lacking *Meis1* die with hemorrhaging in the neural tube and trunk from E11.5-E14.5 [100]. Hematopoietic organs are underdeveloped and show low CFC content [100]. Along with its delayed or reduced development, hematopoietic clusters in the DA, UA and VA are decreased in size and number, and *Runx1* expression is nearly absent [100]. While these $Meis1^{-/-}$ null embryos show defects in hematopoiesis, further work must be done to determine the specific stage at which *Meis1* is important in EHT. *Meis1*

may be important in the endothelium as in the case of *Hoxa3*, in cluster formation like *Sox17*, or throughout the process as *Runx1* [26, 90, 94] (Figure 1.5). Additionally, the known interactions between Meis1 and Hox proteins involved in the development of endoderm, and body plan specification of the embryo, could be affected by pan-deletion of *Meis1* [99]. Defects in structural development of the embryo could lead to non-specific effects on HSC niches like the FL [99]. The use of a conditional mouse model, restricting *Meis1* deletion to the endothelium, is important in determining the role of *Meis1* in EHT.

1.4 Scope, Hypothesis and Aims of Present Study

HSCs are crucial to the long term survival of an organism, providing mature blood cells, which transport nutrients and O_2, and protect our bodies from infection. Commonly mutated genes in AML such as *Runx1* are crucial for both normal HSC development as well as in the progression of leukemia. Knowledge about the development of HSCs will allow us to think critically about *ex vivo* methods of HSC generation to supplement the clinical need for transplantable HSCs. Micro-environmental conditions and genes involved in HSC development may be used to expand transplantable HSCs *ex vivo*, or generate them *de novo* from a patient's cells. As morphology changes rapidly throughout development, and access to mid-gestation human embryos is limited, mouse embryos provide a useful model for this work. By elucidating TFs important early on in the process of EHT, from endothelial cell to hematopoietic cluster formation, our work gives support to research involving the direct conversion of endothelial cells to HSCs.

We hypothesize that Meis1, a TF up-regulated in E10.5 HE, is important for EHT in the mouse DA at E9.5 and that knockdown through Cre-mediated excision of *Meis1* in VEC-expressing endothelial cells will result in defects in hematopoietic cell development.

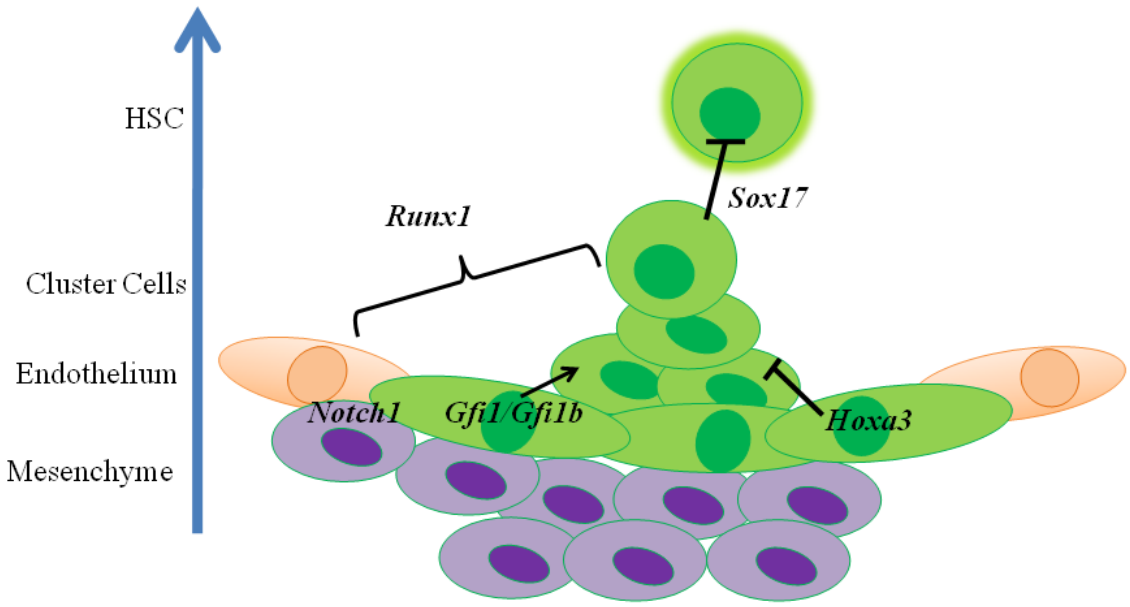

Figure 1.5 Known regulators in hematopoietic cluster formation and EHT

Simplified diagram depicting the spatial roles of *Hoxa3, Runx1, Sox17, Gfi1/Gfi1b* and *Notch1* signalling in EHT of a hematopoietic cluster in E10.5 DA. Expression of *Runx1* is thought to be downstream of *Notch1* signalling which occurs in the endothelium and surrounding mesenchyme [80, 101]. *Runx1* is important throughout the process of EHT from HE specification to cluster formation and maintenance, causing upregulation of downstream genes *Gfi1/Gfi1b* which are important for cluster emergence [88, 89, 102]. This is in contrast to *Hoxa3* expression which inhibits cluster formation in the endothelium, and interacts with *Sox17* which maintains cluster cell identity at the cost of HSC emergence controlled in part by *Sox17* [90, 94]. Blue arrow indicates progression of EHT from basal cell layers to HSC at the terminus of a cluster. Black arrows, and bracket indicate region of importance for indicated gene in EHT (ie. cluster formation or HSC emergence), and inhibition represented by T. Purple cells indicate mesenchymal cell layer, peach cells indicate vascular endothelium, green cells indicate *Runx1* expressing HE and cluster cells, glowing cell indicates HSC.

Aim1: To establish a reproducible *ex vivo* cellular co-culture assay to allow EHT to progress in E9.5 HE cells isolated from mouse DAs

HE cells from E9.5 Runx1+24mCNE-GFP transgenic DAs were isolated by FACS and cultured in an OP9 co-culture system based on a combination of assays from the literature. This assay allows EHT to progress *ex vivo*, and hematopoietic development of these cells was determined through the use of flow cytometry for the acquisition of hematopoietic markers. Inhibitors of this process were introduced to modulate this process in our *ex vivo* system.

Aim 2: To identify transcription factors up-regulated in HE and define the role of *Meis1* in EHT in the DA

Bulk endothelial cells were sorted from E10.5 wild-type DAs, and Runx1+24mCNE-GFP depleted endothelial cells were sorted from E10.5 DAs isolated from transgenic littermates. RNA-seq was carried out for both populations, which were then compared to infer expression of genes in Runx1+24mCNE-GFP expressing HE cells. Up-regulated TFs were identified from this comparison, and the TF Meis1 was chosen for further examination. The manipulation of *Meis1* expression in endothelial cells of the E9.5 DA was accomplished through the use of a conditional mouse model, containing Cre-mediated excision of *Meis1* in VEC-expressing endothelial cells. E9.5 DAs were cultured in our *ex vivo* assay to validate the role of *Meis1* in EHT.

2. Methods

2.1 Transgenic Mice

2.1.1 Runx1+24mCNE-GFP Transgenic Mouse

Runx1+24mCNE-GFP mice were generously provided by Dr. Motomi Osato [46]. These mice were crossed with wild-type C57BL/6J mice to generate a colony of mice heterozygous for the transgene. Heterozygous mice were crossed together, or with wild-type mice in timed matings. These crosses generated both wild-type embryos, and those containing the Runx1+24mCNE-GFP transgene. Transgenic Runx1+24mCNE-GFP expressing mice were identified with the genotyping primers F-EGFP 5'-CACATGAAGCAGCACGACTT-3' and R-EGFP 5'-TGCTCAGGTAGTGGTTGTCG-3'. This transgenic mouse allowed for the identification of HE cells identified by expression of the +24mCNE intronic enhancer through the expression of GFP.

2.1.2 Meis1$^{fl/fl\ VeCre}$ Transgenic Mouse

Homozygous floxed *Meis1* mice (*Meis1*$^{fl/fl}$) containing loxP sites flanking exon 8 were generously provided by Dr. Keith Humphries. These mice were originally generated by Drs. Nancy Jenkins and Neil Copeland [103]. These parental F_0 mice were crossed with *VeCre* mice originally generated by Drs. Xiaoyan Jiang and Connie Eaves (Figure 2.1). *VeCre* mice contain Cre recombinase under the control of the VEC promoter. The first generation (F_1) mice heterozygous for *Meis1*$^{fl/fl}$ and *VeCre* were crossed again with *Meis1*$^{fl/fl}$ parental mice or F1 heterozygotes. This allowed for the generation of embryos containing both copies of *Meis1* exon 8 flanked by loxP sites, allowing Cre mediated excision of exon 8, and lack of *Meis1* expression

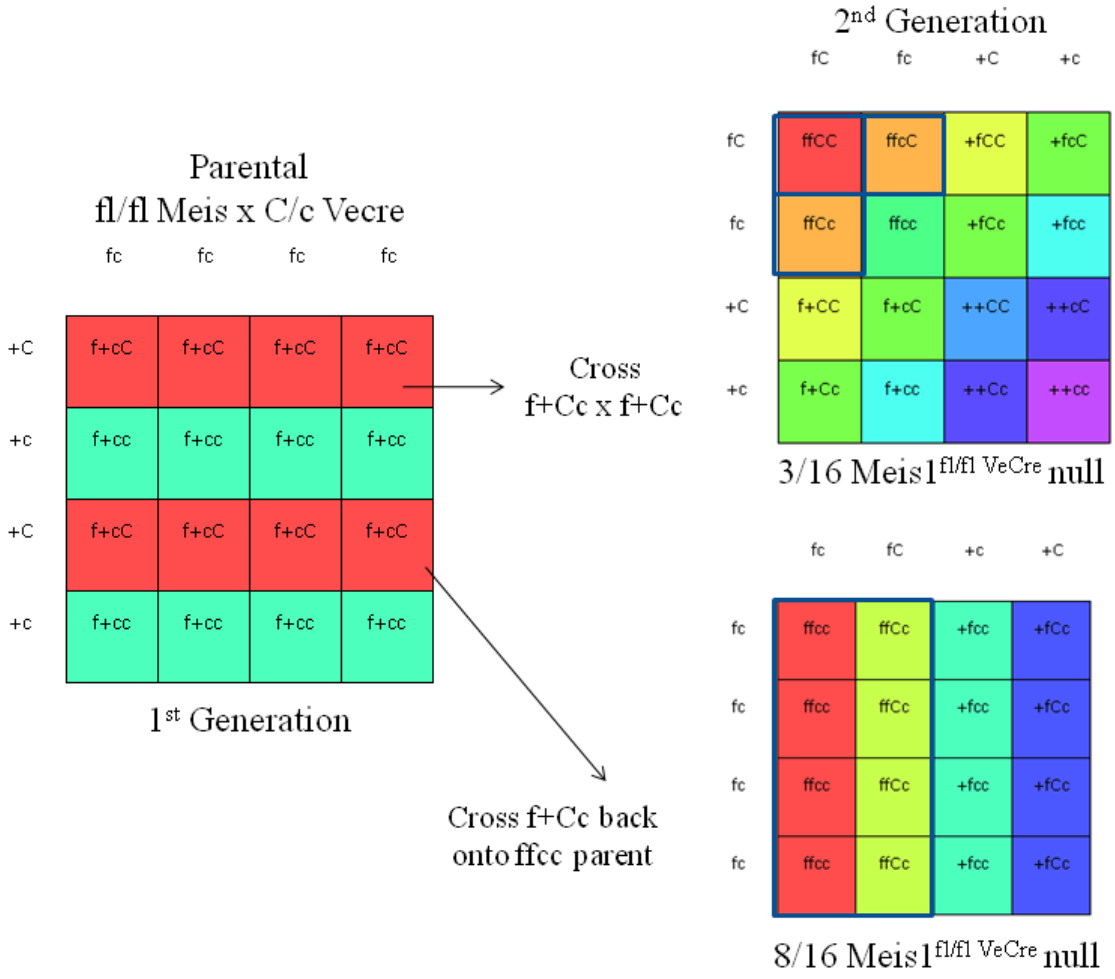

Figure 2.1 Mating scheme to generate *Meis1*$^{fl/fl\ VeCre}$ null embryos

Mating scheme showing initial cross of mouse homozygous for Meis1 fl/fl (ff) crossed with mouse Heterozygous for VeCre (Cc). f = floxed; + = wild-type Meis1 exon 8; C = VeCre; c = lacking Cre recombinase. First generation mice were either crossed back onto parental Meis1$^{fl/fl}$ mouse, or two first generation mice heterozygous for floxed Meis1 exon 8 and VeCre were crossed. Meis1$^{fl/fl}$ mice described further in Miller *et al.* [103].

in VEC^{pos} endothelial cells. These matings also generated wild-type littermates lacking *Meis1*$^{fl/fl}$ or *VeCre* expression. Figure 2.1 shows the frequencies of genotypes due to this mating scheme. The deletion of *Meis1* exon 8 results in functional deletion of the protein, as no truncated sequence was identified by southern blot of the parental line [103]. This model of *Meis1* excision allowed us to examine the generation of hematopoietic cells in VEC^{pos} HE which lacked *Meis1* expression.

Meis1 transgenic embryos were genotyped using 4 sets of primer pairs. These primer sequences are shown in Table 2.1 along with annealing sites in Figure 2.2. CreF and CreR primers were used to identify the presence or absence of the *VeCre* transgene. Set F1-R2 amplified the region containing the loxP sites, producing a 440 base pair (bp) product when loxP sites were inserted within the wild-type locus, and a 332 bp product when no loxP sites were present and only wild-type alleles were present (Figure 2.2). Primer set F1R1 was used to confirm the presence of floxed *Meis1* exon 8, or alternately its successful excision, only amplifying when uncollapsed floxed exon 8 was present. Primer set F2R2 was used to detect the presence of collapsed *Meis1* exon 8. The combination of these four sets of primers, including the different product sizes, were interpreted together to determine the genotype of single embryos. See Table 2.2 for a summary of genotyping results. Ambiguous genotyping was repeated, and embryos were excluded if a clear genotype could not be discerned. All primers were synthesized by Integrated DNA Technologies, Inc. (Coralville, IA). For the purposes of this thesis Meis1$^{fl/fl\ VeCre}$ will refer to transgenic litters containing both wild-type embryos and *Meis1*$^{fl/fl\ VeCre}$ null littermates with *Meis1* exon 8 excised in VEC^{pos} cells. All experiments involving animal use are approved by and conform to the guidelines of the Animal Care Committee of the University of British Columbia (Vancouver, British Columbia).

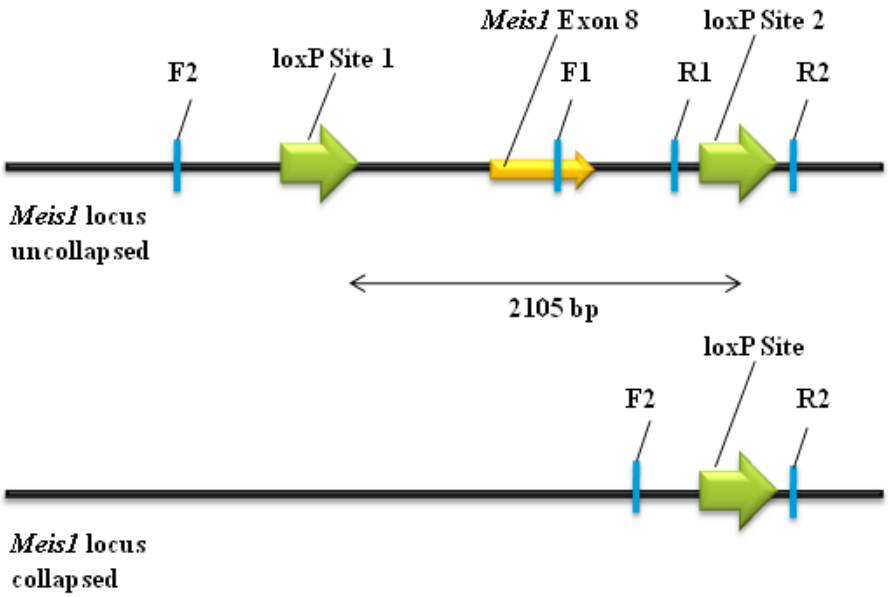

Figure 2.2 Schematic of *Meis1* floxed exon 8 in uncollapsed and collapsed state

Locations of primer binding denoted by F1, F2, R1, R2 (Table 2.1). Exon 8 is represented by yellow arrow. See Table 2.2 for interpretation of genotyping results. Adapted from Miller *et al.* [103].

Table 2.1 Genotyping primers for Meis1$^{fl/fl\ VeCre}$ embryos

	Sequence 5' → 3'
CreF	GTTTCGAATTTACTGACCG
CreR	CGCCGCATAACCAGTGAAAC
F1	CCAAAGTAGCCACCAATATCATGA
R1	GAAGTTATTAGGTGGATCCAAGCT
F2	CATTGACTTAGGTGTATGGGTGTC
R2	AGCGTCACTTGGAAAAGCAATGAT

Table 2.2 Interpretation of Meis1$^{fl/fl\ VeCre}$ genotyping results based on 4 primer sets

Primer set				
Cre	F1R2	F1R1	F2R2	Genotype
No	332	No	No	Wild-type
No	440	Yes	No	Wild-type
No	332 and 440	Yes	No	Wild-type
Yes	332 and 440	Yes	Yes	Heterozygous
Yes	440	Yes	Yes	*Meis1* null

2.2 Timed Matings and Embryo Generation

In order to generate embryos of specific embryonic time-points, timed matings were set up between 2-3 female mice and 1 male stud. Pairs were set up in the evening and the presence or absence of a vaginal plug in the female was determined the next morning. If present, the pregnant female was moved to a separate cage, and the age of the embryos was noted as E0.5. This process was repeated for all timed matings to generate E9.5–E14.5 embryos for sorting, sectioning, and culture experiments.

Staging of embryos was based on somite counts as well as morphological features. At E9.5 embryos have twisted to gain their characteristic fetal shape, and embryos are pale, though the unpaired DAs are visible and contain some blood. Only small forelimb buds are present and the head has not yet formed a prominent forebrain. At E10.5 forelimbs are present and rear limb buds have formed. The eye is translucent, and the head has not fused at the forebrain. At E11.5 both forelimbs and rear limbs have formed, the embryo is more opaque and the DA is visibly

filled with blood. The eye has also gained black pigmentation and the head fold has fused. Only embryos that were staged correctly for each individual experiment were used.

2.3 Embryo Dissection

On the day of each experiment, E9.5-E14.5 days post conception; pregnant females were euthanized with carbon dioxide inhalation followed by cervical dislocation. An incision was made on the abdomen and the uterus containing embryos was removed and placed in phosphate buffered saline (PBS). The embryos were rinsed of excess maternal blood, separated, and each embryo was separately dissected from the uterus, placenta and YS using forceps, in fresh PBS to avoid contamination between littermates. Upon removal of the embryo from the YS, which was collected for genotyping or phenotyping, the embryo was then dissected finely using 30g ½" needles attached to 1 mL syringes (BD Biosciences, San Jose, CA). Dissection varied slightly based on the age and fate of the embryos. To ensure a high number of cells collected when sorting for RNA extraction, more tissue was left intact, including the head vasculature. When embryos were to be used for sorting experiments followed by HE cell culture or library generation, finer dissection of the DA was used (Figure 2.3).

Individually dissected DAs were then moved to individual 1.5 mL microfuge tubes (VWR International, Radnor, PA) or wells of a 96-well plate (BD Biosciences, San Jose, CA) containing PBS + 2% heat inactivated fetal bovine serum (HI-FBS) (Thermo Fisher Scientific, Walton, MA) until all embryos were dissected. As an alternative to genotyping, Runx1+24mCNE-GFP embryos were phenotyped by measuring GFP fluorescence present in embryonic tissues. For phenotyping Runx1+24mCNE-GFP transgenic embryos, extra pieces of embryonic tissue such as the head and YS were collected in parallel to be measured for the presence of GFP by flow cytometry. Transgenic embryos and wild-type littermates were then

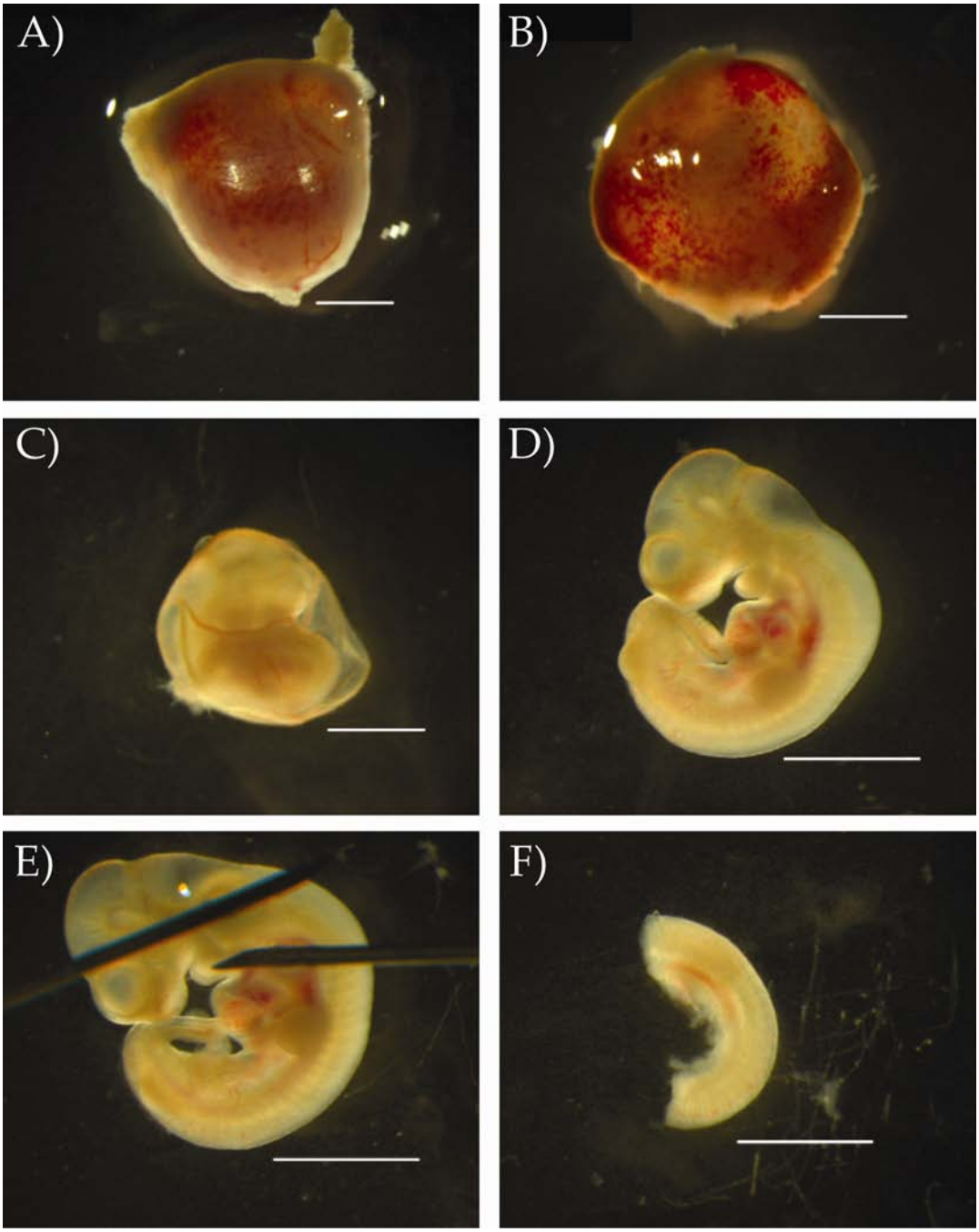

Figure 2.3 Dissection of E10.5 DA

Steps in dissection process to isolate E10.5 DA. A) Embryo in uterine muscle, B) Embryo in deciduum and placenta, C) Embryo in YS, D) Embryo removed from YS, E) Dissection of Embryo with 30g ½" needles, F) DA isolated with somites intact. Scale bar 0.2 cm.

pooled based on their phenotypes. For Meis1$^{fl/fl\ VeCre}$ embryos, no fluorescent cell marker was present, so embryos were processed separately in 1.5mL microfuge tubes (VWR International, Radnor, PA), while YS was collected in PCR strip tubes (VWR International, Radnor, PA) for digestion and genotyping.

2.4 FACS

After dissection was completed for all embryos of the correct age, tissues were dissociated to single cell suspensions. Embryo tissue was enzymatically dissociated in a solution of 1 mg/mL each of Deoxyribonuclease (DNAse) (Sigma-Aldrich, St. Louis, MO) and Collagenase II (Sigma-Aldrich, St. Louis, MO) dissolved in PBS+2% HI-FBS (Thermo Fisher Scientific, Walton, MA) and filter sterilized with a 0.2 μm filter (Thermo Fisher Scientific, Walton, MA). While in this solution embryos were mechanically dissociated first with 200 μL pipette tip (Sardstedt, Sarstedtstraße, DE) and then using a 1 mL syringe with 26g 5/8" needle (BD Biosciences, San Jose, CA). Pipette tips and syringes were rinsed with DNase/Collagenase prior to, and following dissociation. This rinsing solution was then combined with the sample to minimize the loss of cells. If whole DA was to be plated without sorting, dissociated cell suspensions were spun down at 400 RCF for 5 minutes at room temperature (RT), and resuspended in media for plating directly onto OP9 cell monolayers.

If cells were destined for sorting, the dissociated sample was then treated with 6% rat serum for 5 minutes on ice. Following blocking, cells were drawn up into a 1 mL syringe fitted with a 26g 5/8" needle (BD Biosciences, San Jose, CA), and gently filtered over a 40 μm cell strainer (Thermo Fisher Scientific, Walton, MA) into a clean 5 mL polypropylene or polystyrene tube (BD Biosciences, San Jose, CA), drop wise. The strainer was then rinsed with at least two times the volume of the original cell suspension. Filtered cells were spun down at 400 RCF for 5

minutes, and resuspended in 100 – 200 μL of PBS + 2% FBS (Thermo Fisher Scientific, Walton, MA) + 1 mg/mL sterile filtered DNase (Sigma-Aldrich, St. Louis, MO). Cells were then counted and antibodies were added in 1-2 μL of antibody/10^6 cells from titrations done previously. See Table 2.3 for antibodies and concentrations.

Table 2.3 Antibodies, antigens, and concentration for FACS experiments

	Antigen	Volume per 10^6 cells in 100 μL
Phycoerythrin (PE)	SSEA-1, CD31	1 μL
Allophycocyanin (APC)	c-Kit, CD45.2	2 μL
APC-efluor 780 (ApcCy7)	CD45.2	1 μL
Percp-efluor 710	CD31	1 μL
FITC	GFP	1 μL

When sorting for RNA-seq experiments, cells were stained with PE SSEA-1 (eBioscience, San Diego, CA), APC-efluor 780 CD45.2 (eBioscience, San Diego, CA), PerCP-efluor 710 CD31 (eBioscience, San Diego, CA), APC c-Kit (CD177) (eBioscience, San Diego, CA), and gated as shown in Figure 2.4. When sorting for more heterogeneous populations isolated from Runx1+24mCNE-GFP^{pos} embryos, markers PerCP-efluor 710 CD31 (eBioscience, San Diego, CA), and APC c-Kit (eBioscience, San Diego, CA) may have been excluded. When sorting single Meis1$^{fl/fl\ VeCre}$ embryos, cells were stained with PE SSEA-1 (eBioscience, San Diego, CA), APC-efluor 780 CD45.2 (eBioscience, San Diego, CA) and APC VEC (eBioscience, San Diego, CA). Cells were incubated with antibodies for 30 minutes to 1 hour on ice, then stained with 4',6-diamidino-2-phenylindole (DAPI) (Sigma-Aldrich, St. Louis, MO) for viability, before they were sorted in the Terry Fox Laboratory Flow Core Facility on an Influx II (Cytopeia, Seattle, WA) or FACSAria II cell sorter (BD, San Jose, CA). Data was analyzed after the sort using FlowJo software (Treestar, Ashland, OR). After the sort, cells were spun down at 400 RCF for 6 minutes at RT. The supernatant was removed using a 1000 μL pipette, with its tip

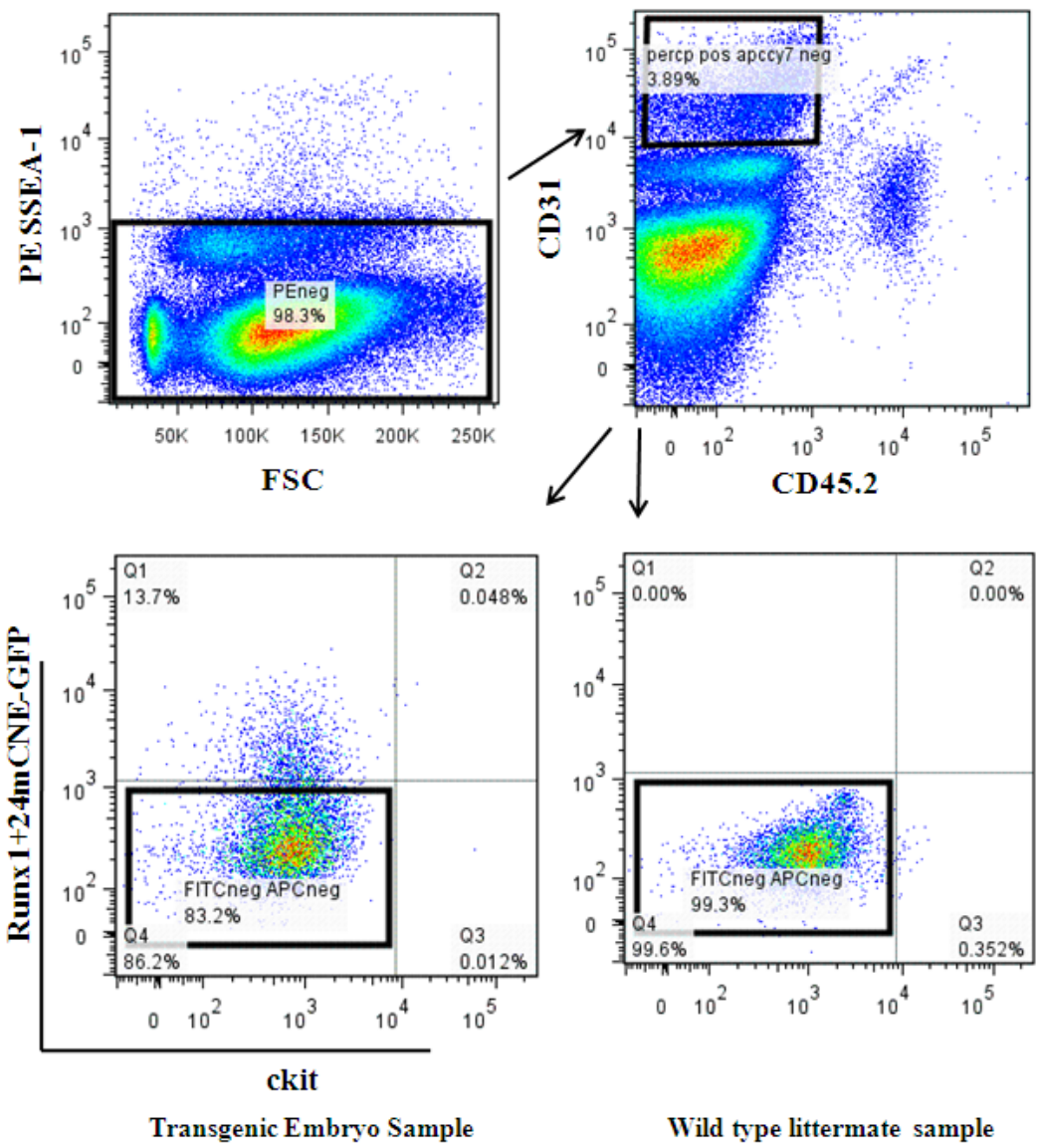

Figure 2.4 Sorting scheme for library construction

Runx1+24mCNE-GFP^{neg} endothelial cells (bottom left) from transgenic Runx1+24mCNE-GFP^{pos} embryos and bulk endothelial cells (bottom right) from wild-type littermates.

connected to an additional 200 μL tip (Sardstedt, Sarstedtstraße, DE) on its end. The cell pellet was then lysed in TriZOL (Invitrogen, Carlsbad, CA) and stored at -80°C, or resuspended in cytokine media for plating in *ex vivo* culture.

2.5 Library Construction

To begin to understand the molecular basis of the differences between endothelial cell subtypes, we first aimed to determine gene expression in HE cells, identified as SSEA-1^{neg}CD31^{pos}c-Kit^{neg}CD45^{neg}Runx1+24mCNE-GFP^{pos} in E10.5 Runx1+24mCNE-GFP transgenic embryos. As the average number of HE cells sorted from embryos with DAs finely dissected is only 50-80 cells per E10.5 transgenic embryo, compared to 150-300 Runx1+24mCNE-GFP negative endothelial cells (SSEA-1^{neg}CD45^{neg}CD31^{pos}c-Kit^{neg}Runx1+24mCNE-GFP^{neg}) per embryo, we chose to use a negative sorting scheme for our libraries. Runx1+24mCNE-GFP negative endothelium, depleted of Runx1+24mCNE-GFP expressing cells, was isolated from transgenic embryos, and bulk endothelium (SSEA-1^{neg}CD45^{neg}CD31^{pos}c-Kit^{neg}) was isolated from wild-type littermates. Following the sort, collected cells were spun down at 400 RCF for 6 minutes, lysed in TriZOL (Invitrogen, Carlsbad, CA), and stored at -80°C until delivery to Canada's Michael Smith Genome Sciences Centre (GSC) Biospecimen core. For more information about library construction see Appendix A.

Following library construction and initial data normalization, RPKM data for both libraries was further analyzed in Microsoft Excel (Microsoft, Redmond, WA). RNA-seq data for bulk endothelial cell and Runx1+24mCNE-GFP depleted endothelial libraries were first refined using an expression cut-off of $\geq$0.3RPKM. Any non-protein coding genes were removed from our list of expressed genes. In order to determine genes up-regulated in HE, differential expression values were calculated by comparing normalized RPKM values for each library. A

cut-off was applied to extract genes exhibiting 1.5-fold change in expression, higher expressed in the bulk endothelial cell library containing HE, as compared to the Runx1+24mCNE-GFP depleted library. 1.5-fold change was used as an alternative to either 2-fold change or a higher value, to generate a larger list including some endothelial cell genes which may be present in both Runx1+24mCNE-GFP^{neg} and bulk endothelial cell libraries. This gene list was further restricted to TFs by overlap with a list of all murine TFs from the GSC. Our next goal was to create a regulatory hierarchy consisting of these up-regulated TFs in order to narrow down our investigation to a few key regulators. The online tool DiRE was used to identify TFs regulating our input genes [104]. DiRE takes into account the locations of a list of co-expressed genes within the genome, and identifies evolutionarily conserved regions (ECRs) surrounding them [104]. These ECRs are then probed for the presence of both intronic and promoter regions which contain regulatory elements and TF binding sites (TFBS) [104]. The relative enrichment for the association of these regulatory elements with the input list is then compared to that of a background gene list [104]. The result of a DiRE analysis includes a list of candidate TFs that bind ECRs significantly closer to the co-expressed input genes, than to a random background list [104]. The candidate TFs from DiRE consist of all mouse TFs, some of which may not be expressed in HE at E10.5. We then filtered this DiRE output for members of the original input list to ensure physiological relevance. This allowed a hierarchy of TF regulation to be constructed which consists only of TFs up-regulated at E10.5 within HE of the DA. This analysis was done online at dire.dcode.org and further data manipulation took place in Microsoft Excel (Microsoft, Redmond, WA) [104]. Biotapestry, online at www.biotapestry.org, was used to illustrate this hierarchy as proposed by DiRE [104, 105].

2.6 Hierarchy Validation

As the libraries and subsequent hierarchy were based on an indirect sequencing method, the validation of TFs as higher expressed in sorted HE was done. HE (SSEA-1^{neg}CD31^{pos}c-Kit^{neg}CD45^{neg}Runx1+24mCNE-GFP^{pos}) and Runx1+24mCNE-GFP^{neg} endothelial cells (SSEA-1^{neg}CD31^{pos}c-Kit^{neg}CD45^{neg} Runx1+24mCNE-GFP^{neg}) cells were sorted from E10.5 embryos, total RNA was extracted from cells using TriZOL (Invitrogen, Carlsbad, CA) based on manufacturer protocols. cDNA was produced with 2.5 μg of total RNA using the Superscript II kit with random primers (Invitrogen, Carlsbad, CA). Quantitative real-time PCR (qRT-PCR) was carried out using 2.5 μL of cDNA and primers for top hierarchy genes, including Runx1 for validation of our sorting scheme. Each primer and cDNA sample was run in triplicate as technical replicates, using an Applied Biosystems 7900HT Fast Real-Time PCR System and using SYBR® Green (Applied Biosystems, Foster City, CA). Table 2.4 describes primers.

Table 2.4 List of qRT-PCR primers

	Forward primer sequence 5'→3'	Reverse primer sequence 5'→3'
mPbx1a	GCCAGACAGGAGGATACAGTG	CTGCCAACCTCCATTAGCAC
mPbx1b	GCCAGACAGGAGGATACAGTG	GTGAGGATCAGTAGGTTCTTGACA
mGata1	GGGAACACTGGGGTTGAA	CCCTGAACTCGTCATACCACT
mGfi1b	GTTGCTGAACCAGAGCCTTC	TTGGGGTGTCACGAGAGG
mGata2	GCTTCACCCCTAAGCAGAGA	TGGCACCACAGTTGACACA
mHes1	CGCACCCTGCAAGTTGGGCA	CTGTGAGCGAAGGCCCCGTT
mStat3	GTTCCTGGCACCTTGGATT	CAACGTGGCATGTGACTCTT
mMeis1	TTGGAATAGAGACCATGATGACAC	GTTATCCCCACTGTGTGAAGTATG
mHoxa9	CCACGCTTGACACTCACACT	CCACGCTTGACACTCACACT
mStat4	CGGCATCTGCTAGCTCAGT	TGCCATAGTTTCATTGTTAGAAGC
mRunx1	GCAGGCAACGATGAAAACTACT	GCAACTTGTGGCGGATTTGTA
mGapdh	TGCAGTGGCAAAGTGGAGAT	TTTGCCGTGAGTGGAGTCATA

2.7 *Ex vivo* Assay

2.7.1 OP9 Co-culture

In order to interrogate these candidate genes of interest in a high-throughput manner, an *ex vivo* assay was developed to allow the differentiation of HE containing cell population SSEA-$1^{neg}CD45^{neg}$Runx1+24mCNE-GFP^{pos} cells into mature hematopoietic cells, as marked by the acquisition of cell surface marker CD45. When culturing cells at a pre-differentiated state it is important to address the culture conditions necessary for both the endothelial and hematopoietic development and maintenance. The cellular co-culture of HE with an OP9 feeder layer, a modified ES cell culture technique, has been used in the past as an *ex vivo* assay for embryonic hematopoiesis. Cellular co-culture allows for the interrogation of specific cell populations isolated from dissociated DAs or other hematopoietic organs.

In the *ex vivo* assay an irradiated OP9 cell feeder layer was prepared the day prior to sorting. OP9 cells were a gift from Dr. Fumio Takei, and were maintained in basal media, α-MEM + 10% HI-FBS + 1% Penicillin-Streptomycin-Glutamine (PSG) (Thermo Fisher Scientific, Walton, MA) (Sigma-Aldrich, St. Louis, MO) supplemented with hematopoietic and endothelial cytokines at the time of plating. OP9 cells were trypsinized and irradiated in suspension at a dose of 40 Gray (Gy). This damages the OP9 DNA enough to stop proliferation, but allows for survival for the duration of the co-culture. OP9s are contact-inhibited, but do not provide optimal support for hematopoietic differentiation when cultured at high density. After irradiation 2500 OP9 cells were plated per well in 400 μL of cytokine media in the inner 8 wells of a tissue culture-treated 24 well plate (BD Biosciences, San Jose, CA). To decrease evaporation the 16 outer wells were filled with PBS. The cytokine media consisted of basal OP9 media made fresh at the time of plating, supplemented with 200 U/mL mIL-3 (eBioscience, San

Diego, CA), 100 ng/mL rhG-CSF (eBioscience, San Diego, CA), 100 ng/mL mSCF (eBioscience, San Diego, CA), 2 U/mL rhEPO (R&D Systems, Minneapolis, MN), 1 ng/mL rhbFGF (StemCell Technologies, Vancouver, BC), and $5x10^{-5}$ M 2-β-mercaptoethanol (Sigma-Aldrich, St. Louis, MO).

Feeder cells were incubated at 20% O_2, at 37°C degrees until the following day when cells isolated from embryos were plated on top of the monolayer. After the sort, cells were pelleted at 400 RCF for 6 min at RT and then resuspended in 100 μL cytokine-containing medium. Sorted cells were plated at 1-3 embryo equivalents (ee) per well depending on the experiment. Additionally if sorted, $CD45^{pos}$ cells were plated as a positive control to measure the capability of the system to allow $CD45^{pos}$ cell expansion.

In the culture of $Meis1^{fl/fl\ VeCre}$ embryos, E9.5 DAs were dissected separately and dissociated in the same manner as the pooled Runx1+24mCNE-GFP embryos. Instead of filtering and staining cell suspensions, tubes were spun down and resuspended directly in 100 uL cytokine containing media for plating.

The work contained in this thesis, in combination with personal communication with Borges *et al* , suggested that the culture of cells isolated from early embryos at a 5% O_2 tension allowed for establishment of an endothelial layer [70]. Cells isolated from E9.5 embryos were cultured for 3 days at 5% O_2, followed by culture at 20% O_2 tension for the final 3 days. After these 6 days all cells, including the OP9 feeder layer were then removed from the plates using the same DNase/Collagenase (Sigma-Aldrich, St. Louis, MO) mixture as was used when digesting the embryos on day 0. The cell suspension was then stained for CD31, and CD45 to determine whether $CD45^{neg}$ HE cells differentiated over this time period. Stained cells were measured for CD31 and CD45 expression using a BD FACSCalibur flow cytometer (BD, San

Jose, CA), and data was analyzed using FlowJo software (Treestar, Ashland, OR). After developing a culture system which allowed an isolated HE cell population about to undergo EHT, we then interrogated this process further using an inhibitor of the process.

2.7.2 Notch Inhibition

Pre-HE cells isolated from E9.5 DAs were sorted as above for the markers SSEA-1^{neg} CD45^{neg}Runx1+24mCNE-GFP^{pos}. Immediately after plating cells the blockade of Notch was attempted by the addition of 0.1 μM γ-secretase inhibitor DFPAA (Calbiochem/Millipore, Billerica, MA) into each experimental well, or dimethyl sulfoxide (DMSO) (Sigma-Aldrich, St. Louis, MO) into control wells. Cells were cultured for 3 days at 5% O_2, 3 days at 20% O_2, and assayed for the acquisition of CD45 by flow cytometry after 6 days.

2.8 Meis1$^{fl/fl\ VeCre}$ Embryo Characterization

2.8.1 Phenotype Analysis

During dissection, images were acquired of intact Meis1$^{fl/fl\ VeCre}$ embryos with the YS removed. Dissections were done on a Leica MZ16 F manual fluorescence stereomicroscope and images were taken with Leica Application Suite (Leica Microsystems, Wetzlar, DE). Images of embryos were analyzed blind to genotype, for the presence of neural tube hemorrhaging or blood pooling outside of vasculature. Genotypes were then assigned to embryos, and the numbers of *Meis1*$^{fl/fl\ VeCre}$ null and wild-type embryos with signs of hemorrhage were tabulated.

2.8.2 Percentage of Cells containing Excised *Meis1*$^{fl/fl}$ Exon 8

To determine the percent of cells containing excised Meis1 exon 8 in cells sorted from *Meis1*$^{fl/fl\ VeCre}$ null embryos, SSEA-1^{neg}CD45^{neg}VEC^{pos} cells were sorted and genomic DNA was isolated using an Invitrogen AllPrep Kit (Invitrogen, Carlsbad, CA). For embryos with sufficient

genomic DNA extracted, 5 ng of genomic DNA per triplicate reaction, per primer set was run, along with positive control genomic DNA. Positive controls displaying 0% collapsed exon 8 (100% intact floxed exon 8) and 100% collapsed (0% intact floxed exon 8, fully excised by Cre) genomic DNA were run as calibrators. Presence or absence of *Meis1*$^{fl/fl}$ exon 8 was determined in comparing samples to calibrators using RQ manager (Applied Biosystems, Foster City, CA) and analyzed in Microsoft Excel (Microsoft, Redmond, WA). Each sample was run in triplicate as technical replicates, for each primer set A, B and C. Samples were run on Applied Biosystems 7900HT Fast Real-Time PCR System and using SYBR® Green (Applied Biosystems, Foster City, CA). Primers are described in Table 2.5.

Table 2.5 List of qRT-PCR primers for percent excision

Meis1_qpcr_A	AGCTTCATTTGAAGTTCCCTATTG	TATTAGGTGGATCCAAGCTTCATT
Meis1_qpcr_B	CTGGACTTTCTCCTTTAGTTGGAT	GGAACTTCATCAGTCAGGTACATA
Meis1_qpcr_C	TATGTACCTGACTGATGAAGTTCC	GCGTCACTTGGAAAAGCAAT

2.8.3 ESLAM Analysis of E14.5 FLs

To examine possible defects in HSC expansion which takes place in the E14.5 embryo, FLs were isolated from one litter of Meis1$^{fl/fl\ VeCre}$ embryos, and analyzed by flow cytometry to determine the number of ESLAM positive cells. E14.5 embryos were isolated from uterine tissue and YSs were collected for genotyping. FLs were removed from each embryo by pinching forceps below the visibly red FL to remove the hind limbs, freeing the liver for further removal by forceps. Livers were collected separately in Eppendorf tubes containing PBS+2% HI-FBS (Thermo Fisher Scientific, Walton, MA) and kept on ice until processing. Mechanical dissociation of FLs involved trituration of the liver with a 1000 μL tip, followed by forcing the cell suspension through a 40 μm cell strainer (Thermo Fisher Scientific, Walton, MA) placed on a 50 mL tube (BD Biosciences, San Jose, CA), with the plunger of a 1 mL syringe (BD

Biosciences, San Jose, CA). The filter was then rinsed, cells were pelleted at 400 RCF for 5 min, and the supernatant was aspirated. The pellet was resuspended in 1 mg/mL DNase (Sigma-Aldrich, St. Louis, MO) dissolved in PBS + 2% HI-FBS (Thermo Fisher Scientific, Walton, MA). After cells were counted, 1 μL of each of the following monoclonal antibody was added per 100 μL of cell suspension; FITC CD45 (LCA) (eBioscience, San Diego, CA), PE EPCR (Stem Cell Technologies, Vancouver, BC), APC CD48 (BioLegend, San Diego, CA), and PE-Cy7 CD150 (BioLegend, San Diego, CA) were incubated with cells for 30 minutes on ice. Stained cells were measured for ESLAM marker binding using a FACSCalibur flow cytometer (BD, San Jose, CA), and the number of $ESLAM^{pos}$ cells for each embryo was quantified using FlowJo software (Treestar, Ashland, OR).

2.8.4 Immunofluorescence Staining

E10.5 embryos were dissected free of the YS with forceps, and heart and limbs were removed using a 30g½" needle. Embryos were fixed in 2% paraformaldehyde (PFA) (Sigma-Aldrich, St. Louis, MO) overnight (or 4% PFA for 5 hours). After fixing they were rinsed in PBS, and incubated with 30% w/v sucrose (Sigma-Aldrich, St. Louis, MO) in PBS overnight for cryopreservation. After the embryos became isotonic with the solution they were moved to Tissue-Tek® O.C.T. Compound (Optimal Cutting Temperature; Sakura Finetek, Torrance, CA) in sectioning moulds and left for 15 min at room temperature (RT) then were moved to -80°C for storage until sectioning. 5 μm sections were taken of the entire embryo, and attached to charged slides. Slides were stored at -80°C until staining.

Cryosections were blocked and permeabilized with 5% chicken serum (Sigma-Aldrich, St. Louis, MO) + 0.2% Triton X-100 (Sigma-Aldrich, St. Louis, MO) in PBS and stained with rat anti-mouse CD41 monoclonal antibody (1/300) (Abcam, Cambridge, UK), and goat anti-

mouse VEC antibody (1/200) (Santa Cruz Biotech, Santa Cruz, CA) overnight at 4°C. Fluorochrome-conjugated secondary antibodies chicken anti-rat Alexa Fluor 488 (Invitrogen, Carlsbad, CA) and chicken anti-goat Alexa Fluor 594 (Invitrogen, Carlsbad, CA) were incubated with all samples at 1/200 for 1-3 hours at RT, and nuclei were stained with 5 mg/mL DAPI (Sigma-Aldrich, St. Louis, MO) for 5 minutes at RT. Immunofluorescent staining was detected with a fluorescent imaging microscope (Axioplan II; Carl Zeiss, Inc.), and images were captured with a digital camera (1350EX; QImaging, Surrey, BC, Canada). Images were analyzed using Eclipse software (EMPIX, Mississauga, ON).

2.9 Statistical Analysis

Results were expressed as mean +/- SEM. Data was analyzed using an unpaired two-tailed student's t-test (p values reported as p=x), and Fisher's exact test (p values reported as p^{Fisher}=x) in GraphPad Prism 6 (GraphPad Software Inc., La Jolla, CA).

3. Results

3.1 RNA-seq Library Construction

170 wild-type and transgenic embryos were dissected and sorted over 14 days from Oct 2011 to Feb 2012 to collect cells for library construction. 49386 Runx+24mCNE-GFP^{neg} cells were collected in total from transgenic embryos and 79703 bulk endothelial cells were collected from wild-type littermates. See Appendix A for additional information.

3.2 Analysis of Whole Transcriptome Data

Differential expression analysis of the RNA-seq libraries allowed for comparison of gene expression between the Runx1+24mCNE-GFP depleted endothelial cell (SSEA-1^{neg}CD31^{pos} c-Kit^{neg}CD45^{neg}Runx1+24mCNE-GFP^{neg}) and bulk endothelial cell (SSEA-1^{neg}CD31^{pos}c-Kit^{neg} CD45^{neg}) libraries. Our gene of interest list was first refined through restriction of the bulk endothelial cell library which, based on our sorting scheme, encompassed the cell types in the Runx1+24mCNE-GFP depleted library. 18365 genes total >0 RPKM were present in the bulk endothelial cell library, and when an expression cutoff of $\geq$0.3 RPKM was used 13825 genes remained. We then removed any non-protein coding genes which resulted in 12512 protein coding genes expressed at $\geq$0.3RPKM. RPKM values for the bulk endothelial cell library were divided by values for the Runx1+24mCNE-GFP depleted library to generate fold change values. A cutoff of 1.5-fold change was used to restrict the list to genes higher expressed in bulk endothelial cells, as compared to Runx1+24mCNE-GFP depleted cells. This resulted in 2348 genes which were expressed at $\geq$0.3 RPKM, 1.5-fold higher expressed in the bulk endothelial cell library, and protein coding. We then overlapped our 2348 total genes with a list of 1653

mouse TFs. This resulted in a list of 228 TF expressed at E10.5 in the DA, hypothesized to be up-regulated in Runx1+24mCNE^{pos} HE.

In order to pull out a multi-leveled hierarchy consisting of interactions between our 228 up-regulated TFs, our list was input into DiRE with a random background of 5000 genes set. 55 of our 228 input genes were proposed to be regulated by 94 different mouse genes using DiRE [92]. When this output was filtered to include only genes present in our list of 228 up-regulated TFs, 9 were found to regulate other downstream TFs. The TFs Pbx1, Gata1, Gfi1b, Hes1, Gata2, Stat3, Stat4, Meis1, Hoxa9 were all found to regulate anywhere from 1 to 10 genes found in our list of 228. The hierarchy that resulted from this process was illustrated using BioTapestry to better visualize these relationships (Figure 3.1).

3.3 Hierarchy Validation

As the sequencing libraries were generated based on a negative comparison method to determine genes up-regulated in HE, we wanted to validate the enrichment of our top regulators in sorted HE. SSEA-1^{neg}CD45^{neg}CD31^{pos}Ckit^{neg}Runx+24mCNE-GFP^{pos} HE, and Runx+24mCNE^{neg} vascular endothelium were sorted for this validation. qRT-PCR was carried out for the 9 genes at the top of the hierarchy over 3 separate experiments using cDNA prepared from pooled cells sorted from 11-21 embryos per sort (Figure 3.2). *Gata1, Gfi1b, Meis1* and *Stat4* showed over 2-fold expression increase in E10.5 Runx1+24mCNE-GFP^{pos} HE when compared to Runx1+24mCNE-GFP^{neg} endothelium. *Gata2, Hoxa9, Pbx1, Stat3,* and *Hes1* showed less than 2-fold change in E10.5 Runx1+24mCNE-GFP^{pos}. *Hes1* actually showed slightly higher expression in Runx1+24mCNE-GFP^{neg} cells (Table 3.1). *Runx1* was not found to be up-regulated in our negative comparison of the two libraries, which may have been due to biases introduced with mRNA transcript selection during library construction. An additional

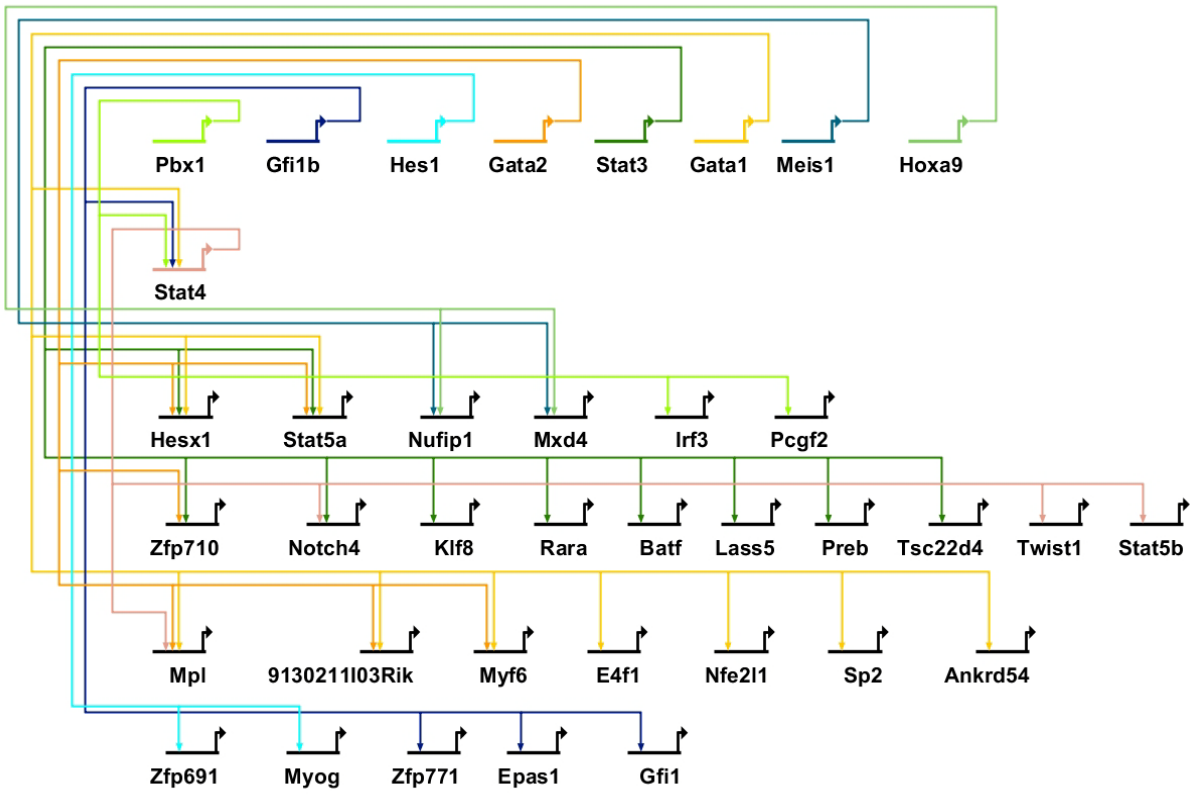

Figure 3.1 Hierarchy of regulators involved in EHT at E10.5

Hierarchy displaying relationships between members of our list of 228 up-regulated TFs as proposed by DiRE and visualized in BioTapestry. 9 top hierarchy regulators are observed in the top row of the tree, followed by secondary regulator Stat4 and resulting downstream members. This diagram visualizes relationships based only on the DiRE results and does not include previously discovered relationships from the literature.

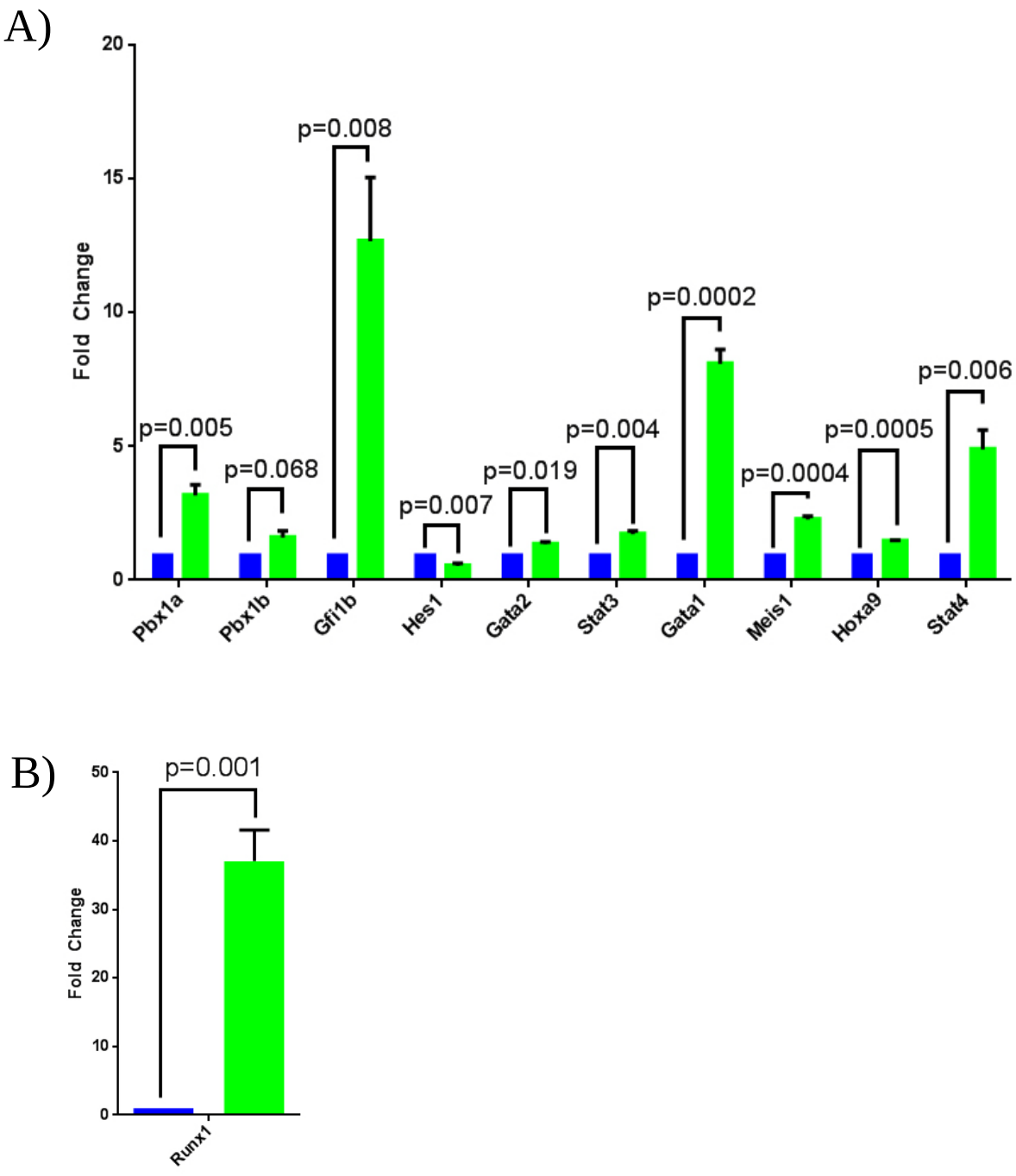

Figure 3.2 qRT-PCR fold change for top hierarchy genes
qRT-PCR results for 9 top hierarchy genes normalized to GAPDH for each sample. Graph compares fold change for expression in SSEA-1^{neg}CD45^{neg}CD31^{pos}c-Kit^{neg}Runx+24mCNE-GFP^{pos} (green) to SSEA-1^{neg}CD45^{neg}CD31^{pos}c-Kit^{neg}Runx+24mCNE-GFP^{neg} (blue) expression, set to 1. B) Increased expression of *Runx1* in Runx1+24mCNE-GFP^{pos} sorted cell populations as compared to negative cells validate correlation between HE sorting scheme and expression of *Runx1*. Unpaired 2-tailed t-test and SEM shown on graph.

Table 3.1 Comparison of the expression of top hierarchy genes in E10.5 HE

	qRT-PCR fold change	Library RPKM fold change
Pbx1a	**3.17**	**1.841**
Pbx1b	**1.595**	**1.841**
Gata1	**8.077**	**6.423**
Gfi1b	**12.665**	**4.139**
Hes1	**-1.75***	**1.733**
Gata2	**1.337**	**1.762**
Stat3	**1.719**	**2.212**
Stat4	**4.885**	**3.092**
Meis1	**2.272**	**2.160**
Hoxa9	**1.453**	**1.960**

validation was done to confirm our HE sorting scheme based on the +24mCNE-GFP marker, validating the increased expression of *Runx1* in these Runx1+24mCNE-GFP^{pos} sorted cells as compared to Runx1+24mCNE-GFP^{neg} sorted cells (Figure 3.2b).

3.4 *Ex vivo* Assay

3.4.1 Oxygen Tension in E9.5 *Ex vivo* Co-culture

E9.5 pre-HE cells (SSEA-1^{neg}CD45^{neg}CD31^{pos}c-Kit^{neg}Runx+24mCNE-GFP^{pos}) were sorted from pooled transgenic DAs and cultured at 37°C, 20% O_2 for 6 days. After 6 days, no CD45^{pos} or GFP^{pos} cells were observed by flow cytometry analysis in any wells. As such a finely sorted population may exclude cells which provide extrinsic signals to developing HE, a more heterogeneous population containing pre-HE was chosen. Additionally as embryos were isolated from an earlier time-point than usual for HE cell culture, we looked at the effect of O_2 concentration on establishing an endothelial culture for later differentiation [63].

Cells were sorted from E9.5 embryos based on their CD45 expression to determine the growth capacity for hematopoietic and non-hematopoietic cell populations in our assays at this

time-point. Cells were sorted based on CD45 expression into SSEA-1^{neg}CD45^{pos}, SSEA-1^{neg} CD45^{mid} and SSEA-1^{neg}CD45^{neg} populations, which were plated at 3 embryo equivalents (ee) into replicate wells. Replicates were split between two 24-well plates (BD Biosciences, San Jose, CA) and cultured at either low, 5% O_2, or regular, 20% O_2 for 6 days. To determine if there were HE cells in culture, bulk Runx1+24mCNE-GFP was measured. For this first experiment the actual number of cells per well after day 6 of culture was not measured, so percentages of the total cell populations present were reported. The number of bulk Runx1+24mCNE-GFP^{pos} cells was significantly higher at 5% O_2 than 20% O_2 when CD45^{neg} and CD45^{mid} cells were cultured ($p=0.00032$, $p=0.022$ respectively). No Runx1+24mCNE-GFP^{pos} cells were present in the CD45^{pos} plated population at either O_2 tension (Figure 3.3A). There was no significant difference in the number of CD45^{pos} cells after 6 days in culture for any of the sorted cell populations at either O_2 tension, though there was a trend of increased CD45 expression in cells cultured at 20% O_2 for 6 days (Figure 3.3B). These experiments confirmed the ability for CD45^{neg} cells to gain CD45^{pos} expression and maintain Runx1+24mCNE-GFP^{pos} cells in culture.

Our next step was to refine this CD45^{neg} population further using Runx1+24mCNE-GFP expression. We compared the capacity of sorted E9.5 SSEA-1^{neg}CD45^{neg}Runx1+24mCNE-GFP^{pos} pre-HE and SSEA-1^{neg}CD45^{neg} Runx1+24mCNE-GFP^{neg} endothelial cells in generating bulk hematopoietic CD45^{pos} cells and HE (CD45^{neg}CD31^{pos}Runx1+24mCNE-GFP^{pos}) cells after 6 days of culture at 5% O_2. Though it was not significant, the results of this experiment suggested that SSEA-1^{neg}CD45^{neg} Runx1+24mCNE-GFP^{pos} cells have a higher potency of HE cell maintenance in culture, per plated cell ($p=0.061$) (Figure 3.4A). This is likely due to their advantage in simply maintaining Runx1+24mCNE-GFP expression already achieved within

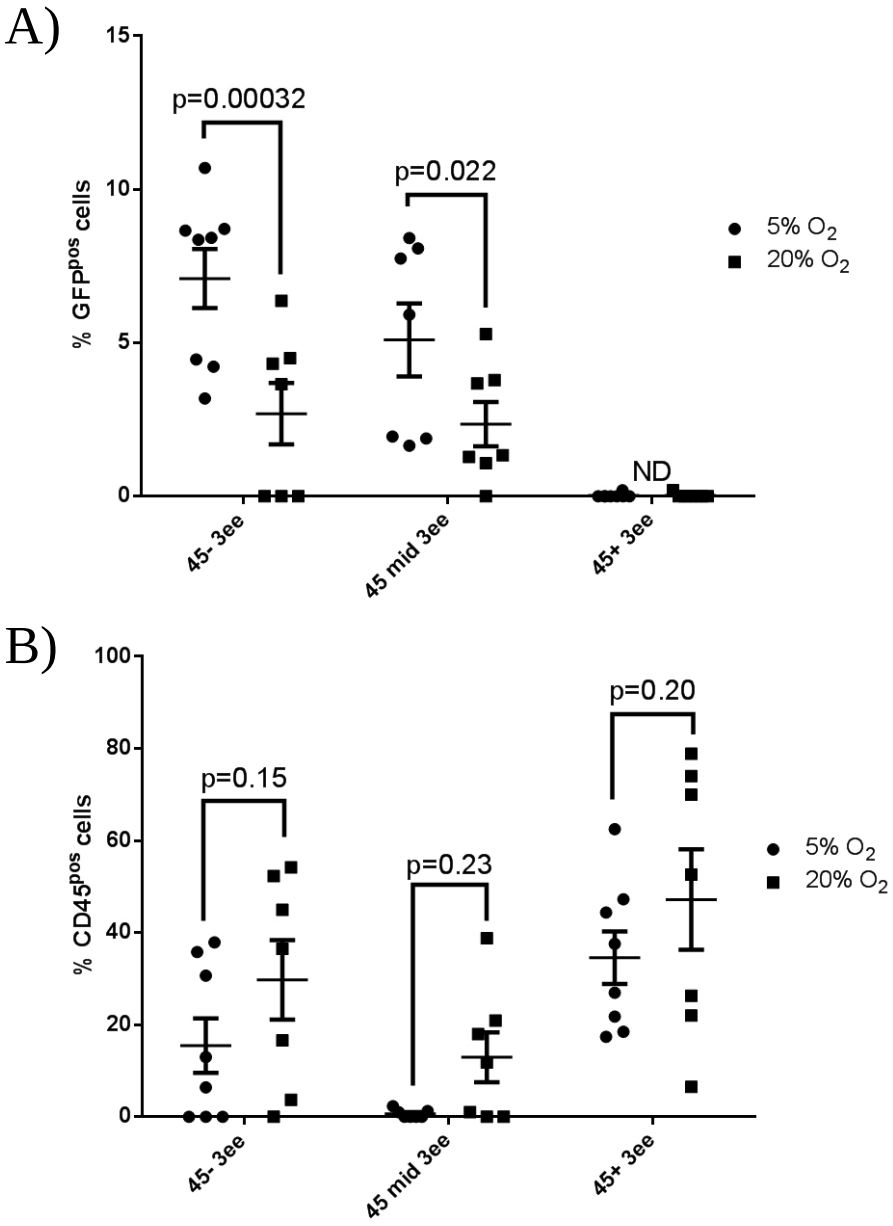

Figure 3.3 Effect of O_2 tension on generation of CD45 and GFP in sorted cells

Percentage of GFP^{pos} and $CD45^{pos}$ cells generated by $CD45^{neg}$ (45-), $CD45^{mid}$ (45 mid), $CD45^{pos}$ (45+) wells at 5% O_2 (●) or 20% O_2 (■). Actual values are not shown as cell numbers were not counted at time of analysis. A) Percentage Runx1+24mCNE-GFP^{pos} cells was significantly higher for $CD45^{neg}$ and $CD45^{mid}$ populations at 5% O_2, and no Runx1+24mCNE-GFP was observed in wells containing $CD45^{pos}$ plated cells at either O_2 tension. B) No significant difference was observed in the percentage $CD45^{pos}$ cells at day 6 between 5% or 20% O_2 tensions for any cell population, though a trend of higher percentage $CD45^{pos}$ was observed in all populations for 5% O_2 compared to 20% O_2. All wells contained 3 embryo equivalents (ee) of cells per well. N=8 for 5% O_2, N=7 for 20% O_2. Data shown from 3 experiments. Unpaired 2-tailed t-test and SEM shown on graph.

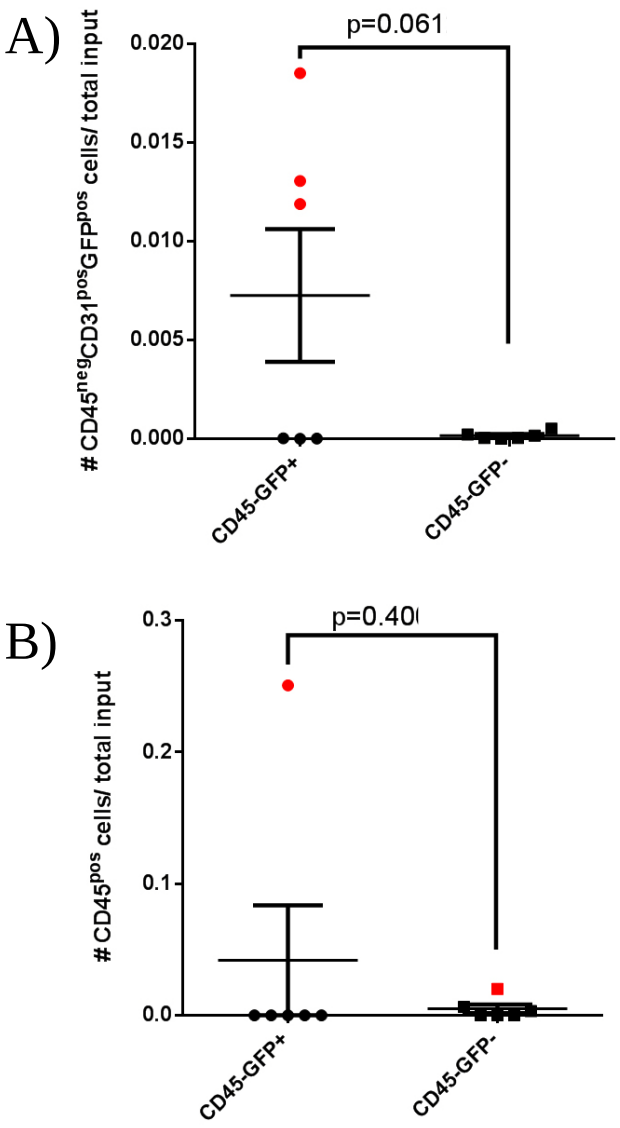

Figure 3.4 5% O_2 culture of $CD45^{neg}GFP^{pos}$ and $CD45^{neg}GFP^{neg}$ cell populations

Differences in the number of $CD45^{neg}CD31^{pos}$ Runx1+24mCNE-GFP^{pos} HE cells and $CD45^{pos}$ hematopoietic cells generated by SSEA-$1^{neg}CD45^{neg}$ Runx1+24mCNE-GFP^{pos} (CD45-GFP+, ●) and SSEA-$1^{neg}CD45^{neg}$ Runx1+24mCNE-GFP^{neg} (CD45-GFP-, ■) cell cultured for 6 days at 5% O_2 normalized to input cell number. Red points (●) signify values $\geq$1% cut-off value. Data shown from three experiments. A) The number of $CD45^{neg}CD31^{pos}$ Runx1+24mCNE-GFP^{pos} HE cells generated by SSEA-$1^{neg}CD45^{neg}$ Runx1+24mCNE-GFP^{pos} cells was not significantly different than generated by SSEA-$1^{neg}CD45^{neg}$ Runx1+24mCNE-GFP^{neg} cells. B) No significant difference was observed between the populations for $CD45^{pos}$ cell generation at this O_2 tension. N=6 wells at 2 embryo equivalents (ee) per well. Unpaired 2-tailed t-test and SEM shown on graph.

these cells. However the development of HE cells from plated SSEA-1^{neg}CD45^{neg} Runx1+24mCNE-GFP^{neg} cells was also observed in culture, at a reduced frequency. This suggests that some cells in this population have the ability to gain Runx1+24mCNE-GFP expression *ex vivo*. There was no significant difference in the number of CD45^{pos} cells generated by each population as the generation of hematopoietic cells from these more refined sorted populations at 5% O_2 is rare (p=0.40) (Figure 3.4B).

It is important to normalize output values to input cell number when comparing the ability of these two populations for CD45^{pos} and HE cell generation. The SSEA-1^{neg}CD45^{neg} Runx1+24mCNE-GFP^{pos} cell population is about 4-fold smaller, about 1200 cells per embryo, than the more heterogeneous SSEA-1^{neg}CD45^{neg}Runx1+24mCNE-GFP^{neg} population, about 30,000 cells per embryo.

In an attempt to compensate for the rarity of CD45^{pos} and HE cell growth *ex vivo* when normalized per input cell, we used a cut-off of $\geq$1% (1/100 cells plated generates 1 CD45^{pos} cell) to allow the comparison of proportions between positive wells which exceed this threshold, and negative wells which do not. With this in mind, the number of wells with $\geq$1% HE cells was not significantly higher for SSEA-1^{neg}CD45^{neg} Runx1+24mCNE-GFP^{pos} wells when compared by Fisher's exact test ($\geq$1% represented by ●, p^{Fisher} =0.18) (Figure 3.4). More replicates are needed to determine the significance of this trend. Both SSEA-1^{neg} CD45^{neg}Runx1+24mCNE-GFP^{pos} wells and SSEA-1^{neg}CD45^{neg} Runx1+24mCNE-GFP^{neg} wells generated 1/6 wells containing $\geq$1% CD45^{pos} cells per input cell which was not significant by Fisher's exact test (p^{Fisher} =1.0). However the frequency of CD45^{pos} cell generation was much higher for the one SSEA-1^{neg}CD45^{neg}Runx1+24mCNE-GFP^{pos} plated well which exceeded the $\geq$1% threshold when compared to the SSEA-1^{neg}CD45^{neg} Runx1+24mCNE-GFP^{neg} well (1/4 versus 1/50 respectively).

This suggests that the plated cell population marked by SSEA-1^{neg}CD45^{neg}Runx1+24mCNE-GFP^{pos} has a more potent ability to maintain HE cultured at 5% O_2. Both populations are capable of HE production or maintenance, and CD45^{pos}cell development *ex vivo*. We chose to use the more refined population of SSEA-1^{neg}CD45^{neg}Runx1+24mCNE-GFP^{pos} pre-HE for further experiments. The need for an assay which allows consistent generation of CD45^{pos} hematopoietic cells, while allowing the growth of HE is important to assay EHT at this time-point.

3.4.2 Effect of Oxygen Tension Change During Culture

To allow for the complex process of EHT to occur *ex vivo*, maintaining endothelial cell growth as well as CD45 generation, we looked at transitioning between 5% and 20% O_2 during culture [63, 70]. SSEA-1^{neg}CD45^{neg}Runx1+24mCNE-GFP^{pos} cells sorted from E9.5 embryos were plated at 2ee per well and cultured in replicates at three conditions. The three conditions consisted of 20% O_2 and 5% O_2 tension combinations, 20% O_2 for 6 days (20%), 2 days at 5% O_2 followed by 4 days at 20% O_2 (2-4), and 3 days at 5% O_2 followed by 3 days at 20% O_2 (3-3). When the number of HE cells were measured after 6 days, cells cultured at 3-3 appeared to generate the highest values of HE, however this difference was not significant when compared to 20% O_2 conditions (3-3 p=0.14) (Figure 3.5A). 2-4 conditions did not show an increase in HE compared to 20% O_2, nor was a trend in HE maintenance observed (p=0.79). As there appears to be a trend for an increase in HE in the 3-3 group as compared to 20% O_2, Fisher's exact test was performed. When Fisher's exact test was used to determine the proportion of 3-3 wells crossing the $\geq$1% threshold, compared to 20% O_2 the difference was not significant although there appears to be a trend (p^{Fisher}=0.094). The same comparison for 20% to 2-4 O_2 was not significant (p^{Fisher}=1.000). There were no significant differences in CD45^{pos} cell generation when comparing 20% O_2 to 2-4 or 3-3 conditions by unpaired t-test (2-4 p=0.25, 3-3 p=0.20) (Figure 3.5B).

A)

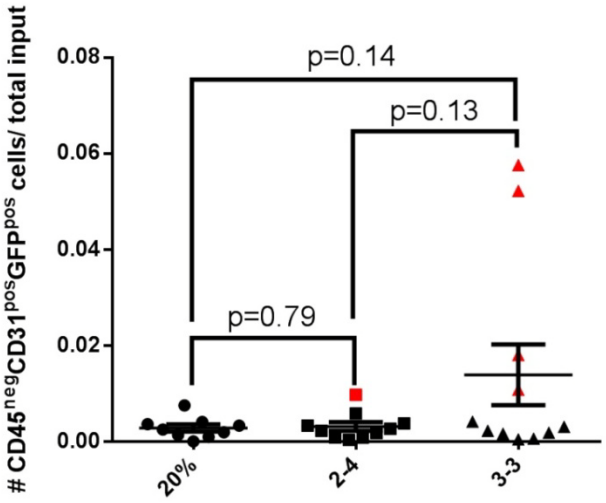

B)

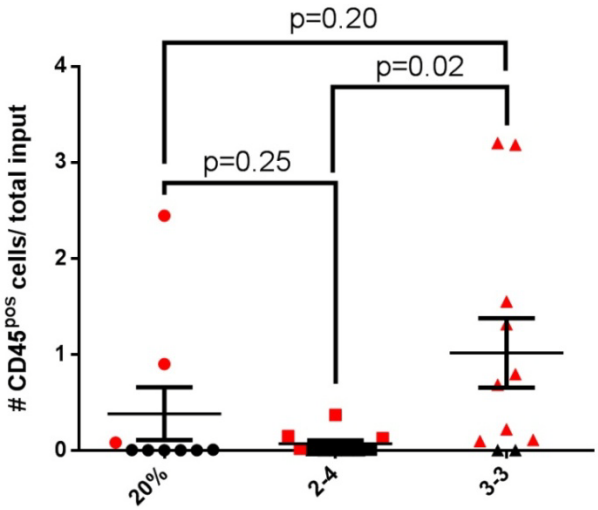

Figure 3.5 Effect of O_2 tension transition during culture

Differences in the capacity for SSEA-1^{neg} CD45^{neg} Runx1+24mCNE-GFP^{pos} cells to generate CD45^{neg} CD31^{pos}Runx1+24mCNE-GFP^{pos} HE cells and CD45^{pos} hematopoietic cells at 3 different O_2 conditions. 20% - 6 days at 20% O_2 (N=9), 2-4 – 2 days at 5% O_2 followed by 4 days at 20% O_2 (N=10), 3-3 – 3 days at 5% O_2 followed by 3 days at 20% O_2 (N=11). Data shown from 4 experiments. Red points (●) signify values beyond the >1% threshold. A) The number of CD45^{neg}CD31^{pos} Runx1+24mCNE-GFP^{pos} cells per input SSEA-1^{neg} CD45^{neg}Runx1 +24mCNE-GFP^{pos} cell plated after 6 days of culture was not significantly higher in 3-3 culture as compared to 20% O_2 or 2-4 conditions. B) There was no significant difference in the number of CD45^{pos} cells in either of the 2-4 or 3-3 transition cultures after 6 days as compared to 20% O_2 culture conditions. 3-3 generated significantly more CD45^{pos} cells than 2-4. Unpaired 2-tailed t-test and SEM shown on graph.

However the 3-3 treatment generated significantly more $CD45^{pos}$ cells when compared to 2-4 ($p=0.02$). When Fisher's exact test was used to compare the proportion of wells in 2-4 conditions which exceeded the >1% threshold for $CD45^{pos}$ cell generation, compared to 20% O_2, there was no significant difference between these treatments ($p^{Fisher}=1.0$). This comparison was significant when the proportion of $CD45^{pos}$ cells generated in 20% O_2 wells was compared to the proportion generated in 3-3 conditions ($p^{Fisher}=0.032$). Together this data suggests that the culture of cells at 5% O_2 may allow for an increase in HE establishment, and that 3-3 conditions result in a higher proportion of wells producing >1% $CD45^{pos}$ cells per input cell (Figure 3.5B).

3.4.3 Notch Inhibitor Manipulation

We next examined the effect of inhibiting Notch signalling using a γ-secretase inhibitor in our *ex vivo* assay. SSEA-$1^{neg}CD45^{neg}$Runx1+24mCNE-GFP^{pos} cells were sorted from E9.5 embryos, plated at 2ee per well and cultured in 3-3 transition culture. The effect of 0.1 μM DFPAA addition did not significantly affect the number of HE cells in culture ($p=0.34$) (Figure 3.6A). The proportion of wells containing ≥1% HE per input was not significant by Fisher's exact test ($p^{Fisher}=1.0$). The addition of 0.1 μM DFPAA appeared to cause a decrease in the number of wells which generated $CD45^{pos}$ cells although this was not significant ($p=0.16$) (Figure 3.6B). As the highest values for $CD45^{pos}$ cell generation were found in the DMSO treated wells, Fisher's exact test was performed, and the proportion of wells which exceeded the ≥1% threshold was not significant ($p^{Fisher}=0.65$). This suggests that the inhibition of Notch signalling by DFPAA does not significantly affect the growth of HE in culture, nor the production of $CD45^{pos}$ cells. DFPAA treated wells appear to have decreased potential for generating high numbers of HE and $CD45^{pos}$ cells when compared to DMSO treated wells.

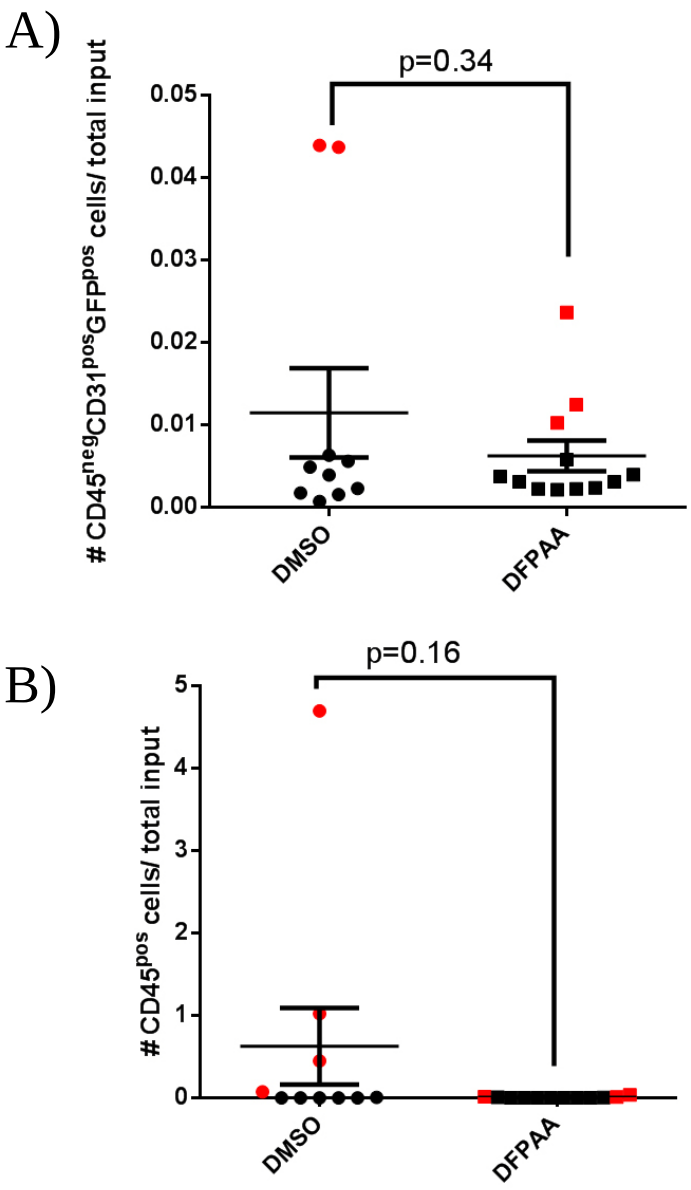

Figure 3.6 The effect of 0.1 µM DFPAA addition to *ex vivo* culture

The effect of 0.1µM DFPAA (N=12) or DMSO (N=10) on the culture of 2ee per well of SSEA-1^{neg}CD45^{neg}Runx1+24mCNE-GFP^{pos} cells at 3-3 O_2. 0.1µM γ-secretase inhibitor DFPAA was added to each well at the time of plating. A) CD45^{neg}CD31^{pos} Runx1+24mCNE-GFP^{pos} HE cell growth was not significantly affected by addition of DFPAA (p=0.3390). B) CD45^{pos} cell generation was not significantly affected by addition of DFPAA (p=0.1578). Red points (●) signify values beyond the ≥1% threshold. Values normalized to input cell number. Data shown from three experiments. Unpaired 2-tailed t-test and SEM shown on graph.

3.5 Meis1$^{fl/fl\ VeCre}$ Embryos

3.5.1 Percent Excision of *Meis1*$^{fl/fl}$ Exon 8 in VEC^{pos} Cells

As the activity of Cre recombinase is variable from cell to cell, we looked at percent of VEC^{pos} endothelial cells containing excised *Meis1*$^{fl/fl}$ exon 8 to determine embryo-to-embryo variability introduced by Cre recombinase activity [106]. SSEA-1^{neg}CD45^{neg}VEC^{pos} cells were sorted from single E10.5 DAs, YSs were saved for genotyping, and genomic DNA was extracted from confirmed *Meis1*$^{fl/fl\ VeCre}$ null embryos. Both null littermates showed that over 95% of endothelial cells contained excised *Meis1*$^{fl/fl}$ exon 8. Along with performing percent excision qRT-PCR on the sorted cells, data from the sort allowed us to get surface marker expression data for these single DAs for VEC, and CD45. There was no significant decrease in the number of CD45^{pos} hematopoietic cells from the DAs of two *Meis1*$^{fl/fl\ VeCre}$ null embryos when compared to two wild-type littermates (p=0.36) (Figure 3.7A). The development of CD45^{neg}VEC^{pos} endothelial cells was not significantly affected by *Meis1*$^{fl/fl}$ exon 8 (p=0.22) (Figure 3.7B).

From these preliminary experiments there was no significant deficiency in the number of hematopoietic or endothelial cells in *Meis1*$^{fl/fl\ VeCre}$ null embryos at E10.5. We decided to determine whether a more pronounced difference would be seen in older embryos as Meis1$^{-/-}$ mice die between E11.5-E14.5 [100]. For our *Meis1*$^{fl/fl\ VeCre}$ null embryos, as with the E10.5 embryos, data was collected from single DAs of E11.5 embryos. No significant difference in either CD45^{pos} or CD45^{neg}VEC^{pos} cells was observed, although cell counts were more variable amongst individual *Meis1*$^{flfl\ VeCre}$ null embryos than wild-type embryos (p=0.94 and p=0.23 respectively) (Figure 3.7C and D). Genomic DNA was extracted in a sufficient amount for percent excision qRT-PCR from one *Meis1*$^{fl/fl\ VeCre}$ null embryo, and it was found that less than 50% of CD45^{neg}VEC^{pos} contained excised *Meis1*$^{fl/fl}$ exon 8. The masking of an

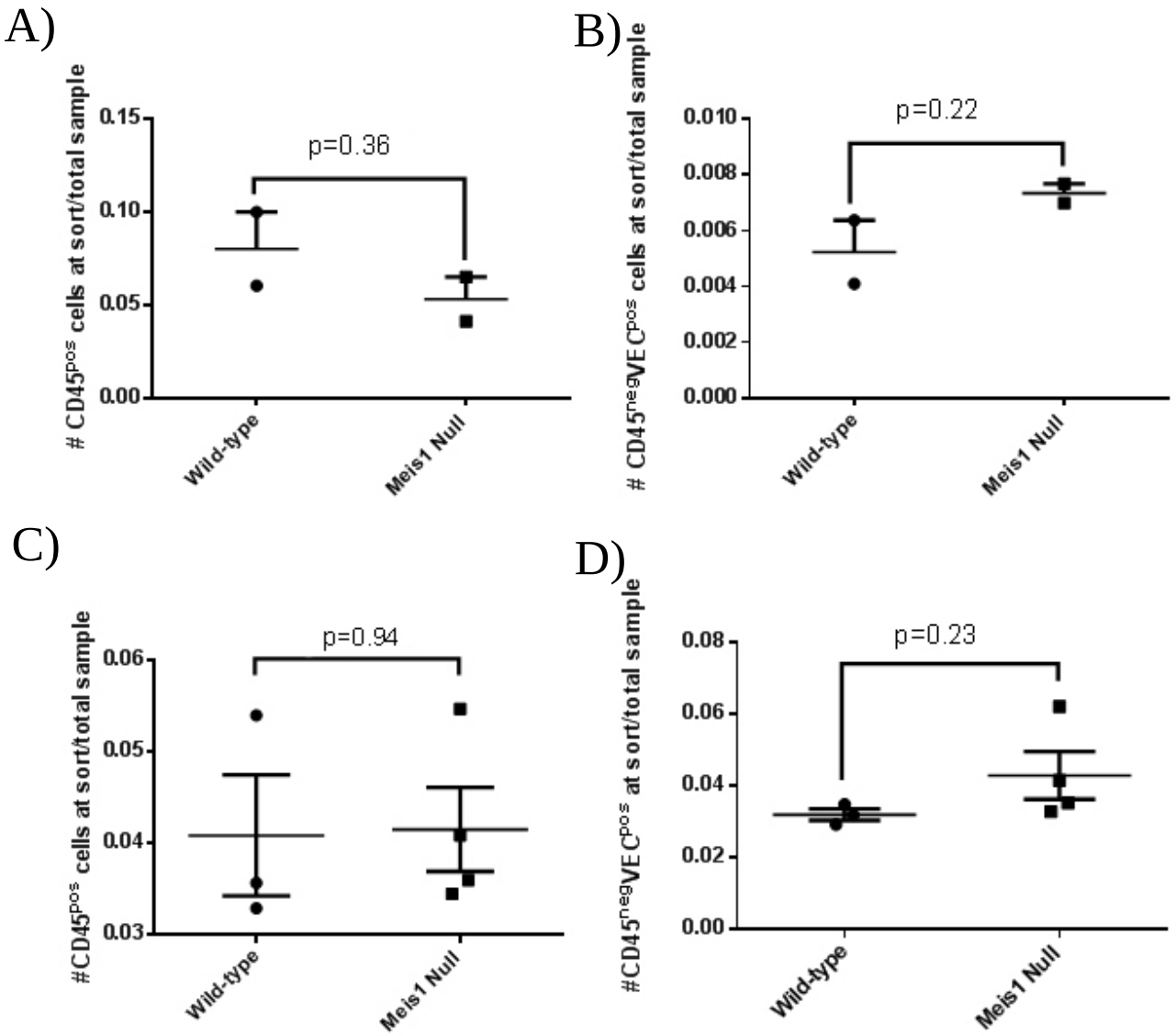

Figure 3.7 Flow analysis of single DAs from E10.5 and E11.5 embryos

Staining and flow cytometry analysis of single E10.5 (N=2 wild-type and N=2 *Meis1*$^{fl/fl\ VeCre}$ null) and E11.5 DAs (N=3 wild-type and N=4 *Meis1*$^{fl/fl\ VeCre}$ null). A) E10.5 *Meis1*$^{fl/fl\ VeCre}$ null embryos show no significant difference in the number of CD45^{pos} cells as compared to wild-type littermates. B) There is no significant difference in the number of CD45^{neg}VEC^{pos} cells in E10.5 *Meis1*$^{fl/fl\ VeCre}$ null embryos compared to wild-type littermates. C) E11.5 *Meis1*$^{fl/fl\ VeCre}$ null DAs show no significant difference in the number of CD45^{pos} or D) CD45^{neg}VEC^{pos} cells compared to wild-type embryos at the time of sort. Data shown is normalized to the total number of cells in each sample. Unpaired 2-tailed t-test and SEM shown on graph.

immunophenotypic effect of *Meis1* loss may be due to low *Meis1*$^{fl/fl}$ exon 8 excision.

3.5.2 Quantification of ESLAM^{pos} Cells in E14.5 FL

There was an opportunity for a preliminary experiment to quantify the number of ESLAM cells in E14.5 FLs of wild-type and *Meis1*$^{fl/fl\ VeCre}$ null embryos. Statistics could not be performed as there was only one wild-type embryo while three were *Meis1*$^{fl/fl\ VeCre}$ null. However all *Meis1*$^{fl/fl\ VeCre}$ null embryos showed drastically reduced ESLAM numbers in comparison to the one wild-type value (Figure 3.8). The normal reported range is 260-760 ESLAMs per E14.5 FL in wild-type mice, and all three of our *Meis1*$^{fl/fl\ VeCre}$ null embryos fall below this range [4, 107]. If this effect is replicated in later experiments, *Meis1*$^{fl/fl\ VeCre}$ null embryos may exhibit a defect in HSC expansion in the FL in comparison to wild-type littermates.

3.5.3 Hemorrhagic Phenotype in *Meis1*$^{fl/fl\ VeCre}$ Null Embryos

Defects in endothelial cell development and subsequent hematopoietic cell production can lead to a hemorrhage in developing embryos. The E14.5 embryos used for ESLAM staining were also observed for this possible phenotype at the time of dissection. No signs of hemorrhage were observed in the wild-type embryos, as they should have normal HSCs and formation of the vasculature (Figure 3.9). The three *Meis1*$^{fl/fl\ VeCre}$ null embryos did not show hemorrhage, despite the low ESLAM numbers observed in their FLs which may result in dysregulated blood production. Hemorrhage in our *Meis1*$^{fl/fl\ VeCre}$ null embryos may have been missed due to the small number small number of *Meis1*$^{fl/fl\ VeCre}$ null replicates, as this phenotype is rare in *Meis1*$^{-/-}$ mice.

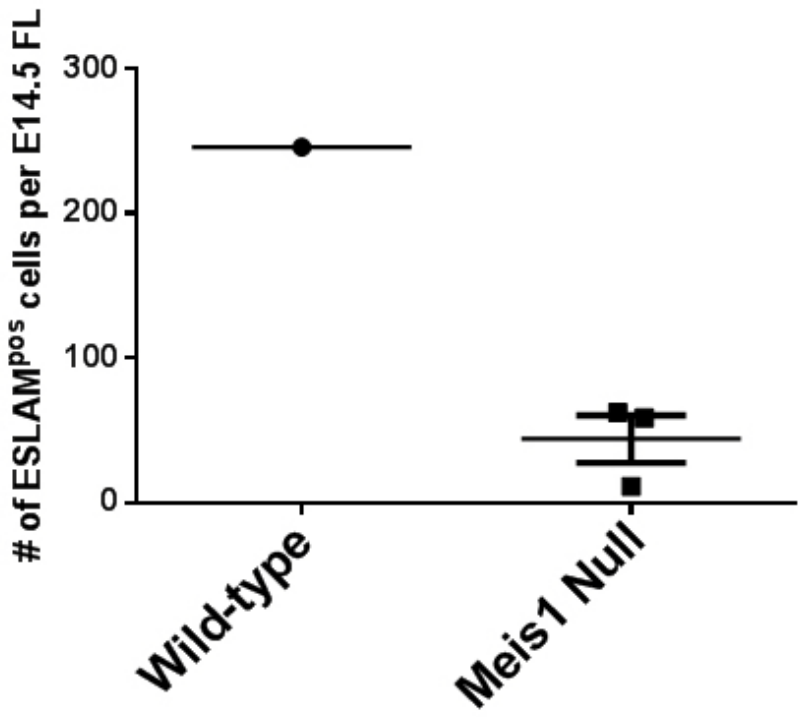

Figure 3.8 Number of ESLAM cells in E14.5 FL of Meis1$^{fl/fl\ VeCre}$ embryos

Number of ESLAM (CD45^{pos}EPCR^{pos}CD48^{neg}CD150^{pos}*)* cells during FACS analysis of single wild-type (N=1) and *Meis1$^{fl/fl\ VeCre}$* null (N=3) E14.5 FLs. *Meis1$^{fl/fl\ VeCre}$* null embryos displayed up to a 4-fold decrease in the number of ESLAM cells when compared to one wild-type embryo. SEM shown on graph.

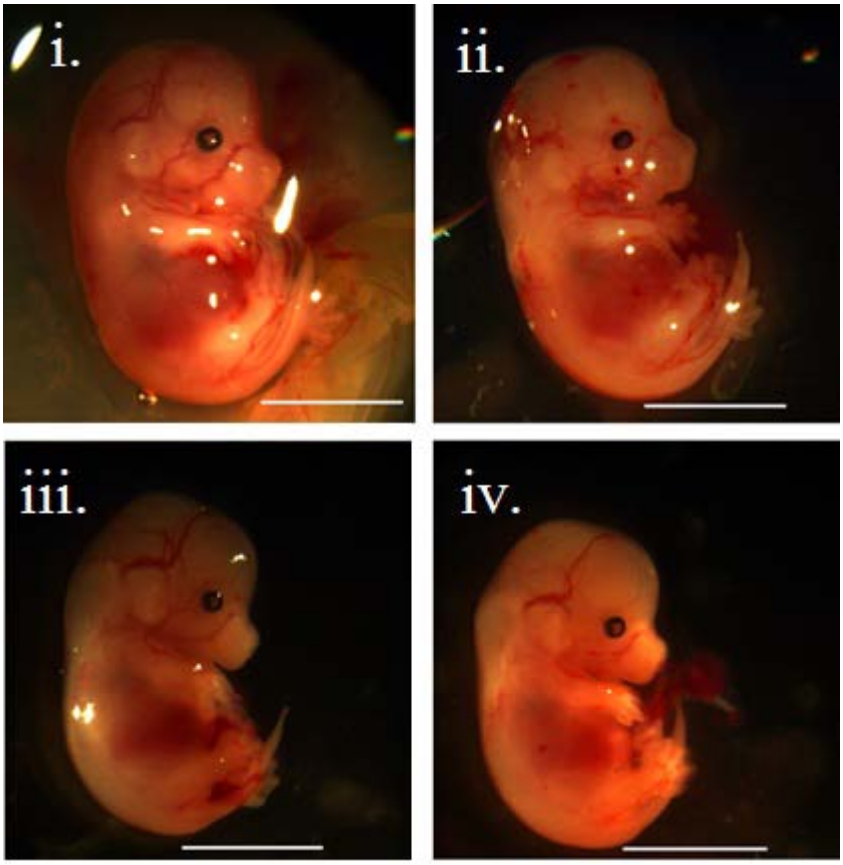

Figure 3.9 Phenotypic examination of E14.5 Meis1$^{fl/fl\ VeCre}$ embryos

E14.5 wild-type embryo (i), and *Meis1*$^{fl/fl\ VeCre}$ null littermates (ii-iv). Scale bar 0.5 cm.

3.5.4 Whole DA Culture of Meis1$^{fl/fl\ VeCre}$ Embryos

In addition to culturing sorted cells isolated from embryonic tissues, our *ex vivo* co-culture assay allows the culture of whole unsorted organs. Using OP9 cell co-culture, at 3-3 O_2 tension, whole unsorted E9.5 DAs from Meis1$^{fl/fl\ VeCre}$ embryos were cultured. This allowed for the measurement of the maintenance and production of CD45^{pos} hematopoietic cells *ex vivo*. DAs were isolated and cultured in individual wells. After 6 days wells containing wild-type and *Meis1*$^{fl/fl\ VeCre}$ null embryos were analyzed for their capacity to generate or expand CD45^{pos} cells. When assayed after 6 days, there was no significant difference in the number of CD45^{pos} hematopoietic cells generated by wild-type and *Meis1*$^{fl/fl\ VeCre}$ null embryos (p=0.17) (Figure 3.10). This suggests that there is no defect in the production of CD45^{pos} cells from *Meis1*$^{fl/fl\ VeCre}$ null embryos at E9.5. However, the possibility of the expansion of pre-existing CD45^{pos} cells may mask any defect in CD45^{pos} cell generation from pre-HE.

3.5.5 Immunofluorescent Staining of Meis1$^{fl/fl\ VeCre}$ Embryos

Single representative sections from E10.5 wild-type and *Meis1* $^{fl/fl\ VeCre}$ null embryos containing the largest contiguous section of DA were stained for VEC and CD41. Sections were analyzed for the number of CD41^{pos} cells located along the length of VEC^{pos} DA. CD41^{pos} cells counted were divided by the total length of the DA present. Data from two wild-type and four *Meis1*$^{fl/fl\ VeCre}$ null embryos were collected. There was no significant difference between the numbers of CD41^{pos} cells in the E10.5 DA of wild-type and *Meis1*$^{fl/fl\ VeCre}$ null embryos quantitated in this manner (p=0.70) (Figure 3.11). Representative images of hematopoietic clusters in wild-type and *Meis1*$^{fl/fl\ VeCre}$ null embryos are shown (Figure 3.12).

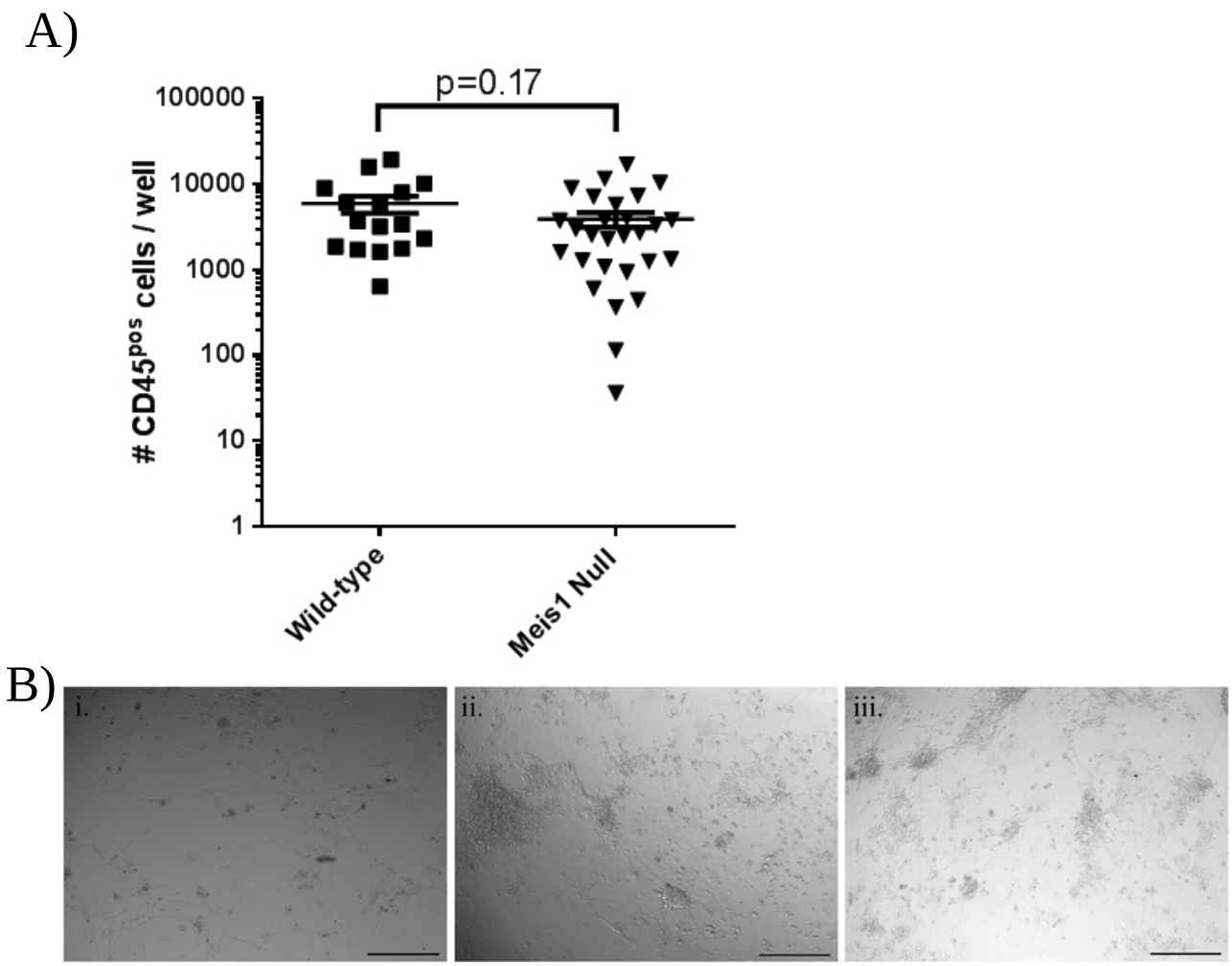

Figure 3.10 Analysis of Meis1$^{fl/fl\ VeCre}$ E9.5 DAs in *ex vivo* culture

A) Graph displaying the number of CD45^{pos} cells per well containing single E9.5 wild-type (N=16) or null (N=28) DAs. CD45^{pos} cells have either developed from CD45^{neg} pre-HE or expanded from circulating hematopoietic cells present in the DA. Combined data from four experiments shown. Unpaired 2-tailed t-test and SEM shown on graph. B) Representative images of *ex vivo* culture wells. i) OP9 cell monolayer only, ii) wild-type well, iii) *Meis1*$^{fl/fl\ VeCre}$ null embryo well. Images taken at 10X magnification with 250 μm scale bar shown.

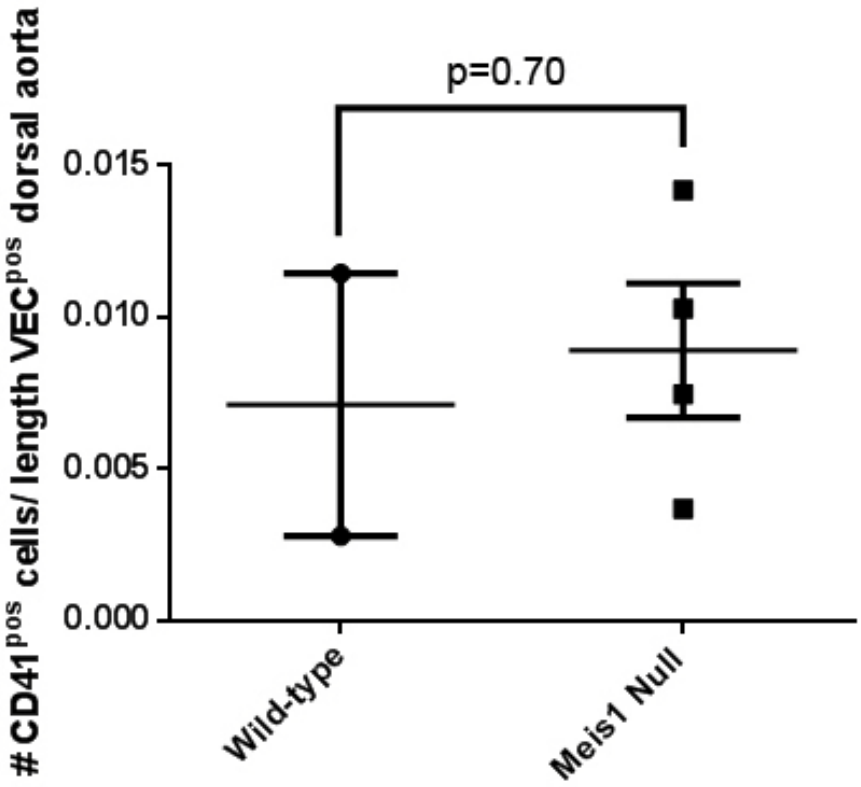

Figure 3.11 Enumeration of CD41^{pos} cells in E10.5 DA sections

The number of CD41^{pos} cells emerging from the surface of VEC^{pos} endothelial cell layer was not significantly different for wild-type (N=2) and *Meis1*$^{fl/fl\ VeCre}$ null (N=4) embryos as shown on graph. Cells counted at 40x objective and normalized based on total length VEC^{pos} DA counted. Unpaired 2-tailed t-test and SEM shown on graph.

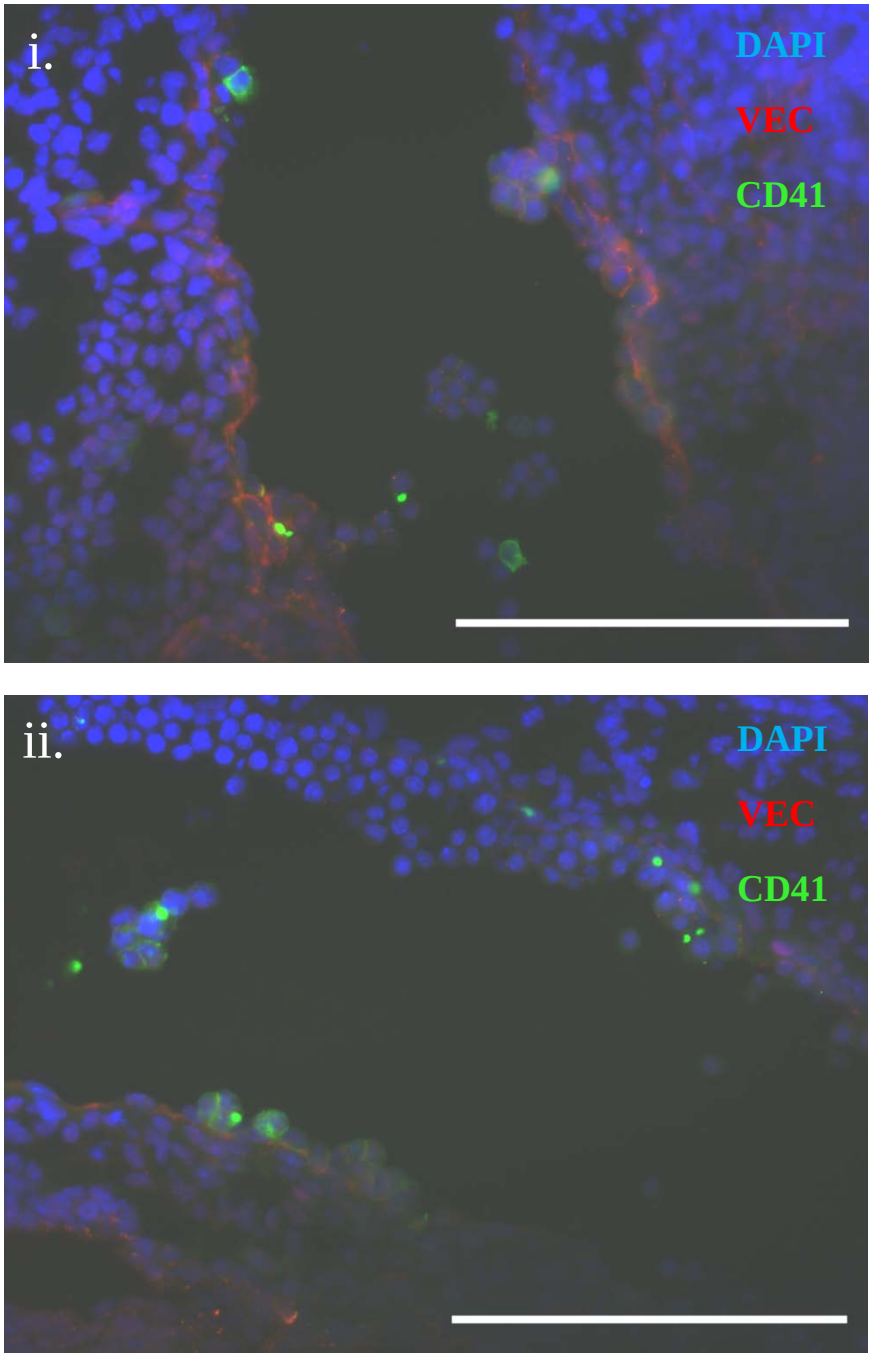

Figure 3.12 Immunofluorescence imaging of E10.5 Meis1$^{fl/fl\ VeCre}$ DAs

Images of representative sections from i) wild-type and ii) *Meis1*$^{fl/fl\ VeCre}$ null embryos at 40X magnification which show no discernable structural differences, and no significant difference in the number of CD41^{pos} cells present along VEC^{pos} DA. Scale bar 150 μm.

4. Discussion

Development of an *ex vivo* assay for the interrogation of EHT is crucial to better understand genes and conditions involved in this complex trans-differentiation process. As the cell markers which identify these transitional cell populations continue to be identified, a functional assay to determine their contributions to EHT is needed. These transitional cells retain many aspects of their endothelial identity, and do not contain hematopoietic potential at early stages of development. Traditional methods such as transplantation do not provide a functional read-out for cells at these earlier endothelial stages of EHT. The work in this thesis attempts to provide an assay for the hematopoietic potential of these early pre-HE cell populations. Variability in the progression of EHT to the production of hematopoietic cells is present in our assay, and may be improved upon in later experiments. The assay could then be used to screen the novel genes identified in our RNA-seq analysis. Additionally it would be important to validate genes previously reported in the literature as important for EHT, which have been assayed by other methods. In the future, information given by the interrogation of genes in this assay could be used for direct conversion of endothelial cells to hematopoietic cells *ex vivo*.

4.1 Analysis of RNA-seq Libraries

Our sequencing libraries were generated through the collection of bulk endothelial cells from E10.5 wild-type DAs, and compared to Runx1+24mCNE-GFP depleted endothelial cells from E10.5 transgenic embryos. We used a sorting scheme to determine the gene expression in a rare population of cells indirectly, allowing us to collect material in a shorter period of time, while allowing multiple experiments to be run from the same sample. However this indirect method may have resulted in the loss of some lower expressed TFs important in EHT. In particular, *Runx1*, thought of as a positive control due to its known role in HE, did not emerge in

our up-regulated TF analysis of the libraries [28, 46]. When the up-regulated genes were extracted by comparison of the two sequencing libraries, *Runx1* showed a fold change of 1.0258. Originally we hypothesized that as the Runx1+24mCNE-GFP depleted library was sorted based only on the expression of the +24 enhancer of *Runx1*, perhaps additional *Runx1* expression in cells not involving the activation of this enhancer was obscuring the difference between the two libraries. The +24 enhancer was shown to mark a specific subpopulation of *Runx1* expressing cells involved in hematopoiesis, but not other endogenously *Runx1* expressing cells [46]. We hypothesized that some *Runx1* transcripts may still be transcribed within the Runx1+24mCNE-GFP-depleted endothelial cell library. In order to confirm this, the expression of *Runx1* was measured through use of qRT-PCR primers which are common to all 5 isoforms, spanning the junction of exons 4 and 5. Expression was measured in Runx1+24mCNE-GFP^{pos} sorted HE as compared to Runx1+24mCNE-GFP^{neg} endothelium. In these cell populations, *Runx1* was shown to be expressed in Runx1+24mCNE-GFP^{pos} cells 40-fold higher than in Runx1+24mCNE-GFP^{neg} cells, which showed undetectable levels of expression. Therefore, the Runx1+24mCNE-GFP^{neg} endothelial cell library sorted and sequenced should contain minimal *Runx1* expression when sorted based on +24mCNE enhancer expression.

Upon closer examination of sequencing data, there appeared to be a large bias in the number of reads aligning to the 3' end of *Runx1*, while 5' reads were largely absent. The lack of coverage in our RNA-seq libraries resulted in a lower reported RPKM value for *Runx1* gene expression, as reads are only counted if they align into transcripts along the entire gene. This is likely due to the 3' bias involved with library generation, as mRNA transcripts are first positively selected using oligoDT primers which bind to their poly-A tail [108]. The use of poly-A selection is thought to cause 3' bias as transcripts selected in this manner must, by definition for

poly-A binding, contain this region of the gene. Furthermore, as the transcripts generated by the distal promoter are 2-4 exons longer, they are more likely to have been fragmented during selection. This fragmentation would cause a decrease in reads from the distal isoforms as the 5' end was lost [108]. This bias can be overcome by using a new negative selection technique involving ribosomal RNA depletion, which avoids poly-A selection and its associated biases [108]. Conscious of the 3' bias, we re-analyzed the libraries instead normalizing to the number of reads on the 3'-most exon of each gene, an alternative to quantifying reads which cover the entire locus. With this analysis the expression of *Runx1* was slightly increased, however as this bias occurred and was corrected in both libraries, fold change increased only slightly to 1.4928, just under our 1.5-fold cut-off threshold. Libraries containing complete sequencing of the 5' end would be necessary for determining the importance of the recently identified *Runx1* isoforms in EHT of the DA at E10.5. This is particularly important as unique roles have been suggested for *Runx1* isoforms throughout different stages of hematopoietic development, although consensus has not been met on this topic [46, 76, 78, 109]. A definite explanation for the incongruous results between the RNA-seq libraries and the expression of *Runx1* remains to be elucidated, and is further complicated by the multiple isoforms and splice variants which characterize *Runx1*.

Despite this challenge, many other genes known to be involved in HE did emerge from our analysis, including *Gfi1b*, and *Gata2*, and other genes have been reported as important in hematopoiesis, including *Pbx1*, *Hoxa9*, *Meis1*, *Gata1*, *Stat3*, *Stat4* and *Hes1*. Our sequencing method did determine important known and candidate regulators of EHT, though known master regulators such as *Runx1* were missed likely due to technical limitations of the RNA-seq library generation. It would be important to isolate the sorted populations used for sequencing, and interrogate the expression of each *Runx*1 isoform in these cells, along with sorted HE.

4.2 Validation of RNA-seq Results

qRT-PCR validation of the library in sorted HE cells showed that 5/9 (*Pbx1a, Gata1, Gfi1b, Stat4,* and *Meis1*) of the up-regulated TFs were expressed at a higher level in Runx1+24mCNE-GFP^{pos} HE than Runx1+24mCNE-GFP^{neg} endothelial cells at E10.5. *Pbx1b*, *Gata2*, and *Stat3* were enriched less than 2-fold between Runx1+24mCNE-GFP^{pos} cells as compared to Runx1+24mCNE-GFP^{neg} cells, however they exhibited a similar relationship in differential expression values between the two sequencing libraries as well, all less than 2-fold enriched in bulk endothelial cells. *Hes1* was the only gene higher expressed in sorted Runx1+24mCNE-GFP^{neg} endothelial cells, but even this relationship was less than 2-fold change. *Hes1* has been shown to be specifically expressed in intra-aortal clusters of the E10.5 DA [110]. The exclusion of c-Kit^{pos} cells in our HE sort therefore excludes the majority of cells expressing *Hes1*, and acts to mitigate the possible difference in expression between Runx1+24mCNE-GFP^{pos} and Runx1+24mCNE-GFP^{neg} HE cells. Overall the RNA-seq libraries created allowed us to identify multiple genes already known to be important in EHT, as well as others known in hematopoiesis. The direct sequencing of Runx1+24mCNE^{neg} endothelial cells, c-Kit^{neg}Runx1+24mCNE-GFP^{pos} HE and c-Kit^{pos} Runx1+24mCNE-GFP^{pos} cluster cells would allow us to identify minimally expressed genes that are unique to these transitioning cell populations, creating a more complete picture of EHT within the embryo.

4.3 *Ex vivo* Co-culture Assay

In order to validate the functional role of TFs identified in the analysis of our RNA-seq libraries, we aimed to establish an *ex vivo* culture system for E9.5 pre-HE. The rationale for the use of E9.5 embryos to validate these TFs identified at E10.5 was to allow the knockdown of these genes in endothelium before their peak of expression at E10.5. Our original experiment to

culture finely sorted E9.5 SSEA-1^{neg}CD45^{neg} CD31^{pos} c-Kit^{neg}Runx1+24mCNE-GFP^{pos} endothelial cells before the acquisition of hematopoietic markers CD45 and c-Kit showed no growth in *ex vivo* culture, despite the hypothesis that this population contains potential for hematopoietic growth and sequential acquisition of these markers *in vivo*. It is possible that these cells were too immature to grow outside of the embryonic environment, either unable to sustain expression of pathways allowing EHT when dissociated from an endothelial layer, or lacking extracellular signals from surrounding cells they would encounter *in vivo* [88, 101, 111].

Fraser *et al*. compared the potential for hematopoietic growth in enzymatically dissociated cells isolated from E9.5 DAs, to that in mechanically dissociated cells [58]. They found that only enzymatically dissociated cells, sorted on VEC^{pos}CD45^{neg}, and not the loosely-attached cluster cells isolated mechanically were capable of forming hematopoietic colonies, and CD31^{pos} endothelial cell networks. This suggests that endothelial cells enzymatically dissociated from the wall of the DA contain pre-HE, not the more loosely attached cells in the lumen at E9.5 [58]. The reason our finely sorted pre-HE did not grow *ex vivo*, is likely unaffected, and in fact possibly helped by their enzymatic dissociation from the DA. It is possible that they are missing extracellular signals from their niche, when cultured in an OP9 co-culture environment, outside of the DA.

There is evidence that signalling from sub aortic patches influence the development of hematopoietic clusters in the DA [88, 111]. It was found that Gata3$^{-/-}$ embryos died at E11.5, but that *Gata3* is not expressed in cluster cells of the DA [111]. Instead *Gata3* expression was observed in sub-aortic patches of the mesenchyme, where it is involved in sympathetic nervous system (SNS) development and the production of catecholamines [111]. The addition of catecholamines to *ex vivo* culture of whole DAs isolated from E11.5 Gata3$^{-/-}$ embryos rescued

hematopoietic cell generation and increased repopulation of irradiated adult recipients [111]. This positive effect in donor repopulation was observed even when catecholamines were added to wild-type AGM cultures [111]. Richard *et al.* showed that the effect of signalling between mesodermal sub-aortic patches and the endothelium is extremely localized [88]. By severing tissue between the lateral plate and DA of an avian embryo on one side, they were able to prevent the migration of mesoderm toward the centreline, where the DA is located [88]. On the side of the DA lacking mesodermal signalling, neither *Runx1* expression nor hematopoietic clusters are present, while the intact side develops normally [88]. Expression of *Notch1* in these patches has also been shown to be important in this process [101]. The effect of catecholamines and Notch signalling from supportive cells surrounding the DA are key examples of factors critical for cluster emergence, despite their location beyond the HE. It is likely that the difficulty in growing finely sorted pre-HE cells in isolation from the DA involves the lack of these exogenous signals which would normally be produced within the embryo.

In order to interrogate the activity of a more heterogeneous cell population, increasing the possibility for signalling between developing hemogenic and vascular endothelial cells, we went back to validate that $CD45^{pos}$ cell generation was possible from bulk $CD45^{neg}$ cells. We were able to further refine this $CD45^{neg}$ sorted population through the use of the Runx1+24mCNE-GFP marker in our mouse, found to mark HE cells [46]. The inclusion of CD45 and Runx1+24mCNE-GFP markers allowed us to specifically interrogate the activity of HE cells in culture. The Runx1+24mCNE-GFP^{pos} cell population is made up largely of HE at this early time-point, as primitive hematopoietic cells which express this enhancer do not develop in the DA until E10.5 [46].

Although possibly limiting, in that we may be depleting cells of supportive mesodermal tissue, the use of sorted cell populations allows us to specifically define which cells are undergoing EHT in the DA. Previous experiments in the literature involving the culture of embryos from early time-points were to facilitate transplantation into adult recipients [28, 112]. These techniques employed whole organ culture without FACS sorting of specific cell populations [28, 112]. These cultures serve the purpose of allowing development of hematopoietic cells from a specific organ without nonspecific input from other regions of the embryo, and were necessary to identify intra-embryonic hematopoiesis [28]. In light of this, the need for an assay to allow the *ex vivo* culture of specific cell populations is important to delineate the process of EHT. The culture of HE cells isolated from E10.5 or E11.5 DAs, specifically of mature cluster cells expressing CD45 or c-Kit have shown consistent hematopoietic growth *ex vivo* [58, 102, 113, 114]. After the peak at E10.5, until E11.5, it has been observed that cluster numbers decrease as hematopoiesis shifts towards the FL [42]. This is important to remember as we are interested in manipulating genes in endothelium still retaining HE potential, prior to cluster formation and EHT.

In order to be successful in the culture of E9.5 embryos, containing pre-HE which holds potential for manipulation, and development, we found that a less refined sorting scheme was necessary. The use of sorted $CD45^{neg}$Runx1+24mCNE-GFP^{pos} cells, not gated on CD31 expression, may allow endothelial cells further along the process of EHT to be included, if they have already begun down-regulating endothelial makers to emerge from the endothelial layer. As well, our relaxed sorting scheme does not exclude the very few cells at E9.5 which may express c-Kit. As c-Kit expression is acquired by cells following *Runx1* expression, c-Kit^{pos} cells are not the strictly pre-HE that we are investigating [42, 102]. If we were to culture c-Kit^{pos} HE from

E10.5 embryos, our assay could be allowing cells pointed in the path of differentiation to continue along this trajectory, unaffected by any culture manipulation. This may be true in our E9.5 culture as well, though by combining an earlier E9.5 time-point, and Runx1+24mCNE-GFP expression, these assay conditions are our best option to study EHT. If we are still able to block this transition and acquisition of CD45 in early HE our assay is an important tool in interrogating genes involved in EHT. Further manipulation of our *ex vivo* co-culture assay through the use of viral transduction for shRNA constructs, or the addition of other γ-secretase inhibitors is an important step to validating the importance of our assay.

The specificity of the Runx1+24mCNE-GFP marker was an important factor in validating our assay. Although *Runx1* is expressed in mesoderm surrounding the DA, the +24mCNE-GFP marker is not active in these cells [46]. It is possible that effect of the less stringent sorting scheme on an increase in cell number, and therefore increased density of cells in our *ex vivo* assay causes a positive effect in cell growth alone. Additionally interactions within the entire population of Runx1+24mCNE-GFP^{pos} cells, including cells which have already begun to down-regulate CD31 expression, may be important. A supportive relationship is suggested when you compare the size of each cell population. The number of total Runx1+24mCNE-GFP cells in the DA at E10.5 (~30,000) greatly outnumbers the 1 LT-HSC proposed to exist in the embryo at this time, as well as the 15 HSCs present after DA culture [28, 29, 46]. The majority of HE cells present at E9.5-E10.5 therefore do not undergo EHT to the conclusion of pre-HSC production. Instead these cells may be playing a supportive role through the secretion of cytokines, or the generation of more restricted EMPs [54].

4.4 Effect of Oxygen Tension During *Ex vivo C*ulture

Pre-HE isolated from E9.5 cells may require different conditions to maintain endothelial identity, and establish themselves at this early time-point, before hematopoietic potential can been gained. Before the establishment of an endothelial layer in the embryo, the culture of mesodermal precursors isolated from E7.5 embryos has been used to assay these earlier populations for their endothelial and hematopoietic potential [63]. A balance between culture conditions is needed to allow the growth of these transitional endothelial cells, undergoing down-regulation of endothelial genes upon hematopoietic commitment [89, 94]. Borges *et al.* cultured E7.5 mesodermal cells separately at 5% O_2 with cytokines such as VEGF and bFGF to examine the endothelial potential of sorted cell populations [63, 70]. Separately, cells were cultured at 20% O_2 with hematopoietic cytokines IL-3, SCF, EPO, and G-CSF, to assay hematopoietic potential. It was reported that endothelial growth from such an early time-point was only observed when cells were cultured at 5% O_2 [63].

With this knowledge, and the significant increase in Runx1+24mCNE-GFP expression observed in $CD45^{neg}$ and $CD45^{mid}$ cells cultured at 5% O_2, we were encouraged to examine the effect of culturing cells in 2-4, and 3-3 transitional culture periods. This transitional culture method for sorted HE cells has not been previously reported in the literature. The highest Runx1+24mCNE-GFP values per well were observed in 3-3 culture conditions, possibly due to the longest period of 5% O_2 exposure. Runx1+24mCNE-GFP expression was also higher in the 2-4 treatment when compared to 6 days at 20% O_2 but this was not significant. The establishment and maintenance of Runx1+24mCNE-GFP expressing endothelial cells during 5% O_2 culture may be partially due to the effect of hypoxia on these cells. Hypoxia is known to cause the production of factors such as VEGF as an angiogenic response, which acts directly on

endothelial cells [69]. It was not tested whether the exogenous addition of VEGF would show an increased effect in the establishment of HE, beyond the trend observed in 5% O_2 culture, but this would be an interesting condition to investigate.

Equally important, the further differentiation into $CD45^{pos}$ hematopoietic cells as a measure of EHT may be affected by O_2 transition as well. This process seems to be more permissive with respect to O_2 tension as there was no significant difference between 5% and 20% O_2 treatments in generating hematopoietic cells. Despite this, we hypothesized that a more established endothelial cell layer, expressing Runx1+24mCNE-GFP would increase the likelihood of hematopoietic growth and differentiation, as $Runx1^{-/-}$ embryos lack this expression in pre-HE, and do not produce hematopoietic cells in culture [19]. The difference in $CD45^{pos}$ cell production between 20% O_2 treatment and 2-4 or 3-3 transitional culture was not significant, though the highest values for $CD45^{pos}$ cell generation were observed in the 3-3 culture.

A major effect on the significance of our *ex vivo* assay is that the variability of each well in maintaining HE cells, and generating $CD45^{pos}$ cells. The results can be interpreted slightly differently if we think about this culture system in the terms of a positive versus negative outcome. This can be used if we consider wells which generated at least 1% of the input SSEA-$1^{neg}CD45^{neg}GFP^{pos}$ cell number in output HE or $CD45^{pos}$ cells as positive, and less than 1% as negative. This cut-off was chosen as almost all wells did produce a few HE, or $CD45^{pos}$ cells, but these numbers were far below 1% when normalized to total input cell number. Thinking of the proportion of positive wells for HE cell maintenance 0/9 wells generated HE at 20% O_2 compared to 4/11 wells in 3-3 conditions. While these proportions appears to be significantly different, it is not significant when tested by Fisher's exact test ($p^{Fishers}$=0.094). The comparison of 20% O_2 and 3-3 culture conditions should be replicated to ensure statistical significance,

however we chose to go further with 3-3 culture based on the trend observed. For $CD45^{pos}$ cell generation, 3/9 wells were positive when cultured at 20% O_2, compared to 9/11 wells for 3-3. When Fisher's exact test was performed the proportion of wells which generated $CD45^{pos}$ cells in 3-3 conditions was significantly higher than at 20% O_2 (p^{Fisher}=0.03). This suggests that the 3-3 cultures allow more consistent hematopoietic cell generation. The combination of possibly increased HE maintenance, with significantly increased $CD45^{pos}$ cell generation in 3-3 conditions resulted in our choice for O_2 tension transition conditions for our *ex vivo* assay. In addition to O_2 concentration, the age and health of OP9 cells in each experiment should be kept consistent to encouraging hematopoietic development *ex vivo*, and decrease variability inherent in the assay.

4.5 Shear Stress and Nitric Oxide in *Ex vivo* Culture

Fluid flow and nitric oxide (NO) signalling within the DA are key regulators of hematopoietic development in this organ [115]. It has been shown that shear stress, and the addition of NO donors in culture, can increase the engraftment of cells from cultured E9.5 DAs when they are transplanted into irradiated adult recipients [115, 116]. While likely a very small effect, as there is no significant difference in CD45 generation between the different O_2 tensions, the shear stress introduced to cells during the transportation of plates from the 5% O_2 incubator to the 20% O_2 incubator cannot be ruled out. The effect of adding NO donors would be an interesting addition to the culture of these developing endothelial cells, as fluid flow present in the developing embryo, generated by the heartbeat, is important for cardiovascular and hematopoietic development [116].

4.6 Effect of Notch Blockage in *Ex vivo* Culture

Notch1 is known to be important for the development of HE and is thought to be upstream of *Runx1* [81]. *Runx1* expression is absent in the DA of Notch1$^{-/-}$ embryos, which can be rescued by enforced *Runx1* expression [81]. Using this knowledge we tested modulation of our *ex vivo* culture assay with the addition of a γ-secretase inhibitor. The use of DAPT, another γ- secretase inhibitor was reported to have numerous effects on cultured DAs isolated from E9.5 embryos, depending on the endpoint at which the cultures were interrogated [88]. Richard *et al.* observed a transient increase in CD45^{pos} cells from E9.5 DA explants at day 3 midway through culture, but a (non-significant) inversion of that was observed by day 6, due to an increase in apoptosis in these wells [24]. Our decrease in CD45^{pos} cells in DFPAA treated wells at day 6 was also not significant, though the largest values for CD45^{pos} cell generation per input cell plated were in the DMSO treated controls. Additionally, when we erroneously analyzed one experiment (data not shown) at day 5, an increase was observed in the number of CD45^{pos} cells in the DFPAA treated wells, though not significant. It is possible that this initial expansion is due to the growth of primitive progenitors, which are not reliant on Notch signalling for development and undergo apoptosis in the well without the replacement by definitive hematopoietic progenitors which require Notch [80, 86, 110, 117]. Notch signalling has been observed to separate the primitive and definitive waves of hematopoiesis in zebrafish, and primitive hematopoiesis within the YS of Notch1$^{-/-}$ embryos showed no difference from wild-type controls [80, 86, 87, 110]. The fact that our assay involving the culture of sorted E9.5 cells, replicates the results of Notch blockage experiments done in whole organ explant culture, is encouraging in regards to the use of sorted cell populations to assay EHT within the DA.

4.7 Analysis of Single Meis1$^{fl/fl\ VeCre}$ Embryos

Single E10.5 and E11.5 Meis1$^{fl/fl\ VeCre}$ embryos were analyzed through flow cytometry, and immunofluorescent staining of cryosections. When using flow cytometry to compare wild-type and *Meis1*$^{fl/fl\ VeCre}$ null embryos at E10.5 and E11.5, there were no significant differences in the number of CD45^{pos} cells, or CD45^{neg}VEC^{pos} in DAs of either group. Differences between wild-type and *Meis1*$^{fl/fl\ VeCre}$ null embryos could be masked by contribution from primitive hematopoietic cells of the YS, which stain positively for CD45. YS hematopoiesis appeared to be normal in Meis1$^{-/-}$ embryos, and the late stage of lethality of these mice also signal that *Meis1* is not critical for YS hematopoiesis [100]. In Meis1$^{-/-}$ embryos, hemorrhaging and changes in hematopoietic cell number were not described until after E11.5 [100]. The use of a conditional model introduces the variable of Cre activity into how penetrant a phenotype is. It is important to note that although the E10.5 litter contained two embryos with 90% of endothelial cells containing excised *Meis1*$^{fl/fl}$ exon 8, when the E11.5 litter was analyzed only one embryo was measured and only 50% of endothelial cells contained excised *Meis1*$^{fl/fl}$ exon 8. This suggests variability in the activity of Cre in the excision of *Meis1*$^{fl/fl}$ exon 8. It is likely that any phenotype of *Meis1* deletion in these E11.5 embryos was masked by a high percentage of cells containing intact *Meis1*$^{fl/fl}$ exon 8. Additionally Meis1 is known to bind with multiple hox proteins, involved in hematopoiesis and limb development [97-99]. In particular, the relationship between *Hoxa9* and *Meis1* is known in leukemia, and both of these transcription factors were identified in our RNA-seq analysis [97]. As there are multiple *Hox* genes and binding partners, the lack of *Meis1* may be compensated by *Hox* binding with other co-factors. Even *Meis1* excision to a level causing haploinsufficiency in our homozygous floxed embryos may not lead to a phenotypic difference, as Meis1$^{+/-}$ mice showed no phenotype in previous studies [100].

4.8 Hemorrhagic Phenotype in Meis1$^{fl/fl\ VeCre}$ Embryos

When comparing embryos at E9.5 and E10.5 no obvious differences or signs of hemorrhaging were observed between wild-type and *Meis1*$^{fl/fl\ VeCre}$ null embryos. When observing E14.5 embryos used for FL ESLAM staining, as a pronounced effect may be observed in older embryos of a larger size, no difference was observed between one wild-type and three *Meis1*$^{fl/fl\ VeCre}$ null embryos. However, this does not rule out the possibility of a hemorrhagic phenotype being observed if more replicates were examined. In the *Runx1*$^{fl/fl\ VeCre}$ conditional knockout model embryos only 10% of E12.5 embryos exhibit central nervous system hemorrhaging and fetal anemia, and only 65% die in mid-gestation [26]. The Meis1$^{-/-}$ mouse model showed a hemorrhagic phenotype by E11.5 in about a quarter of homozygous deleted embryos, and by E12.5 showed liver size differences and a pale phenotype overall [100]. It is likely that the effects of *Meis1*$^{fl/fl\ VeCre}$ deletion were not penetrant enough to be observed in our small sample size, in addition to the use of a tissue specific model resulting in an even rarer phenotype.

4.9 *Ex vivo* Culture of E9.5 Meis1$^{fl/fl\ VeCre}$ Embryos

One of the goals for both validation of Meis1 as important in EHT, and validation of our *ex vivo* assay for EHT, was to grow DAs isolated from Meis1$^{fl/fl\ VeCre}$ embryos *ex vivo*. As Meis1 embryos are difficult to genotype, requiring the use of 4 primer sets, we decided not to genotype and pool embryos prior to sorting. The allotment of additional time before sorting for genotyping would have resulted in the analysis of embryos closer to an E9.0 time-point than E9.5. Additionally instead of sorting single E9.5 DAs and risking the loss of important HE cells while sorting, we chose to dissect, dissociate, and plate whole DAs isolated from single E9.5 embryos as a pilot experiment. An overall difference in the number of CD45^{pos} cells over 4 experiments

was not significant between wild-type and *Meis1*$^{fl/fl\ VeCre}$ null embryos. The only replicate which showed a significant difference between groups for CD45^{pos} cell generation took place nearly 12 months prior to the final replicates. This could be an artefact, or due to decreasing activity of Cre with increasing generations [106]. Either way, as with the analysis of single E10.5 DAs, contributions of CD45^{pos} cells in circulation cannot be ruled out when whole DAs are plated in culture, resulting in their expansion. It was our assumption that any possible differences in hematopoietic cell function would be large enough to be detected beyond this effect, but either this is not the case, or there is truly no difference. The depletion of CD45^{pos} cells through sorting single DAs is an important future step to determine if it is possible to sort pre-HE cells from single E9.5 DAs, and maintain cell growth. Alternatively we could repeat experiments as done, with whole organ culture, followed by the collection of non-adherent cells from each well of *ex vivo* co-culture, and qRT-PCR to determine *Meis1* expression in these hematopoietic cells produced. This would determine if CD45^{pos} cells generated are from "escaped" cells containing intact *Meis1*$^{fl/fl}$ exon 8, developing normally, or from cells with *Meis1*$^{fl/fl}$ exon 8 excised.

4.10 Quantification of ESLAM Cells in E14.5 Meis1$^{fl/fl\ VeCre}$ FL

The FL is often the next step of interrogation when determining the role of a gene in embryonic hematopoiesis [75, 93, 100]. The number of ESLAM^{pos} cells in wild-type and *Meis1*$^{fl/fl\ VeCre}$ null FLs at E14.5 was quantified. All three of the null FLs at E14.5 showed ESLAM numbers far below the normal range of 260-760 ESLAMS, with 11-62 ESLAMs per E14.5 FL. While no statistics could be performed due to lack of wild-type replicates, the one wild-type was at the lower end of the normal range reported in wild-type mice, at 245 [107]. If this deficiency in hematopoiesis within the FL is confirmed with subsequent experiments, it

confirms the role of *Meis1* in HSC development. Azcoitia *et al.* observed a decrease in absolute numbers of LSKs in the Meis1$^{-/-}$ FL at E12.5 as well [100].

4.11 The Role of Meis1 in the Endothelium and HSC

No significant differences were found between the generation of CD45^{pos} cells in the culture of wild-type and *Meis1*$^{fl/fl\ VeCre}$ null embryos. This assay is meant to interrogate the functional significance of genes in EHT in E9.5 pre-HE. Our preliminary ESLAM data supports the role of *Meis1* at the HSC level, although additional experiments are required to fully support this. *Meis1* is thought to be involved in HSC quiescence, and the lack of quiescence due to *Meis1* loss may cause the increased proliferation and depletion of ESLAM cells of the FL [118]. The E11.5-E14.5 range in which Meis1$^{-/-}$ mice die also supports the role of *Meis1* at the level of the HSC, while it may be dispensable before E11.5 when EHT is occurring [100]. Meis1$^{-/-}$ embryos showed hemorrhaging at E11.5 which may have been due to improper vessel formation through a lack of *Hox* and *Meis1* interactions required for vascular development, while later deaths at E14.5 could be attributed to defective blood production from HSCs lacking *Meis1* [100].

Meis1 was found to bind to the *Hif1α* promoter, and lack of *Meis1* has been correlated with lower *Hif1α* expression, leading to increased oxidative stress within these cells [118, 119]. The increase in reactive O_2 species (ROS) levels may decrease NO production, which as discussed earlier is important for EHT [115, 116, 120]. The involvement of Meis1 with oxidative stress and NO signalling maintains its possible role at the level of the endothelium and EHT, however whether it is crucial for this process remains to be determined [115, 116, 120].

4.12 Summary and Future Directions

The main objective of this thesis was to establish a reproducible assay for the growth of endothelial cells isolated from E9.5 embryos, allowing their transition through EHT *ex vivo*. This assay was then used to interrogate the effect of Notch inhibition through the addition of γ-secretase inhibitors. The addition of DFPAA did not significantly affect the production of HE and hematopoietic cells in our assay, however our results are congruent with the trend previously reported by Richard *et al*. [88]. In future experiments the co-culture of pre-HE with an OP9 cell monolayer in the conditions described in this thesis may be used to interrogate genes using shRNA mediated knockdown, or other inhibitory and stimulatory modulators of EHT. Preliminary experiments were performed using this *ex vivo* assay to compare the hematopoietic potential of DAs isolated from Meis1 $^{fl/fl\ VeCre}$ embryos. We identified *Meis1* through analysis of our RNA-seq libraries, along with 8 other known and novel candidate regulators of EHT. Previous assays to determine the role of genes or compounds in EHT exist in the literature; however there exists no assay including the combination of sorted pre-HE cells isolated from E9.5 embryos, and cultured on an OP9 cell monolayer in O_2 transition culture. While *Meis1* has been identified as important in embryonic hematopoiesis, the use of a conditional mouse model to restrict deletion to the endothelium has not been described in the literature [100]. With pan-deletion of *Meis1*, the confounding effects of *Meis1* loss in embryonic tissue development and HSC niche formation causing the hematopoietic defects observed in this model cannot be ruled out [100].

In the future, it would be important to determine why *Runx1*, beyond bias involved in library construction, shows low differential expression between our RNA-seq libraries. Isoform expression should be investigated in cells isolated using the indirect scheme employed for library

generation, as well as in sorted HE directly. In order to improve upon the *ex vivo* co-culture assay which has been developed, the addition of signalling compounds, or supportive non-hematopoietic cells present within the embryo would be an important conditions to investigate. These supportive cells and compounds might include catecholamines or sub-aortic mesenchymal cells to approximate the SNS support within the embryo, NO donors to approximate fluid flow, VEGF to encourage endothelial cell growth, or Notch-ligand expressing OP9 cells.

Characterization of the *Meis1*$^{fl/fl\ VeCre}$ null embryos must be explored further with respect to determining the range in the number of cells containing *Meis1*$^{fl/fl}$ exon 8 successfully excised between litters and littermates. If the number of generations affects Cre expression, the colony should be refreshed to rule out any complications due to silencing. As the hemorrhagic phenotype may be rare, more embryos of later time-points, E12.5-E14.5 must be examined, along with the replication of ESLAM staining on E14.5 FLs. In order to determine differences in the hematopoietic capacity of *Meis1*$^{fl/fl\ VeCre}$ null endothelial cells in culture, the depletion of differentiated hematopoietic cells from E9.5 DAs is an important technical challenge to explore. Alternatively, the collection of CD45^{pos} cells generated in culture, and percent excision qRT-PCR on these cells, will determine whether CD45^{pos} cells in culture contain intact *Meis1*$^{fl/fl}$ exon 8 or whether cells lacking *Meis1*$^{fl/fl}$ exon 8 are able to generate hematopoietic cells. Finally, the transplant of E10.5 DAs cultured *ex vivo* and injected into irradiated adult recipients would be an important step in characterizing the effect of *Meis1* excision in the embryonic endothelium on HSC development. Overall, the exploration of *Meis1* as a novel regulator of EHT leaves many avenues to explore. The development of an *ex vivo* co-culture assay which allows the maturation of pre-HE provides the opportunity to interrogate additional candidate regulators of EHT within this unique system.

References

1. Till, J.E., E.A. McCulloch, and L. Siminovitch, *A Stochastic Model of Stem Cell Proliferation, Based on the Growth of Spleen Colony-Forming Cells.* Proc Natl Acad Sci U S A, 1964. **51**: p. 29-36.
2. Doulatov, S., et al., *Hematopoiesis: a human perspective.* Cell Stem Cell, 2012. **10**(2): p. 120-36.
3. Jordan, C.T. and I.R. Lemischka, *Clonal and systemic analysis of long-term hematopoiesis in the mouse.* Genes Dev, 1990. **4**(2): p. 220-32.
4. Benz, C., et al., *Hematopoietic stem cell subtypes expand differentially during development and display distinct lymphopoietic programs.* Cell Stem Cell, 2012. **10**(3): p. 273-83.
5. Sieburg, H.B., et al., *The hematopoietic stem compartment consists of a limited number of discrete stem cell subsets.* Blood, 2006. **107**(6): p. 2311-6.
6. Christensen, J.L. and I.L. Weissman, *Flk-2 is a marker in hematopoietic stem cell differentiation: a simple method to isolate long-term stem cells.* Proc Natl Acad Sci U S A, 2001. **98**(25): p. 14541-6.
7. Morrison, S.J. and I.L. Weissman, *The long-term repopulating subset of hematopoietic stem cells is deterministic and isolatable by phenotype.* Immunity, 1994. **1**(8): p. 661-73.
8. Reya, T., et al., *Stem cells, cancer, and cancer stem cells.* Nature, 2001. **414**(6859): p. 105-11.
9. Adolfsson, J., et al., *Identification of Flt3+ lympho-myeloid stem cells lacking erythro-megakaryocytic potential a revised road map for adult blood lineage commitment.* Cell, 2005. **121**(2): p. 295-306.
10. Lancrin, C., et al., *Blood cell generation from the hemangioblast.* J Mol Med (Berl), 2010. **88**(2): p. 167-72.
11. Wada, H., et al., *Adult T-cell progenitors retain myeloid potential.* Nature, 2008. **452**(7188): p. 768-72.
12. Akashi, K.T., D.; Miyamoto, T.; Weissman, I., *A clonogenic common myeloid progenitor that gives rise to all myeloid lineages.* Nature, 2000. **404**: p. 193 - 197.
13. Kondo, M., I.L. Weissman, and K. Akashi, *Identification of clonogenic common lymphoid progenitors in mouse bone marrow.* Cell, 1997. **91**(5): p. 661-72.
14. Godin, I., F. Dieterlen-Lievre, and A. Cumano, *Emergence of multipotent hemopoietic cells in the yolk sac and paraaortic splanchnopleura in mouse embryos, beginning at 8.5 days postcoitus.* Proc Natl Acad Sci U S A, 1995. **92**(3): p. 773-7.
15. Cumano, A., et al., *Intraembryonic, but not yolk sac hematopoietic precursors, isolated before circulation, provide long-term multilineage reconstitution.* Immunity, 2001. **15**(3): p. 477-85.
16. Moore, M.A. and D. Metcalf, *Ontogeny of the haemopoietic system: yolk sac origin of in vivo and in vitro colony forming cells in the developing mouse embryo.* Br J Haematol, 1970. **18**(3): p. 279-96.
17. Mikkola, H.K. and S.H. Orkin, *The journey of developing hematopoietic stem cells.* Development, 2006. **133**(19): p. 3733-44.
18. Murray, P.D.F., *The Development in vitro of the Blood of the Early Chick Embryo.* Proceedings of the Royal Society B: Biological Sciences, 1932. **111**(773): p. 497-521.

19. North, T., et al., *Cbfa2 is required for the formation of intra-aortic hematopoietic clusters.* Development, 1999. **126**(11): p. 2563-75.
20. Swiers, G., N.A. Speck, and M.F. de Bruijn, *Visualizing blood cell emergence from aortic endothelium.* Cell Stem Cell, 2010. **6**(4): p. 289-90.
21. Boisset, J.C., et al., *In vivo imaging of haematopoietic cells emerging from the mouse aortic endothelium.* Nature, 2010. **464**(7285): p. 116-20.
22. Gekas, C., et al., *The placenta is a niche for hematopoietic stem cells.* Dev Cell, 2005. **8**(3): p. 365-75.
23. Li, Z., et al., *Mouse embryonic head as a site for hematopoietic stem cell development.* Cell Stem Cell, 2012. **11**(5): p. 663-75.
24. Nakano, H., et al., *Haemogenic endocardium contributes to transient definitive haematopoiesis.* Nat Commun, 2013. **4**: p. 1564.
25. North, T.E., et al., *Runx1 expression marks long-term repopulating hematopoietic stem cells in the midgestation mouse embryo.* Immunity, 2002. **16**(5): p. 661-72.
26. Chen, M.J., et al., *Runx1 is required for the endothelial to haematopoietic cell transition but not thereafter.* Nature, 2009. **457**(7231): p. 887-91.
27. De Bruijn, M., Speck, N., Peeters, M., Dzierzak, E., *Definitive hematopoietic stem cells first develop within the major arterial regions of the mouse embryo.* EMBO, 2000. **19**(11): p. 2465-2474.
28. Medvinsky, A. and E. Dzierzak, *Definitive hematopoiesis is autonomously initiated by the AGM region.* Cell, 1996. **86**(6): p. 897-906.
29. Muller, A.M., et al., *Development of hematopoietic stem cell activity in the mouse embryo.* Immunity, 1994. **1**(4): p. 291-301.
30. Matsubara, A., et al., *Endomucin, a CD34-like sialomucin, marks hematopoietic stem cells throughout development.* J Exp Med, 2005. **202**(11): p. 1483-92.
31. Yoder, M.C., K. Hiatt, and P. Mukherjee, *In vivo repopulating hematopoietic stem cells are present in the murine yolk sac at day 9.0 postcoitus.* Proc Natl Acad Sci U S A, 1997. **94**(13): p. 6776-80.
32. Rhodes, K.E., et al., *The emergence of hematopoietic stem cells is initiated in the placental vasculature in the absence of circulation.* Cell Stem Cell, 2008. **2**(3): p. 252-63.
33. Zovein, A.C., et al., *Fate tracing reveals the endothelial origin of hematopoietic stem cells.* Cell Stem Cell, 2008. **3**(6): p. 625-36.
34. Micklem, H.S., et al., *Competitive in vivo proliferation of foetal and adult haematopoietic cells in lethally irradiated mice.* J Cell Physiol, 1972. **79**(2): p. 293-8.
35. Bowie, M.B., et al., *Hematopoietic stem cells proliferate until after birth and show a reversible phase-specific engraftment defect.* J Clin Invest, 2006. **116**(10): p. 2808-16.
36. Morrison, S.J., et al., *The purification and characterization of fetal liver hematopoietic stem cells.* Proc Natl Acad Sci U S A, 1995. **92**(22): p. 10302-6.
37. Rebel, V.I., et al., *The repopulation potential of fetal liver hematopoietic stem cells in mice exceeds that of their liver adult bone marrow counterparts.* Blood, 1996. **87**(8): p. 3500-7.
38. Bowie, M.B., et al., *Identification of a new intrinsically timed developmental checkpoint that reprograms key hematopoietic stem cell properties.* Proc Natl Acad Sci U S A, 2007. **104**(14): p. 5878-82.
39. Mizuochi, C., et al., *Intra-aortic clusters undergo endothelial to hematopoietic phenotypic transition during early embryogenesis.* PLoS One, 2012. **7**(4): p. e35763.

40. BDBiosciences *Introduction to Flow Cytometry*. Training and E-Learning, 2014.
41. Taoudi, S., et al., *Extensive hematopoietic stem cell generation in the AGM region via maturation of VE-cadherin+CD45+ pre-definitive HSCs.* Cell Stem Cell, 2008. **3**(1): p. 99-108.
42. Yokomizo, T., et al., *Three-dimensional imaging of whole midgestation murine embryos shows an intravascular localization for all hematopoietic clusters.* Blood, 2011. **117**(23): p. 6132-4.
43. Alva, J.A., et al., *VE-Cadherin-Cre-recombinase transgenic mouse: a tool for lineage analysis and gene deletion in endothelial cells.* Dev Dyn, 2006. **235**(3): p. 759-67.
44. Soriano, P., *Generalized lacZ expression with the ROSA26 Cre reporter strain.* Nat Genet, 1999. **21**(1): p. 70-1.
45. Carmeliet, P.L., M.; Moons, L.; Breviario, F.; Compernolle, V.; Bono, F.; Balconi, G.; Spagnuolo, R.; Oosthuyse, B.; Dewerchin, M., *Targeted Deficiency or Cytosolic Truncation of the VE-cadherin Gene in Mice Impairs VEGF-Mediated Endothelial Survival and Angiogenesis.* Cell, 1999. **98**: p. 147 - 157.
46. Ng, C.E., et al., *A Runx1 intronic enhancer marks hemogenic endothelial cells and hematopoietic stem cells.* Stem Cells, 2010. **28**(10): p. 1869-81.
47. Kodama, H., et al., *Involvement of the c-kit receptor in the adhesion of hematopoietic stem cells to stromal cells.* Exp Hematol, 1994. **22**(10): p. 979-84.
48. Sanchez, M.J., et al., *Characterization of the first definitive hematopoietic stem cells in the AGM and liver of the mouse embryo.* Immunity, 1996. **5**(6): p. 513-25.
49. Ferkowicz, M.J., et al., *CD41 expression defines the onset of primitive and definitive hematopoiesis in the murine embryo.* Development, 2003. **130**(18): p. 4393-403.
50. Mitjavila-Garcia, M.T., et al., *Expression of CD41 on hematopoietic progenitors derived from embryonic hematopoietic cells.* Development, 2002. **129**(8): p. 2003-13.
51. Robin, C., et al., *CD41 is developmentally regulated and differentially expressed on mouse hematopoietic stem cells.* Blood, 2011. **117**(19): p. 5088-91.
52. Okada, S., et al., *In vivo and in vitro stem cell function of c-kit- and Sca-1-positive murine hematopoietic cells.* Blood, 1992. **80**(12): p. 3044-50.
53. Spangrude, G.J., S. Heimfeld, and I.L. Weissman, *Purification and characterization of mouse hematopoietic stem cells.* Science, 1988. **241**(4861): p. 58-62.
54. Chen, M.J., et al., *Erythroid/myeloid progenitors and hematopoietic stem cells originate from distinct populations of endothelial cells.* Cell Stem Cell, 2011. **9**(6): p. 541-52.
55. Robin, C., et al., *An unexpected role for IL-3 in the embryonic development of hematopoietic stem cells.* Dev Cell, 2006. **11**(2): p. 171-80.
56. Yoshida, H., et al., *The murine mutation osteopetrosis is in the coding region of the macrophage colony stimulating factor gene.* Nature, 1990. **345**(6274): p. 442-4.
57. Nakano, T., H. Kodama, and T. Honjo, *Generation of lymphohematopoietic cells from embryonic stem cells in culture.* Science, 1994. **265**(5175): p. 1098-101.
58. Fraser, S.T., et al., *Putative intermediate precursor between hematogenic endothelial cells and blood cells in the developing embryo.* Dev Growth Differ, 2003. **45**(1): p. 63-75.
59. Nishikawa, S.I., et al., *In vitro generation of lymphohematopoietic cells from endothelial cells purified from murine embryos.* Immunity, 1998. **8**(6): p. 761-9.

60. Broudy, V.L., N.; Priestly, G.; Nocka, K.; Wolf, N., *Interaciton of Stem Cell Factor and Its Receptor c-kit Mediates Lodgment and Acute Expansion of Hematopoietic Cells in the Murine Spleen.* Blood, 1996. **88**(1): p. 75 - 81.
61. Wu, H., et al., *Generation of committed erythroid BFU-E and CFU-E progenitors does not require erythropoietin or the erythropoietin receptor.* Cell, 1995. **83**(1): p. 59-67.
62. Nicola, N.A., et al., *Purification of a factor inducing differentiation in murine myelomonocytic leukemia cells. Identification as granulocyte colony-stimulating factor.* J Biol Chem, 1983. **258**(14): p. 9017-23.
63. Borges, L., et al., *A critical role for endoglin in the emergence of blood during embryonic development.* Blood, 2012. **119**(23): p. 5417-28.
64. Mukouyama, Y., et al., *In vitro expansion of murine multipotential hematopoietic progenitors from the embryonic aorta-gonad-mesonephros region.* Immunity, 1998. **8**(1): p. 105-14.
65. Quinn, P. and G.M. Harlow, *The effect of oxygen on the development of preimplantation mouse embryos in vitro.* J Exp Zool, 1978. **206**(1): p. 73-80.
66. Fandrey, J., *Oxygen-dependent and tissue-specific regulation of erythropoietin gene expression.* Am J Physiol Regul Integr Comp Physiol, 2004. **286**(6): p. R977-88.
67. Hata, Y., S.L. Rook, and L.P. Aiello, *Basic fibroblast growth factor induces expression of VEGF receptor KDR through a protein kinase C and p44/p42 mitogen-activated protein kinase-dependent pathway.* Diabetes, 1999. **48**(5): p. 1145-55.
68. Hoeben, A., et al., *Vascular endothelial growth factor and angiogenesis.* Pharmacol Rev, 2004. **56**(4): p. 549-80.
69. Shweiki, D., et al., *Vascular endothelial growth factor induced by hypoxia may mediate hypoxia-initiated angiogenesis.* Nature, 1992. **359**(6398): p. 843-5.
70. Borges, L., *Personal Communication.* September 13, 2012.
71. Gregory, C.J. and A.C. Eaves, *Human marrow cells capable of erythropoietic differentiation in vitro: definition of three erythroid colony responses.* Blood, 1977. **49**(6): p. 855-64.
72. Pereira, C., E. Clarke, and J. Damen, *Hematopoietic colony-forming cell assays.* Methods Mol Biol, 2007. **407**: p. 177-208.
73. Jaffe, L., E.J. Robertson, and E.K. Bikoff, *Distinct patterns of expression of MHC class I and beta 2-microglobulin transcripts at early stages of mouse development.* J Immunol, 1991. **147**(8): p. 2740-9.
74. Nucifora, G. and J.D. Rowley, *AML1 and the 8;21 and 3;21 translocations in acute and chronic myeloid leukemia.* Blood, 1995. **86**(1): p. 1-14.
75. Okuda, T., et al., *AML1, the target of multiple chromosomal translocations in human leukemia, is essential for normal fetal liver hematopoiesis.* Cell, 1996. **84**(2): p. 321-30.
76. Bee, T., et al., *Alternative Runx1 promoter usage in mouse developmental hematopoiesis.* Blood Cells Mol Dis, 2009. **43**(1): p. 35-42.
77. Komeno, Y., et al., *Runx1 exon 6-related alternative splicing isoforms differentially regulate hematopoiesis in mice.* Blood, 2014. **123**(24): p. 3760-9.
78. Bee, T., et al., *The mouse Runx1 +23 hematopoietic stem cell enhancer confers hematopoietic specificity to both Runx1 promoters.* Blood, 2009. **113**(21): p. 5121-4.
79. Burns, C.E., et al., *Hematopoietic stem cell fate is established by the Notch-Runx pathway.* Genes Dev, 2005. **19**(19): p. 2331-42.

80. Kumano, K., et al., *Notch1 but not Notch2 is essential for generating hematopoietic stem cells from endothelial cells.* Immunity, 2003. **18**(5): p. 699-711.
81. Nakagawa, M., et al., *AML1/Runx1 rescues Notch1-null mutation-induced deficiency of para-aortic splanchnopleural hematopoiesis.* Blood, 2006. **108**(10): p. 3329-34.
82. Artavanis-Tsakonas, S., M.D. Rand, and R.J. Lake, *Notch signaling: cell fate control and signal integration in development.* Science, 1999. **284**(5415): p. 770-6.
83. Bray, S.J., *Notch signalling: a simple pathway becomes complex.* Nat Rev Mol Cell Biol, 2006. **7**(9): p. 678-89.
84. Varnum-Finney, B., et al., *The Notch ligand, Jagged-1, influences the development of primitive hematopoietic precursor cells.* Blood, 1998. **91**(11): p. 4084-91.
85. Swiatek, P.J., et al., *Notch1 is essential for postimplantation development in mice.* Genes & Development, 1994. **8**(6): p. 707-719.
86. Hadland, B.K., et al., *A requirement for Notch1 distinguishes 2 phases of definitive hematopoiesis during development.* Blood, 2004. **104**(10): p. 3097-105.
87. Bertrand, J.Y., et al., *Notch signaling distinguishes 2 waves of definitive hematopoiesis in the zebrafish embryo.* Blood, 2010. **115**(14): p. 2777-83.
88. Richard, C., et al., *Endothelio-mesenchymal interaction controls runx1 expression and modulates the notch pathway to initiate aortic hematopoiesis.* Dev Cell, 2013. **24**(6): p. 600-11.
89. Lancrin, C., et al., *GFI1 and GFI1B control the loss of endothelial identity of hemogenic endothelium during hematopoietic commitment.* Blood, 2012. **120**(2): p. 314-22.
90. Clarke, R.L., et al., *The expression of Sox17 identifies and regulates haemogenic endothelium.* Nat Cell Biol, 2013. **15**(5): p. 502-10.
91. Irion, S., et al., *Temporal specification of blood progenitors from mouse embryonic stem cells and induced pluripotent stem cells.* Development, 2010. **137**(17): p. 2829-39.
92. Kim, I., T.L. Saunders, and S.J. Morrison, *Sox17 dependence distinguishes the transcriptional regulation of fetal from adult hematopoietic stem cells.* Cell, 2007. **130**(3): p. 470-83.
93. Nobuhisa, I., et al., *Sox17-mediated maintenance of fetal intra-aortic hematopoietic cell clusters.* Mol Cell Biol, 2014. **34**(11): p. 1976-90.
94. Iacovino, M., et al., *HoxA3 is an apical regulator of haemogenic endothelium.* Nat Cell Biol, 2011. **13**(1): p. 72-8.
95. Kawagoe, H., et al., *Expression of HOX genes, HOX cofactors, and MLL in phenotypically and functionally defined subpopulations of leukemic and normal human hematopoietic cells.* Leukemia, 1999. **13**(5): p. 687-98.
96. Moskow, J.J., et al., *Meis1, a PBX1-related homeobox gene involved in myeloid leukemia in BXH-2 mice.* Mol Cell Biol, 1995. **15**(10): p. 5434-43.
97. Dasse, E., et al., *Distinct regulation of c-myb gene expression by HoxA9, Meis1 and Pbx proteins in normal hematopoietic progenitors and transformed myeloid cells.* Blood Cancer J, 2012. **2**(6): p. e76.
98. Pineault, N., et al., *Differential expression of Hox, Meis1, and Pbx1 genes in primitive cells throughout murine hematopoietic ontogeny.* Exp Hematol, 2002. **30**(1): p. 49-57.
99. Shen, W.F., et al., *AbdB-like Hox proteins stabilize DNA binding by the Meis1 homeodomain proteins.* Mol Cell Biol, 1997. **17**(11): p. 6448-58.

100. Azcoitia, V., et al., *The homeodomain protein Meis1 is essential for definitive hematopoiesis and vascular patterning in the mouse embryo.* Dev Biol, 2005. **280**(2): p. 307-20.
101. Yoon, M.J., et al., *Mind bomb-1 is essential for intraembryonic hematopoiesis in the aortic endothelium and the subaortic patches.* Mol Cell Biol, 2008. **28**(15): p. 4794-804.
102. Yokomizo, T., et al., *Requirement of Runx1/AML1/PEBP2alphaB for the generation of haematopoietic cells from endothelial cells.* Genes Cells, 2001. **6**(1): p. 13-23.
103. Miller, M.E., *VALIDATION OF TWO NOVEL MOUSE MODELS OF CONDITIONAL MEIS1 DELETION TO STUDY ROLES IN ADULT MOUSE HEMATOPOIESIS*, in *THE FACULTY OF GRADUATE AND POSTDOCTORAL STUDIES*. 2014, University of British Columbia: Vancouver, BC.
104. Gotea, V. and I. Ovcharenko, *DiRE: identifying distant regulatory elements of co-expressed genes.* Nucleic Acids Res, 2008. **36**(Web Server issue): p. W133-9.
105. Longabaugh, W.J., E.H. Davidson, and H. Bolouri, *Visualization, documentation, analysis, and communication of large-scale gene regulatory networks.* Biochim Biophys Acta, 2009. **1789**(4): p. 363-74.
106. Schulz, T.J., et al., *Variable expression of Cre recombinase transgenes precludes reliable prediction of tissue-specific gene disruption by tail-biopsy genotyping.* PLoS One, 2007. **2**(10): p. e1013.
107. Copley, M.R., et al., *The Lin28b-let-7-Hmga2 axis determines the higher self-renewal potential of fetal haematopoietic stem cells.* Nat Cell Biol, 2013. **15**(8): p. 916-25.
108. Cui, P., et al., *A comparison between ribo-minus RNA-sequencing and polyA-selected RNA-sequencing.* Genomics, 2010. **96**(5): p. 259-65.
109. Challen, G.A. and M.A. Goodell, *Runx1 isoforms show differential expression patterns during hematopoietic development but have similar functional effects in adult hematopoietic stem cells.* Exp Hematol, 2010. **38**(5): p. 403-16.
110. Miller, C.L., et al., *Studies of W mutant mice provide evidence for alternate mechanisms capable of activating hematopoietic stem cells.* Exp Hematol, 1996. **24**(2): p. 185-94.
111. Fitch, S.R., et al., *Signaling from the sympathetic nervous system regulates hematopoietic stem cell emergence during embryogenesis.* Cell Stem Cell, 2012. **11**(4): p. 554-66.
112. Goyama, S., et al., *The transcriptionally active form of AML1 is required for hematopoietic rescue of the AML1-deficient embryonic para-aortic splanchnopleural (P-Sp) region.* Blood, 2004. **104**(12): p. 3558-64.
113. Ruiz-Herguido, C., et al., *Hematopoietic stem cell development requires transient Wnt/beta-catenin activity.* J Exp Med, 2012. **209**(8): p. 1457-68.
114. Takakura, N., et al., *A role for hematopoietic stem cells in promoting angiogenesis.* Cell, 2000. **102**(2): p. 199-209.
115. Adamo, L., et al., *Biomechanical forces promote embryonic haematopoiesis.* Nature, 2009. **459**(7250): p. 1131-5.
116. Pardanaud, L. and A. Eichmann, *Stem cells: The stress of forming blood cells.* Nature, 2009. **459**(7250): p. 1068-9.
117. Robert-Moreno, A., et al., *Impaired embryonic haematopoiesis yet normal arterial development in the absence of the Notch ligand Jagged1.* EMBO J, 2008. **27**(13): p. 1886-95.
118. Unnisa, Z., et al., *Meis1 preserves hematopoietic stem cells in mice by limiting oxidative stress.* Blood, 2012. **120**(25): p. 4973-81.

119. Kocabas, F., et al., *Meis1 regulates the metabolic phenotype and oxidant defense of hematopoietic stem cells.* Blood, 2012. **120**(25): p. 4963-72.
120. Forstermann, U., *Nitric oxide and oxidative stress in vascular disease.* Pflugers Arch, 2010. **459**(6): p. 923-39.

Appendix A: Additional information regarding RNA-seq Library Construction

At the GSC Biospecimen Core, RNA in the samples was enriched for RNA transcripts which contained a polyadenylated (poly-A) tail at their 3' end through poly-A selection. Poly-A selection enriches for mRNA, microRNA, and snoRNA. cDNA was generated from this enriched RNA, which was not sufficient for unamplified library construction, so samples were amplified using the SMART cDNA Amplification kit (Clontech, Mountain View, CA). Amplified cDNA was then sheared and adapters were ligated for sequencing. Libraries were indexed and run in one lane of an Illumina Hiseq 2000 flow cell. The resulting RNA-seq data was analyzed on the standard GSC pipeline for RNA-seq and aligned to *Mus musculus* genome mm9. Following library construction, additional analysis was done to generate reads per kilobase per million mapped reads (RPKM) values normalized for each library. This normalization allowed the comparison between the two libraries, including differential expression calculations to extract gene expression from HE at E10.5.